γ-secretase modulators and inhibitors in Alzheimer's disease: Influence of genetic background on efficacy and mechanism of action.

Dissertation

zur Erlangung des Grades

Doktor der Naturwissenschaften

Am Fachbereich Biologie

der Johannes Gutenberg-Universität Mainz

Eva Czirr

geb. am 27. Juni 1979 in Kreuztal

Mainz, 2008

Dekan:

1. Berichterstatter:

2. Berichterstatter:

Tag der mündlichen Prüfung: 17. Juni 2008

Contents

Abbreviations

ADAM	a disintegrin and metalloprotease
AICD	APP intracellular domain
ANOVA	analysis of variance
APH	anterior pharynx defective
APLP	amyloid precursor protein-like protein
APP	amyloid precursor protein
APPsw	Swedish mutant APP
Aβ	amyloid-β
BACE	β-site APP cleaving enzyme
COX	cyclooxygenase
C-terminal	carboxy-terminal
CTF	carboxy-terminal fragment
DAPT	N-[N-(3,5-Difluorophenacetyl-L-alanyl)]-S-pheylglycine t-butyl ester
DMSO	dimethylsulfoxid
E.coli	Escherichia coli
ECL	enhanced chemiluminescence
ELISA	enzyme-linked immunosorbent assay
EM	electron microscopy
ER	endoplasmic reticulum
FAD	familial Alzheimer's disease
FLIM	fluorescence lifetime imaging
flPS1	full length presenilin-1
FRET	fluorescence resonance energy transfer
g	gramm
GPI	glycophosphatidylinositol
GSK3-β	glycogen-synthase 3-β
GSM	γ-secretase modulator
HEK	human embryonic kidney
HRP	horse-raddish peroxidase
ICD	intracellular domain
iNOS	inducible nitric oxid synthase
kDa	kilo Dalton
KPI	Kunitz protease inhibitor
LPECL	liquid phase electrochemiluminescence
LTP	long-term potentiation

M	molar
m	milli
n	nano
Nct	nicastrin
NEXT	Notch extracellular truncation
NICD	Notch intracellular domain
NRG-1	neuregulin-1
NSAID	non-steroidal anti-inflammatory drug
N-terminal	amino-terminal
NTF	amino-terminal fragment
p	pico
PBS	phosphate-buffered saline
PD	Parkinson's disease
PDGF	platelet derived growth factor
PEN-2	presenilin enhancer-2
PKC	protein kinase C
PPAR	peroxysome proliferator-activated receptor
PS	presenilin
PS1-WT	wild-type presenilin-1
RIP	regulated intramembrane proteolysis
sAPP	soluble amyloid precursor protein ectodomain
SPP	signal-peptide peptidase
TAE	tris acetic acid
TBS	tris-buffered saline
TMD	transmembrane domain

Amino acids

A	alanine
C	cysteine
D	aspartic acid
E	glutamic acid
F	phenylalanine
G	glycine
I	isoleucine
K	lysine
L	leucine
M	methionine

N	asparagine
P	proline
Q	glutamine
R	arginine
S	serine
T	threonine
V	valine
W	tryptophan
Y	tyrosine

1 Introduction

1.1 Alzheimer's disease

Alzheimer's disease (AD) is the most common age-related neurodegenerative disorder currently affecting more than 20-30 million people worldwide. With increasing life expectancy projections are that by 2050 the European region alone will harbour around 11.2 million patients (Wancata, Musalek et al. 2003). These overwhelming numbers are posing an enormous threat to the public health care system especially as there is at present no disease modifying therapy available. The clinical phenotype of AD is characterised by progressive memory impairment, disordered cognitive function, altered behaviour including paranoia and delusions, loss of social appropriateness and a progressive decline in language functions. As the cognitive decline continues, a slowing of motor functions such as gait and coordination often leads to a picture resembling extrapyramidal motor disorders such as Parkinson's disease (PD). The major pathological hallmarks of AD are widespread neuron loss, intraneuronal neurofibrillary tangle formation and extracellular amyloid plaques (Fig. 1.1.1). The intracellular tangles are comprised of hyperphosphorylated tau protein while the main components of the extracellular plaques are the amyloid-β (Aβ) peptides, proteolytic fragments of the amyloid precursor protein (APP).

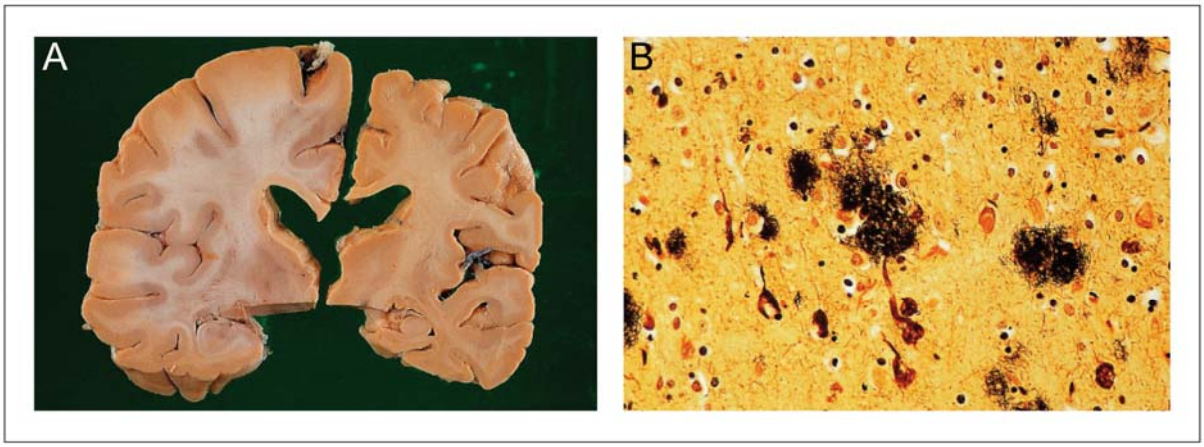

Fig. 1.1.1 Alzheimer's disease (AD) pathology. (A) Brain slices of a normal brain at age 70 (left side) and an AD brain (right side). Note in the AD slice the reduction in volume of white matter with cortical atrophy, mild sulcal widening and gyral thinning, the hippocampus is atrophic. (B) Microscopic picture of cerebral cortex stained with methylamine silver to reveal amyloid plaques and neurofibrillary tangles.

Initial studies in AD patients demonstrated degeneration of cholinergic basal forebrain neurons that innervate the hippocampus and wide areas of the cortex, but later studies

clearly showed that the neuron loss in AD is not specific for a certain subgroup of neurons. This distinguishes Alzheimer's disease from other neurodegenerative disorders where only certain groups of neurons are affected, such as the dopaminergic neurons in the substantia nigra in Parkinson's disease. The cause for the widespread neuron loss in AD patients has not been fully determined but accumulating evidence suggests that aberrant production of the Aβ peptides plays a causal role in disease onset and progression. This theory is outlined in the amyloid hypothesis (Fig. 1.1.2) (Hardy 1997; Hardy and Selkoe 2002). According to this hypothesis, the central disease causing agents in AD are the Aβ peptides and in particular the longer, more aggregation prone Aβ42 peptides. While Aβ40 is the major species produced in humans, Aβ42 is initially deposited in the AD brain (Iwatsubo, Odaka et al. 1994; Golde, Eckman et al. 2000) and animal models have suggested that this species is essential for formation of amyloid plaques (McGowan, Pickford et al. 2005). It is now believed that aberrant production of Aβ subsequently promotes secondary pathologies in the brain such as formation of intracellular neurofibrillary tangles, synaptic dysfunction, enhanced oxidative stress, and inflammatory responses. This finally culminates in neuronal cell death by still unknown mechanisms. Strong support for this hypothesis is drawn from studies of rare cases of familial autosomal-dominantly inherited forms of AD. In affected families, a particularly aggressive early-onset form of the disease is observed. However, histopathologically, these familial forms of AD are indistinguishable from the late-onset sporadic form of the disease. Familial Alzheimer's disease (FAD) is caused by mutations in the *APP*, the *presenilin-1* (PS1) or the *presenilin-2* (PS2) genes. More than 180 mutations have been described to date (http://www.molgen.ua.ac.be/ADMutations/default.cfm?MT=0&ML=0&Page=Home) the vast majority of them being missense mutations in the PS1 gene. Studies in primary fibroblasts from patients with PS1 or PS2 mutations have demonstrated that these mutations selectively increase the production of the Aβ42 peptide (Scheuner, Eckman et al. 1996). In contrast, the rarer mutations in APP can also enhance the production of all Aβ species or promote the aggregation properties of the peptides (Citron, Oltersdorf et al. 1992; Suzuki, Cheung et al. 1994; Tomiyama, Nagata et al. 2008). Moreover, in patients with Down's syndrome (trisomy 21), overexpression of the normal APP gene which is located on the long arm of chromosome 21, causes AD-like pathology and symptoms during middle adult years (Glenner and Wong 1984). More recently, APP locus duplications were also found to cause early-onset autosomal-dominant AD, clearly showing that enhanced APP gene dosage alone is sufficient for early-onset of the disease (Rovelet-Lecrux, Hannequin et al. 2006). Taken together, these findings clearly indicate that overproduction of Aβ is sufficient to initiate the disease process, and that reducing Aβ production could be an efficient means to treat or prevent AD.

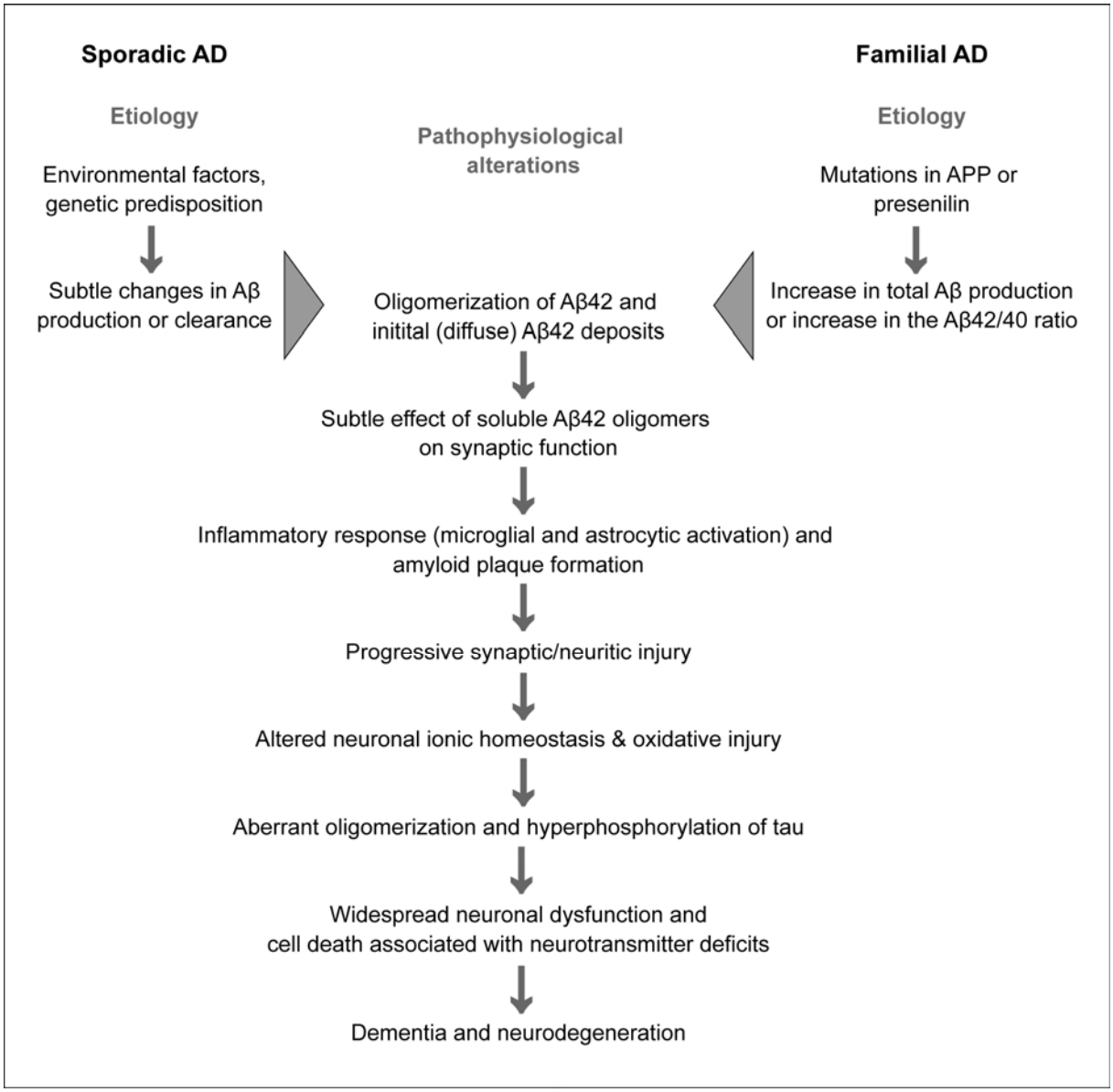

Fig. 1.1.2 The amyloid hypothesis. Sporadic cases of AD, which account for the vast majority of all AD patients, are predominantly caused by aging and unknown environmental factors, but genetic predisposition may also play a role in the late-onset form of the disease. Familial forms of AD are caused by autosomal dominant mutations in the APP gene or the presenilin genes, which cause disease onset typically well before 60 years of age. Both disease courses lead to similar clinical phenotypes and can not be distinguished histopathologically. (modified after (Winklhofer, Tatzelt et al. 2008)).

1.2 APP processing and function

The amyloid precursor protein (APP) was first cloned in 1987 (Goldgaber, Lerman et al. 1987; Kang, Lemaire et al. 1987; Robakis, Wisniewski et al. 1987; Tanzi, Gusella et al. 1987). APP is a 110 – 130 kDa type-I single pass transmembrane protein with a large

ectodomain and a shorter cytoplasmic carboxy-terminal (C-terminal) tail. APP belongs to a larger family of APP-like proteins (APPLPs) with two homologues in mammals, APLP1 and APLP2 (Wasco, Bupp et al. 1992). Both APLPs display substantial homology to APP within their ectodomain and particularly in the cytoplasmic tail, but are largely divergent in the Aβ region. APP exists in at least eight different splice variants with species containing 770, 751 and 695 amino acids being most common. The longer variants, APP770 and APP751, are predominantly expressed in non-neuronal cells, while the APP695 isoform is highly expressed in neurons. The main difference between these splice variants is the presence of a motif that is homologous to the Kunitz-type of serine protease inhibitors (KPI), indicating a possible function of these longer isoforms. Indeed, the KPI containing forms of APP were shown to participate in the coagulation cascade in human platelets (Smith, Higuchi et al. 1990). APP is cotranslationally translocated into the endoplasmic reticulum (ER) and then travels through the intermediate compartments into the Golgi and to the plasma membrane. During its transport along the secretory pathway APP is posttranslationally modified by addition of *N*- and *O*-linked sugars, sulfation, and phosphorylation (Weidemann, König et al. 1989). At the plasma membrane, APP can be internalized into endosomal compartments and then either be degraded through the endosomal-lysosomal pathway or it can be recycled back to the plasma membrane (Kang, Lemaire et al. 1987; Suzuki, Cheung et al. 1994). The best understood and investigated posttranslational modification of APP is its proteolytic processing, which can lead to the formation of the Aβ peptides (Fig. 1.2.1). APP processing occurs via two different pathways, the amyloidogenic and the non-amyloidogenic pathway. Approximately 90 % of all APP molecules are processed in the non-amyloidogenic pathway with ectodomain shedding by α-secretase being the first cleavage event. α-secretase cleavage is mediated by proteins of the *a disintegrin and metalloprotease domain* family (ADAM) with ADAM9, ADAM10 and ADAM17 being the most likely candidates (Asai, Hattori et al. 2003). α-secretase processing leads to shedding of the large soluble ectodomain of APP (sAPPα) and leaves behind a C-terminal membrane spanning fragment of 83 amino acids (CTFα/C83) (Esch, Keim et al. 1990; Sisodia, Koo et al. 1990). As α-cleavage occurs within the Aβ region of APP it precludes subsequent Aβ production. The C-terminal stub is further processed by γ-secretase, which cleaves membrane spanning protein stubs that are generated by ectodomain shedding within their transmembrane domain (TMD). γ-secretase cleavage of CTFα leads to the release of the APP intracellular domain (AICD) and to the formation of a 3 kDa protein fragment termed p3, that is released into the extracellular or luminal space (Haass, Hung et al. 1993). The AICD has been proposed to play a role in transcriptional activation (von Rotz, Kohli et al. 2004; Pardossi-Piquard, Petit et al. 2005; Zhang, Wang et al. 2007).

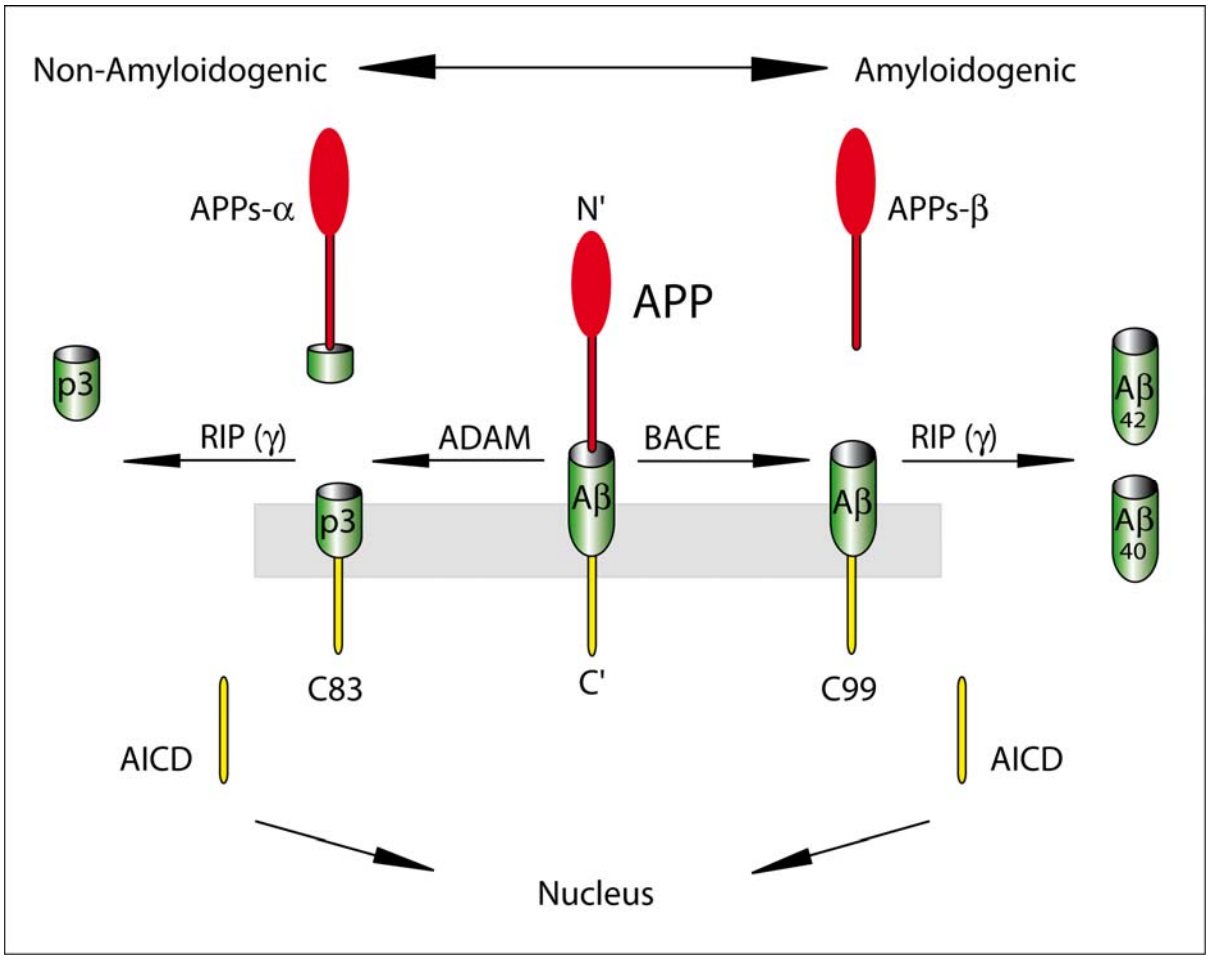

Fig. 1.2.1 APP processing. APP can be processed either via the amyloidogenic or the non-amyloidogenic pathway. In the non-amyloidogenic pathway, APP is first cleaved by α-secretase (ADAM) in the middle of the Aβ domain, generating a soluble ectodomain (sAPPα) and a membrane-bound C-terminal stub of 83 amino acids (CTFα/C83). C83 is then cleaved by γ-secretase releasing the APP intracellular domain (AICD) and the p3 fragment. In the amyloidogenic pathway, APP is initially cleaved by β-secretase (BACE1), generating a shorter soluble ectodomain (sAPPβ) and a C-terminal membrane-bound stub of 99 amino acids (CTFβ/C99). C99 is then further processed by γ-secretase releasing the AICD fragment and Aβ peptides of varying length. (AICD – APP intracellular domain; RIP – regulated intramembrane proteolysis; γ – γ-secretase)

The amyloidogenic processing of APP follows a similar pattern. The first cleavage is mediated by the *β-site APP cleaving enzyme* (BACE1) (Citron, Teplow et al. 1995; Hussain, Powell et al. 1999; Sinha, Anderson et al. 1999; Vassar, Bennett et al. 1999; Yan, Bienkowski et al. 1999) and releases a slightly shorter soluble ectodomain, referred to as sAPPβ and leaves behind a 99 amino acid membrane-bound, C-terminal fragment (CTFβ/C99). BACE1 cleavage generates the N-terminal end of the Aβ peptides. CTFβ is then processed by γ-secretase, liberating the AICD and producing Aβ peptides of different lengths (Haass, Schlossmacher et al. 1992).

More than 20 mutations in the APP gene causing FAD have been identified to date and they can be divided into three groups: 1. mutations that improve BACE1 cleavage and lead to higher overall Aβ production (Citron, Oltersdorf et al. 1992), 2. mutations at the γ-cleavage site, which increase production of Aβ42 (Murrell, Hake et al. 2000), and 3. mutations in the middle of the Aβ region, which enhance the aggregation properties of the peptide (Nilsberth, Westlind-Danielsson et al. 2001). The identification of APP mutations causing familial forms of AD has led to the development of mouse models that resemble many features of AD and most faithfully the amyloid pathology. One of the first models with significant pathological accumulation of Aβ was the PDAPP mouse line. These mice express APP with the Indiana mutation (V717F) under the platelet derived growth factor (PDGF) promoter and amyloid deposition starts at about 6 month of age (Games, Adams et al. 1995). Another widely used transgenic mouse model is the Tg2576 mouse line, which overexpresses APP with the Swedish mutation (K670N/M671L) under the control of the hamster prion promoter, and displays amyloid deposition between 9 and 11 months of age (Hsiao, Chapman et al. 1996). APP with the Swedish mutation carries two point mutations, which result in two amino acid exchanges at the BACE cleavage site (K670N/M671L). These amino acid changes make APP a better substrate for BACE and the enzyme cleaves more efficiently, resulting in more Aβ production. These APP transgenic mouse models only insufficiently recapitulate the AD pathology and lack neurofibrillary tangles and neuron loss. Subsequently, more complete models with tau pathology and neuronal loss have been developed which express a combination of several transgenes including FAD mutant PS and mutant tau (Oddo, Caccamo et al. 2003; Oakley, Cole et al. 2006; Radde, Bolmont et al. 2006).

Even though APP has been cloned more than 20 years ago its physiological function is still unknown. A variety of functions for APP as a growth factor, a cell-surface receptor with signalling properties, an adhesion molecule, and a transcriptional regulator have been proposed. APP knock-out mice are viable and show only minor deficits, such as reduced growth and brain weight, reduced grip strength, hypersensitivity to seizures and slightly impaired spatial learning and long-term potentiation (LTP) (Mueller, Cristina et al. 1994; Zheng, Jiang et al. 1995; Li, Stark et al. 1996). This minor phenotype could be due to functional redundancy between APP and its homologues APLP1 and APLP2. Knock-out mice for either one of the APLPs are also viable, but combining a knock-out for APP and APLP2 or for APLP1 and APLP2 results in postnatal lethality (von Koch, Zheng et al. 1997; Heber, Herms et al. 2000). Knock-out mice for all three proteins, APP, APLP1 and APLP2 also die postnatally and display cranial dysplasias resembling human type II lissencephaly (Herms , Anliker et al. 2004). These results clearly indicate that APP and the APLPs possess important functions during development and presumably also during adult life.

Various signalling functions have been linked to the soluble ectodomain of APP. sAPP can stimulate growth of fibroblasts in culture (Park, Gimbel et al. 2006) and was found to be neuroprotective (Mattson, Cheng et al. 1993) as well as to mediate axonal and dendritic outgrowth (Perez, Zheng et al. 1997). The finding that transgenic expression of sAPPα is sufficient to rescue the abnormalities of APP knock-out mice, including their deficits in LTP, suggests that sAPPα plays a role in learning and memory and indicates that the soluble ectodomain is the most important part for APP function in general (Ring, Weyer et al. 2007). APP structurally resembles a cell-surface receptor, but so far no extracellular ligand has been confirmed. It was recently reported that TAG1, a glycophosphatidylinositol (GPI)-linked recognition molecule, serves as a functional ligand of APP (Ma, Futagawa et al. 2008). The authors were able to demonstrate a γ-secretase dependent increase in AICD release upon interaction of APP and TAG1. They further described a TAG1-APP signalling pathway that negatively modulates neurogenesis. If confirmed, TAG1 would be the first functional ligand of APP that influences an intracellular signalling pathway.

APP has further been proposed to function as an adhesion molecule and it was shown to bind to extracellular matrix proteins such as heparin and collagen (Multhaup 1994; Beher, Hesse et al. 1996). Many more proteins were found to bind to APP and to influence Aβ production, for example the transmembrane lipoprotein receptor LRP and the transmembrane receptor protein SORL1 (Andersen, Reiche et al. 2005; Bu, Cam et al. 2006; Waldron, Jaeger et al. 2006). An APP interacting protein that has generated much interest is Fe65. Fe65 binds to the cytoplasmic tail of APP and it can form ternary complexes with the AICD and the histone acetyltransferase Tip60. This complex has been detected in the nucleus and it has been proposed to mediate transcription (Cao and Sudhof 2001; Cao and Sudhof 2004). A number of putative target genes, such as tetraspanin, APP itself, glycogen synthase 3-β (GSK3-β) and neprilysin have been identified (Baek, Ohgi et al. 2002; Kim, Kim et al. 2003; von Rotz, Kohli et al. 2004; Pardossi-Piquard, Petit et al. 2005). Some of these putative target genes seem particularly interesting in the context of AD, for example neprilysin, which is an Aβ degrading enzyme (Iwata, Tsubuki et al. 2001; Leissring, Farris et al. 2003). However, the function of AICD as a transcriptional activator or coactivator is still under debate, as a recent study by Hébert et al. could not confirm the previously reported target genes (Hebert, Serneels et al. 2006).

1.3 γ-secretase

γ-secretase is an aspartyl-protease (Wolfe, Xia et al. 1999) that cleaves type-1 transmembrane proteins after ectodomain shedding in the middle of their TMD. This process

is called regulated intramembrane proteolysis (RIP) (Brown, Ye et al. 2000). γ-secretase is a multiprotein complex consisting of at least four different proteins, nicastrin (Yu, Nishimura et al. 2000), anterior pharynx defective-1 (APH-1) (Goutte, Tsunozaki et al. 2002), presenilin enhancer-2 (PEN2) and the presenilin proteins, PS1 or PS2. These four proteins are necessary and sufficient to form an active γ-secretase complex (Fig. 1.3.1) (Edbauer, Winkler et al. 2003; Kimberly, LaVoie et al. 2003). Two other proteins have been suggested to be modulators of γ-secretase activity and components of the γ-secretase complex, CD147 and TMP21. Both proteins are not essential for γ-secretase function and whether they are indeed integral components of the complex awaits confirmation (Zhou, Zhou et al. 2005; Chen, Hasegawa et al. 2006).

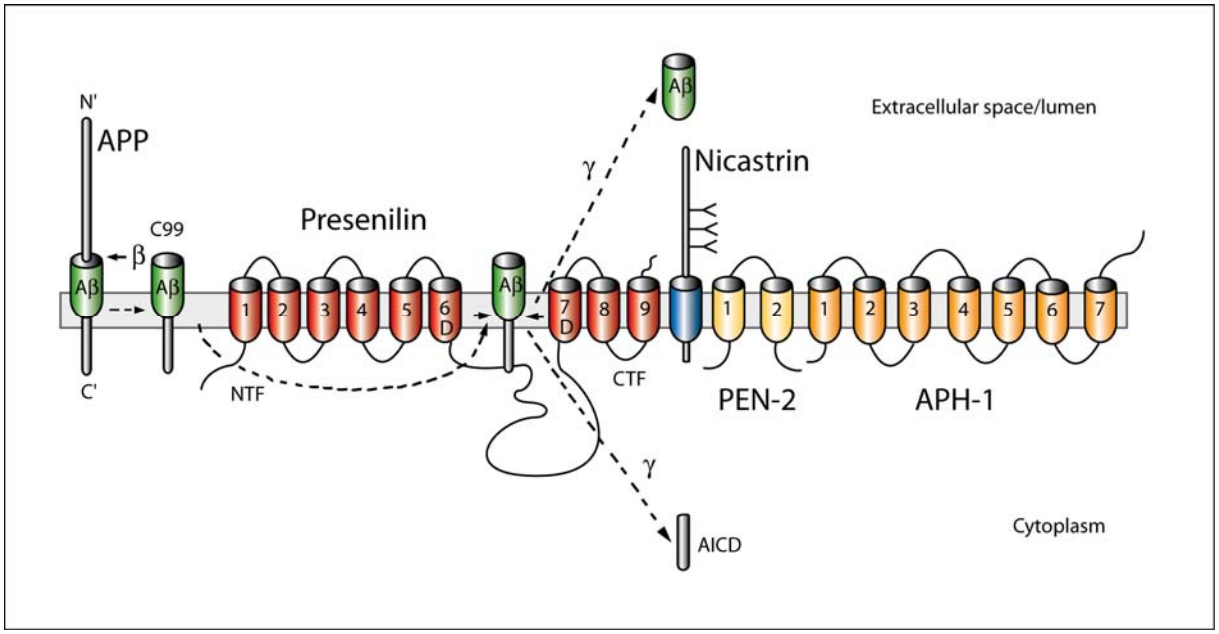

Fig. 1.3.1 The γ-secretase complex. The γ-secretase complex consists of four different membrane spanning proteins, presenilin, nicastrin, PEN-2 and APH-1. γ-secretase cleaves type-I transmembrane proteins after ectodomain shedding in the middle of their transmembrane domain. Here, the β-cleaved APP C-terminal stub (C99) is processed into the APP intracellular domain (AICD) and the Aβ peptide. (PEN-2 – presenilin enhancer-2; APH-1 – anterior pharynx defective-1; CTF – carboxy-terminal fragment; NTF – amino-terminal fragment) (modified after (Haass and Steiner 2002))

The catalytic center of the complex is formed by the PS proteins which contain the two catalytically active aspartate residues in TMDs 6 and 7. Exchange of either aspartate by other amino acids renders γ-secretase catalytically inactive (Wolfe, Xia et al. 1999; Nyabi, Bentahir et al. 2003). The PS genes were initially identified by genetic association with rare cases of FAD (Levylahad, Wasco et al. 1995; Rogaev, Sherrington et al. 1995). The PS proteins are integral membrane proteins with nine TMDs (Laudon, Hansson et al. 2005; Oh and Turner 2005; Spasic, Tolia et al. 2006) and are endoproteolytically processed into an

amino-terminal and a carboxy-terminal fragment (NTF and CTF respectively) (Brunkan, Martinez et al. 2005). However, proteolytic processing is not a requirement for the formation of an active γ-secretase complex as the FAD associated PS1-ΔExon9 mutation is proteolytically active even though the mutant protein lacks the endoproteolytic cleavage site (Steiner, Romig et al. 1999).

Nicastrin is a highly glycosylated type-1 transmembrane protein (Herreman, Van Gassen et al. 2003) and seems to be the initial substrate receptor in the γ-secretase complex (Shah, Lee et al. 2005). No distinct functions have been attributed to the other γ-secretase components, APH-1 and PEN-2 so far. PEN-2 contains two TMDs and the N- and C-terminus are both protruding into the lumen/extracellular space, while APH-1 seems to possess 7 TMDs. Two different APH-1 genes in humans, APH-1A and APH-1B, and three in rodents that can be alternatively spliced have been identified. APH-1A and APH-1B as well as PS1 and PS2 are incorporated mutually exclusive into the γ-secretase complex. Hence, at least four different γ-secretase complexes can be formed in humans and up to six in rodents (Hébert, Serneels et al. 2004; Shirotani, Edbauer et al. 2004b). Whether these distinct complexes are differentially expressed, have different functions or play different roles during development is still under investigation.

All components of the γ-secretase complex colocalize in the endoplasmic reticulum (ER) and their assembly occurs in a stepwise manner. Initially a subcomplex of nicastrin and APH-1 is formed which is stable even in the absence of PS and PEN2 (Shirotani, Edbauer et al. 2004a). The complex of Nicastrin and APH-1 then associates with full length PS (flPS), and this trimeric complex is finally joined by PEN-2 which facilitates PS endoproteolysis (LaVoie, Fraering et al. 2003; Niimura, Isoo et al. 2005). Whether full assembly of the complex already occurs within the ER or later in the secretory pathway (Capell, Beher et al. 2005) is not fully resolved. Recent reports indicate that ER-Golgi recycling mechanisms might play a role in complex assembly (Kaether, Scheuermann et al. 2007; Spasic, Raemaekers et al. 2007).

The exact stoichiometry of the four components in the active γ-secretase complex is unknown. Recent data indicates a 1:1:1:1 assembly (Sato, Diehl et al. 2007), but a final picture of the γ-secretase structure and stoichiometry will only be available after crystallisation of the complex is achieved. Low resolution electron-microscopy (EM) pictures of purified γ-secretase complexes show a globular structure with a large aqueous central chamber (Lazarov, Fraering et al. 2006). This is consistent with the finding of a water accessible hydrophilic pore in PS1 between TMDs 6 and 7, which contain the catalytically active aspartate residues (Sato, Morohashi et al. 2006; Tolia, Chavez-Gutierrez et al. 2006). This water accessible pore also provides a potential explanation for how γ-secretase can perform proteolysis within the hydrophobic environment of the membrane.

More than 20 substrates for γ-secretase have been identified to date [for a review see (Parks and Curtis 2007)] and more are expected. All identified proteins are type-1 transmembrane proteins and the prerequisite for γ-secretase dependent cleavage is ectodomain shedding. APP is one of the many γ-secretase substrates and has been most intensely studied. Cleavage of the APP βCTF by γ-secretase produces a number of Aβ-peptides, with species ending after 40 and 42 amino acids being the most abundant forms. Besides these two peptide species γ-cleavage also produces to a lesser extend longer and shorter Aβ forms ending after 46, 45, 43, 38, 37, 34 or 33 amino acid residues. Cleavage generating a peptide of 46 amino acids has been termed ζ-cleavage and seems to precede formation of the other peptides (Zhao, Cui et al. 2005). The longer peptides such as Aβ45 and Aβ46 can only be detected intracellularly while the shorter forms are secreted. How these different peptides are produced is not known, but evidence points to a sequential cleavage mechanism in which the shorter forms are generated by γ-secretase processing of longer peptides. Some interdependence between the generation of Aβ40, Aβ43 and Aβ46 has been demonstrated and a sequential cleavage model was postulated (Qi-Takahara, Morishima-Kawashima et al. 2005).

Another important substrate is the Notch receptor (Levitan, Doyle et al. 1996; Baumeister, Leimer et al. 1997), and γ-secretase mediated Notch signalling is important for cell-fate decisions during development and throughout the adult lifespan. The Notch receptor is processed in a similar fashion as APP. Upon interaction with its ligand Notch undergoes cleavage at site 2 (S2) within its ectodomain. The ligand-bound ectodomain is endocytosed (Parks, Klueg et al. 2000), while the Notch extracellular truncation (NEXT) fragment remains embedded in the membrane (Mumm, Schroeter et al. 2000). NEXT serves as a substrate for γ-secretase and cleavage at site 3 (S3) releases the Notch intracellular domain (NICD), which translocates into the nucleus and drives the transcription of target genes (Schroeter, Kisslinger et al. 1998) such as Hes-1, a homeobox gene encoding a basic helix-loop-helix transcription factor (Thomas and Rathjen 1992; Kopan, Nye et al. 1994). γ-secretase cleavage of the NEXT fragment also leads to the release of Notch Aβ-like peptides named Nβ, which do not seem to possess aggregation properties and whose function, if any, is unclear (Okochi, Steiner et al. 2002; Okochi, Fukumori et al. 2006). The deficiency in Notch signalling most likely accounts for the lethality of PS1 knock-out mice, which are phenocopies of Notch knock-out mice and show gross abnormalities in formation of the axial skeleton and severely impaired neurogenesis (Shen, Bronson et al. 1997; Wong, Zheng et al. 1997; De Strooper, Saftig et al. 1998). The phenotype of PS1/2 double knock-out mice is even more severe and these mice display additional defects that may be due to the loss of PS cleavage of other substrates (Donoviel, Hadjantonakis et al. 1999; Herreman, Hartmann et al. 1999). A knock-out of PS2 alone is not lethal and these mice display only a mild

pulmonary fibrosis and haemorrhage with age (Herreman, Hartmann et al. 1999). Hence, PS1 is able to largely compensate for loss of PS2 function.

PS has also been shown to have γ-secretase independent functions, most notably in calcium regulation. A consistent observation has been that induced release of calcium from ER stores is strongly increased by FAD-associated PS-mutants (Smith, Green et al. 2005; Stutzmann 2005). These results have led to the hypothesis that altered calcium homeostasis in patients with AD might contribute to neuronal dysfunction and cell death. Additionally and somewhat contradictory, it was recently demonstrated that PS forms ER calcium leak channels. Mutations in one of the catalytically active aspartates did not abolish this function, showing that it is independent of γ-secretase activity. However, FAD-associated PS1 mutations exert strong dominant-negative effects on leak channel function and thus interfere with calcium homeostasis (Tu, Nelson et al. 2006). Other proposed but less characterized functions of PS proteins include protein trafficking, cell adhesion, synaptic function and tau phosphorylation (Marambaud, Shioi et al. 2002; Baki, Shioi et al. 2004; Haas, Frank et al. 2005; Wang, Tang et al. 2006; Zhang, Haapasalo et al. 2006).

Since the first report of a PS1 mutation in 1995 (Sherrington, Rogaev et al. 1995) more than 150 mutations in PS1 and about 10 in PS2 have been described, all leading to aggressive forms of FAD with an onset as early as 24 years of age (Moehlmann, Winkler et al. 2002). The FAD associated mutations in PS1 and PS2 are evenly distributed over the whole molecule (Fig. 1.3.2) and their only common characteristic is their influence on APP processing: all FAD associated PS mutations identified to date increase the Aβ42 to Aβ40 ratio (Borchelt, Thinakaran et al. 1996; Scheuner, Eckman et al. 1996; Citron, Westaway et al. 1997). Almost all FAD associated PS1 or PS2 mutations are missense mutations leading to the exchange of one amino acid residue against another, only very few mutations are insertions or deletions. The shift in the Aβ42/40 ratio is often caused by a decrease in Aβ40 production rather than an increase in Aβ42 levels (Bentahir, Nyabi et al. 2006). Some FAD PS1 mutations also display reduced production of AICD and NICD. For example, the PS1-ΔExon9 mutation, a complex PS1 mutation caused by a splice site mutation leading to deletion of exon9 was shown to produce less Aβ40, AICD, and NICD as compared to wild-type PS1, but Aβ42 generation was not changed. This suggests that incorporation of these mutant PS molecules into the γ-secretase complex might result in reduced proteolytic activity of the enzyme, which would be consistent with the view that FAD mutations cause a loss-of-function phenotype (De Strooper 2007; Wolfe 2007). However, other FAD PS1 mutations (i.e PS1-G384A) were shown to increase Aβ42 production without a significant effect on Aβ40 levels (Bentahir, Nyabi et al. 2006). Whether the possible loss of γ-secretase activity caused by some FAD PS mutations contributes to the phenotype in FAD patients is not clear, but

since not all FAD PS mutations seem to display a reduced proteolytic activity, their only common denominator remains the effect on the Aβ42/40 ratio.

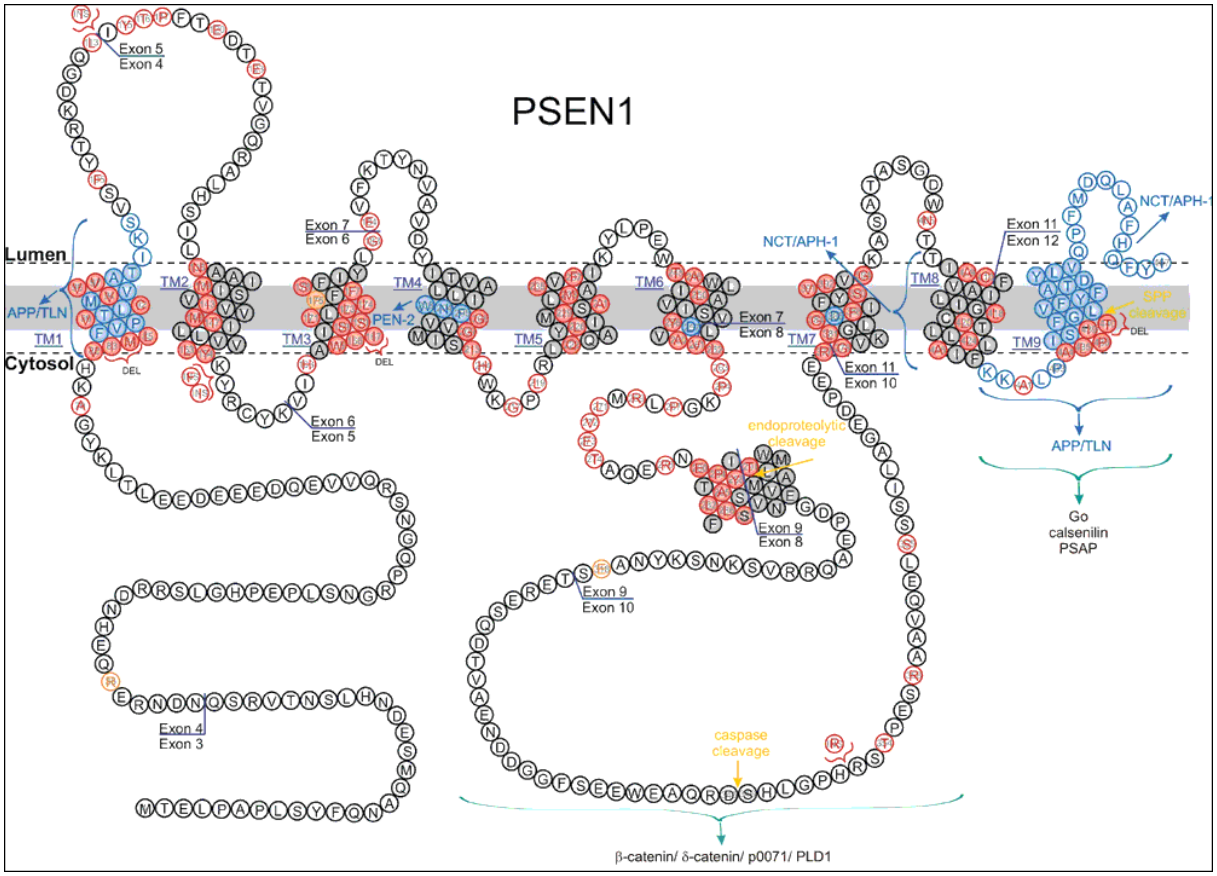

Fig. 1.3.2 Presenilin-1. Presenilin proteins contain the catalytically active aspartates in transmembrane domains 6 and 7. During maturation of the γ-secretase complex PS1 is processed into an N-terminal and a C-terminal fragment. Amino acids depicted in red are known FAD PS1 mutations. Amino acids depicted in blue are interaction sites with other proteins in the γ-secretase complex. The yellow arrows show the endoproteolytic cleavage site and a caspase cleavage site.

1.4 Treatment strategies for Alzheimer's disease

Currently only two types of drugs are approved specifically for treatment of Alzheimer's disease symptoms, cholinesterase inhibitors and the N-methyl-D-aspartate (NMDA) receptor antagonist mematine. Both kinds of drugs do not change disease progression and only temporarily ameliorate disease symptoms and cognitive decline. Acetylcholinesterase inhibitors seem to work by reducing the transmitter deficit caused by the progressive loss of cholinergic neurons in the brains of AD patients. With the emergence of the amyloid hypothesis Aβ production became a major target for drug development efforts and this spurred the hope of being able to attenuate or even halt disease progression. The most

promising drug targets are the secretases, BACE1 and γ-secretase, that are the two major players in Aβ generation. However, activation of the α-secretases and the non-amyloidogenic processing pathway is also under investigation. Inhibitors of Aβ aggregation as well as therapeutic strategies that lead to enhanced degradation of Aβ and clearance of amyloid plaques from the brain are other important prospects for intervention in AD.

BACE1 cleavage of APP is the initial and rate limiting step in the production of Aβ peptides. Furthermore, BACE1 knock out mice are viable and display more than 90 % reduction in Aβ generation (Cai, Wang et al. 2001; Luo, Bolon et al. 2001). The BACE1 active center was crystallized and the structure was determined at 1.9 angstrom resolution (Hong, Koelsch et al. 2000). This showed that the active center is rather large and flexible, which makes the development of potent small molecule inhibitors that are able to cross the blood-brain barrier very difficult. It was also found that, while BACE1 knock-out mice do not show gross abnormalities, they do have defects in peripheral nerve myelination and axon bundling. These deficits are most likely caused by reduced processing of type III neuregulin-1 (NRG-1), which was identified as a new substrate for BACE1 (Hu, Hicks et al. 2006; Willem, Garratt et al. 2006). Whether pharmacological inhibition of BACE1 activity in adult life would also have effects on nerve myelination needs to be clarified, but a recent study showed that BACE1 inhibition in adult mice did not have an effect on brain NRG1 processing despite a notable reduction in Aβ production (Sankaranarayanan, Price et al. 2007). The first BACE1 inhibitors that were developed had peptide-like structures and were modelled after the BACE1 cleavage site of APP with the FAD-associated Swedish mutation (APPsw) (Sinha, Anderson et al. 1999), but these large peptidomimetics are highly unlikely to cross the blood-brain barrier. Therefore, efforts have focused on remodelling these peptide-like inhibitors to reduce their size and increase their potency (Shuto, Kasai et al. 2003; Hom, Gailunas et al. 2004), but other substance classes are also being investigated for their ability to inhibit BACE1. Only few of these compounds have been published outside of patent applications and none have entered clinical trials so far.

The α-secretases have also been proposed as potential therapeutic targets. Overexpression of a known α-secretase, ADAM10, in an APP transgenic mouse model of AD increased sAPPα production, decreased Aβ generation and reduced cognitive defects (Postina, Schroeder et al. 2004). These results provide proof of concept that enhancing α-secretase activity results in reduced amyloid pathology. Direct activation of α-secretase by pharmacological means is difficult. Some compounds have been shown to indirectly influence its activity often by activating protein kinase C (PKC) mediated signalling pathways, which results in altered trafficking and subcellular localization of APP, α-secretase or both

(Gandy and Greengard 1994; Koo 1997; Vardy, Catto et al. 2005). A green tea polyphenol (-)-epigallocatechin-3-gallate may also activate ADAM10 and this effect might contribute to its efficacy in reducing Aβ pathology in APP transgenic mouse models (Levites, Amit et al. 2003; Rezai-Zadeh, Shytle et al. 2005; Obregon, Rezai-Zadeh et al. 2006). Nonetheless to date there is only insufficient evidence to support use of α-secretase activating compounds in AD therapy.

Another very promising therapeutic approach to reduce amyloid pathology is vaccination. Pre-clinical studies in AD mouse models have shown that the amyloid pathology can be strongly reduced by either active or passive immunisation with Aβ42 peptides or anti-Aβ monoclonal antibodies. Active immunisation in an APP transgenic AD mouse model was able to prevent plaque formation, neuritic dystrophy and astrogliosis when administered prior to AD-type neuropathology and markedly reduced the extend and progression of these pathologies when administered to older animals (Schenk, Barbour et al. 1999). Peripheral application of anti-Aβ antibodies also led to reduced amyloid plaque burden and associated pathology (Bard, Cannon et al. 2000). There is still no consensus how either form of Aβ immunotherapy prevents Aβ deposition (Das and Golde 2002; Schenk 2002). Unfortunately, a clinical trial with active immunisation had to be stopped due to meningoencephalitis in 6 % of the vaccinated individuals (Nicoll, Wilkinson et al. 2003; Orgogozo, Gilman et al. 2003; Gilman, Koller et al. 2005). Continuing analysis of the halted trial suggested that the treatment might have been effective, and that it was able to clear brain amyloid and to slow cognitive decline in some patients (Hock, Konietzko et al. 2003; Masliah, Hansen et al. 2005). Despite the setbacks of the first clinical trial, a phase-II clinical trial with a humanized monoclonal anti-Aβ antibody (Bapineuzumab™, AAB-001) is ongoing, but no results have been reported so far.

Inhibition of γ-secretase is also under investigation as a possible treatment option for AD, as it also has the potential to completely abolish Aβ production. Potent inhibitors of γ-secretase activity have been developed, some with an IC50 of less than 100 pM, and they have been tested extensively in cellular and animal models of AD. Difficulties are evident considering the pivotal role of γ-secretase in the Notch signalling pathway. Indeed, cell based assays showed that inhibition of γ-secretase completely blocked NICD formation (Lewis, Perez Revuelta et al. 2003). It was also shown that treatment of zebrafish embryos with a γ-secretase inhibitor affected embryonic development in a manner indistinguishable from deficiencies in Notch signalling (Geling, Steiner et al. 2002). In addition, long term treatment of an AD mouse model with a potent inhibitor of γ-secretase activity led to severe effects including degeneration of the thymus, altered B-cell maturation and drastically altered tissue

morphology in the intestines (Wong, Manfra et al. 2004).The observed side effects in animal models seem to disqualify these compounds for treatment of patients. Nonetheless, the development of γ-secretase inhibitors continues and compounds that can distinguish between inhibition of APP-cleavage and inhibition of Notch-cleavage are being developed, but none have entered the clinic so far (Netzer, Dou et al. 2003; Fraering, Ye et al. 2005). One pan-γ-secretase inhibitor that has recently completed a phase II clinical study is LY-450139. The patients received 100 mg/day or 140 mg/day, and Aβ40 levels in plasma and cerebrospinal fluid (CSF) were recorded. Aβ40 reduction in plasma was significant, but in CSF only marginal, non-significant reductions of Aβ40 were observed. However, some of the patients dropped out after occurrence of side-effects such as diarrhea and elevations in white blood cell counts (Fleisher, Raman et al. 2007; Siemers, Dean et al. 2007). A phase III trial is planned but has not yet started.

1.5 γ-secretase modulation

The main disease causing agent in AD seems to be Aβ42. Aβ42 is the peptide initially deposited in AD brain (Iwatsubo, Odaka et al. 1994; Golde, Eckman et al. 2000), it aggregates faster than Aβ40, and it was shown to be toxic in cell culture (Yankner, Dawes et al. 1989; Yankner, Duffy et al. 1990). Moreover, transgenic mice expressing Aβ42 alone in the absence of APP develop a robust amyloid pathology, while mice expressing Aβ40 alone do not develop overt amyloid pathology (McGowan, Pickford et al. 2005). Taken together with the problematic toxicity profile of γ-secretase inhibitors, these results argue that modulation of γ-secretase leading to reduced Aβ42 production without affecting AICD or NICD formation could be an equally effective but safer approach for AD therapy.

In 2001 three non-steroidal anti-inflammatory drugs (NSAIDs) with specific Aβ42-lowering activity were first identified, ibuprofen, sulindac sulfide and indomethacin (Weggen, Eriksen et al. 2001). For all three compounds a 70 – 80 % reduction in Aβ42 with a concomitant increase in Aβ38 levels was observed, without significant effects on Aβ40 levels (Fig. 1.5.1). This inverse correlation between the generation of Aβ42 and Aβ38 peptides has led to the initial idea that the production of these two peptide species might be related. A report in 2005 demonstrated that some NSAIDs and related compounds such as celcoxib and fenofibrate can act as inverse modulators of γ-secretase activity and increase Aβ42 levels while concomitantly decreasing Aβ38 (Kukar, Murphy et al. 2005). Furthermore, similar results were obtained with some γ-secretase inhibitors when used at subinhibitory concentrations they increased Aβ42 production while decreasing Aβ38 (Zhao, Tan et al. 2007). These observations clearly demonstrate that γ-secretase can be modulated to generate less and to generate more Aβ42. In addition, they point to a coordinated production of Aβ42 and Aβ38

and a possible product-precursor relationship. Since the initial report that some NSAIDs can specifically lower Aβ42-production, several groups have confirmed these findings (Morihara, Chu et al. 2002; Takahashi, Hayashi et al. 2003; Yan, Zhang et al. 2003; Zhou, Su et al. 2003; Peretto, Radaelli et al. 2005).

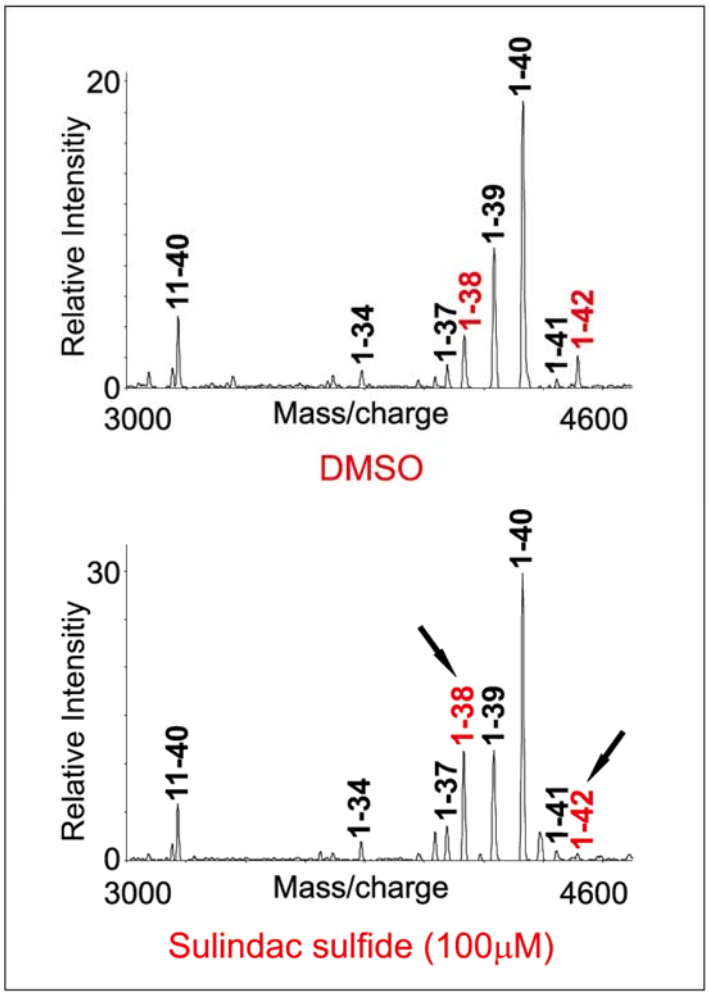

Fig. 1.5.1 Mass spectrometry analyis of Aβ peptides after treatment with the GSM sulindac sulfide. APP CHO cells were treated with 100 μM sulindac sulfide and Aβ peptides were immunoprecipitated from conditioned media. Peptides were then analyzed by matrix-assisted laser desorption/ionization time of flight (MALDI-TOF). Sulindac sulfide treatment (lower panel) causes a decrease in Aβ42 peptides and a concomitant increase in Aβ38 as compared to vehicle treated control (upper panel) (from (Weggen, Eriksen et al. 2001)).

NSAIDs have long been suspected to have beneficial effects in AD. Initial evidence came from epidemiological studies showing that prolonged use of NSAIDs lowered the risk of developing AD (McGeer, McGeer et al. 1990; Launer 2003). The most convincing of these epidemiological studies is the “Rotterdam study”, a prospective, population-based cohort study of almost 7000 patients. This report is especially informative since the NSAID use of every subject was documented in computerized pharmacy records, eliminating recall bias and reducing the chance for misclassification of drug exposure. The study showed an 80 % risk reduction associated with NSAID use for more than 2 years, and further did not find any risk reduction for vascular dementia suggesting specificity for AD (in t' Veld, Ruitenberg et al. 2001). Until the discovery that some NSAIDs are also able to target Aβ42 production, the

reduced risk for AD associated with prolonged NSAID use was mainly attributed to the anti-inflammatory properties of these compounds. The main pharmacological targets of NSAIDs are the cyclooxygenases (COX), COX-1 and COX-2, which play an important role in the synthesis of inflammatory prostaglandins. While COX-1 is constitutively expressed in most tissues and generates proinflammatory as well as protective prostanoids that are critical for the maintenance of the gastric mucosa, COX-2 expression is generally inducible. COX-2 expression is typically upregulated at sites of inflammation, although there is detectable basal expression in neurons (Simmons, Botting et al. 2004; Warner and Mitchell 2004). Both isoforms are inhibited to varying degrees by NSAIDs in the nanomolar to low micromolar range. Clinically useful NSAIDs comprise drugs with preference for COX-1 like flurbiprofen, indomethacin and aspirin, drugs with little selectivity like sulindac sulfide, naproxen and ibuprofen, and newer COX-2 specific inhibitors like celecoxib and rofecoxib (Warner and Mitchell 2004). Other COX independent targets of NSAIDs include the peroxisome proliferator-activated receptors (PPARs). PPARs belong to a family of ligand-activated receptors that activate or trans-repress target genes involved in lipid and glucose metabolism and adipocyte differentiation (Lehrke and Lazar 2005). PPARγ activation has been shown to inhibit expression of pro-inflammatory genes such as inducible nitric oxide synthase (iNOS) and several cytokines (Jiang, Ting et al. 1998). Some NSAIDs including indomethacin, ibuprofen, and naproxen also function as PPARγ agonists indicating that the anti-inflammatory properties of these compounds are not only mediated through inhibition of COX.

The initial report about Aβ42-lowering NSAIDs by Weggen et al. also demonstrated that these compounds had no effect on other APP cleavage events besides Aβ generation, and that they did not affect production of the Notch intracellular domain (Weggen, Eriksen et al. 2001). Therefore, in contrast to γ-secretase inhibitors, no effects on Notch signalling would be expected. By utilizing double knock-out cells for COX-1 and COX-2 it was also shown that NSAIDs exert their Aβ42-lowering activity independent of COX inhibition (Weggen, Eriksen et al. 2001). Later, it was reported that purified enantiomers of ibuprofen and flurbiprofen that lack COX inhibitory activity are still able to reduce Aβ42 production providing additional support for a COX-independent mechanism (Morihara, Chu et al. 2002; Eriksen, Sagi et al. 2003). NSAIDs also affect various other molecular pathways including nuclear factor κB activation, lipoxygenases, Rho GTPases, and PPAR signalling (Lehmann, Lenhard et al. 1997; He, Chan et al. 1999; Baron and Sandler 2000; Zhou, Su et al. 2003) and any of these pathways could potentially lower Aβ42 levels. However subsequent studies have failed to show that these pathways decrease Aβ42 production (Sagi, Weggen et al. 2003; Sastre, Dewachter et al. 2003; Sung, Yang et al. 2004; Kukar, Murphy et al. 2005; Leuchtenberger, Beher et al. 2006; Leuchtenberger, Kummer et al. 2006). In contrast, accumulating evidence

indicates that NSAIDs exert their Aβ42-lowering function through direct modulation of γ-secretase activity. The strongest support for this hypothesis is drawn from the finding that NSAIDs are able to lower Aβ42 and concomitantly increase Aβ38 in cell free γ-secretase assays, which exclude involvement of protein trafficking events and many intracellular signalling pathways (Eriksen, Sagi et al. 2003; Takahashi, Hayashi et al. 2003; Weggen, Eriksen et al. 2003; Beher 2004). More indirect evidence for direct modulation of γ-secretase activity is drawn from the observation that certain FAD associated PS1 mutations are able to alter the cellular response to Aβ42-lowering NSAIDs (Weggen, Eriksen et al. 2003). The FAD associated mutation PS1-M146L was shown to enhance the Aβ42-lowering activity of NSAIDs meaning that a larger reduction in Aβ42 levels was achieved in cells expressing mutant PS1 as compared to cells expressing PS1-WT at identical NSAID concentrations. In stark contrast, the PS1-ΔExon9 mutation strongly attenuated the Aβ42 response and rendered cells almost completely non-responsive to treatment with Aβ42-lowering NSAIDs. These results demonstrate that mutations in PS1 can modulate the cellular response to Aβ42-lowering NSAIDs in both directions, to a stronger and to a lesser effect. Finally, studies using fluorescence lifetime imaging (FLIM) have shown that Aβ42-lowering NSAIDs alter the proximity between PS1 and its substrate APP, and change PS1 conformation. In these FLIM studies, the PS1-NTF and the PS1-CTF were labelled with different fluorophores. When these fluorophores came into close proximity, fluorescence resonance energy transfer occured (FRET) and the lifetime of the fluorescence was reduced. The authors showed that treatment of cells with the Aβ42-lowering NSAID ibuprofen resulted in an enhanced lifetime of fluorescence whereas treatment with naproxen, an NSAID without Aβ42-lowering activity, did not change the fluorescence lifetime (Lleo, Berezovska et al. 2004). These results suggest an allosteric mechanism for γ-secretase modulation. However, the binding partner of Aβ42-lowering NSAIDs within the γ-secretase complex is still unknown.

In conclusion, NSAIDs are the founding members of a new class of γ-secretase modulators (GSMs) that specifically target Aβ42 production (Czirr and Weggen 2006). These GSMs have the crucials advantage over classical pan-γ-secretase inhibitors that they do not affect the formation of intracellular signalling domains of γ-secretase substrates and consequently do not perturb Notch signalling (Weggen, Eriksen et al. 2001; Takahashi, Hayashi et al. 2003; Weggen, Eriksen et al. 2003; Beher, Clarke et al. 2004; Gasparini, Rusconi et al. 2004). Still, Aβ42-lowering NSAIDs such as ibuprofen or sulindac sulfide are not the new AD drugs from old. Pharmacological treatment of primarily elderly patients for a prolonged period of time requires compounds with a very benign toxicity profile, but NSAID doses needed to decrease Aβ42 levels in cell culture as well as in brain of AD mouse models are higher than the approved doses for treatment of other diseases. Accordingly, side-effects associated with long-term NSAID dosing in humans including gastrointestinal bleedings constrain the clinical

use especially in elderly patients. Most importantly, clinical studies with several classical NSAIDs have also generally failed to prevent cognitive decline in AD patients (Weggen, Czirr et al. 2007). Therefore, instead of treating patients with current NSAIDs the focus has shifted to the development of GSMs that lack COX activity and, as a result, would be expected to have fewer side-effects. One compound, the *R*-enantiomer of flurbiprofen (Flurizan™, MPC-7869) has already entered phase III clinical trials. A completed phase-II trial in 207 subjects with mild to moderate AD reported that mild subjects that had received the highest dose of 800 mg twice-daily showed statistically significant benefits in their ability to perform activities of daily living and positive trends towards stabilization of cognitive functions. The drug was well tolerated even up to the highest dose of 800 mg twice a day. However, efficacy of *R*-flurbiprofen to lower Aβ42 levels in plasma or CSF of patients was not reported in this trial. Results from the ongoing phase-III trial are expected by mid-2008.

Only few improved GSMs with markedly reduced IC50 for Aβ42 reduction have been reported so far. Peretto et al. published improved analogues of flurbiprofen with increased potency against Aβ42 and reduced COX activity (Peretto, Radaelli et al. 2005). Very recently a highly potent NSAID derivative, GSM-1, was published and shown to strongly reduce Aβ42 levels in brains of an AD mouse model (Page, Baumann et al. 2007). Mice were treated with a single dose of GSM-1 and Aβ levels in brain homogenates were quantified 4 h post-administration. The authors showed a dose-dependent decrease in Aβ42 levels with approximately 50 % Aβ42 reduction after administration of 10 mg/kg of GSM-1 with no effects on Aβ40 levels.

1.6 Objectives

Accumulating evidence indicates that γ-secretase modulators (GSMs) exert their Aβ42-lowering activity by direct modulation of γ-secretase. The binding site of GSMs in the γ-secretase complex has not been identified, but current results implicate the presenilin (PS) proteins, which harbour the active center of γ-secretase, as possible binding partners. Support for this hypothesis is drawn from the observation that some FAD-associated PS1 mutations modulate the cellular response to GSMs and also to γ-secretase inhibitors, which are known to directly interact with PS1. A particularly interesting mutation is PS1-ΔExon9, a complex deletion mutant that blocks endoproteolysis of PS1 and renders cells completely non-responsive to GSMs. However, the molecular basis for this insensitivity of PS1-ΔExon9 to GSMs is not known. Accordingly, we wanted to investigate the following question:

(1) What causes the diminished response of the PS1-ΔExon9 mutation to GSMs? Does the deleted region (Δ291-319) contain the proposed binding site of GSMs within the γ-secretase complex?

(2) Is the insensitivity of the Ps1-ΔExon9 mutation restricted to the GSM sulindac sulfide and the transition-state γ-secretase inhibitor L-685,458, or is this effect common to GSMs and γ-secretase inhibitors and related to their mechanism of action?

(3) Do other FAD-associated PS1 mutations show a similar phenotype?

(4) Animal models of AD often express FAD-associated PS mutations. Are these animal models suitable tools to investigate the in vivo effect of compounds that target the γ-secretase complex such as GSMs and γ-secretase inhibitors?

(5) GSMs concomitantly increase Ab38 production indicating closely coordinated generation of Aβ42 and Aβ38. If confirmed, a potential precursor-product relationship between these peptides would support the sequential cleavage model of γ-secretase, which proposes that Aβ peptides are generated by sequential trimming of longer into shorter peptides. With tte PS1-ΔExon9 mutation displaying a diminished Aβ42 response to GSM treatment, is Aβ38 production similarly affected or independently regulated from Aβ42 production?

2 Material

2.1 Mouse strains

Name	Transgene	
Tg2576	Single transgenic mouse model expressing human APP695 with the Swedish mutation (K670N/M671L) under the control of the hamster prion protein promoter.	(Hsiao, Chapman et al. 1996; Hsiao 1998)
APPPS	Double-transgenic mouse model expressing human APP695 with the Swedish mutation and PS1 with the L166P mutation both under the control of the Thy1 minigene promoter.	(Radde, Bolmont et al. 2006)

2.2 Cell lines

APP CHO	Chinese hamster ovary cells with stable overexpression of APP751.	(Weggen, Eriksen et al. 2003)
APP CHO PS1-WT	APP CHO cells with stable overexpression of wild-type PS1.	(Weggen, Eriksen et al. 2003)
APP CHO PS1-ΔExon9	APP CHO cells with stable overexpression of PS1-ΔExon9.	(Weggen, Eriksen et al. 2003)
APP CHO PS1-Δ291-319	APP CHO cells with stable overexpression of PS1-Δ291-319.	
APP CHO PS1-M292D	APP CHO cells with stable overexpression of PS1-M292D.	
APP CHO PS1-S290C	APP CHO cells with stable overexpression of PS1-S290C.	
APP CHO PS1-S290C/M292D	APP CHO cells with stable overexpression of PS1-S290C/M292D.	
APP CHO PS1-M292D/M146L	APP CHO cells with stable overexpression of PS1-M292D/M146L.	
APP CHO PS1-P117L	APP CHO cells with stable	

	overexpression of PS1-P117L.	
APP CHO PS1-L166P	APP CHO cells with stable overexpression of PS1-L166P.	
APP CHO PS1-G384A	APP CHO cells with stable overexpression of PS1-G384A.	
GP2-293	HEK293 based cell line with stable expression of the viral gag and pol proteins.	(Emi, Friedmann et al. 1991; Burns, Friedmann et al. 1993)

2.3 Bacterial strains

Strain	**Genotype**
DH5α	F^- Φ80*lac*ZΔM15 Δ(*lac*ZYA-*arg*F)U169*rec*A1 *end* A1 *hsd*R17(r_K^-, m_K^+) *pho*A *sup*E44 *thi*-1 *gyr* A96 *rel*A1λ^-
XL1-Blue supercompetent cells	recA endA1 gyrA96 thi-1 hsdR17 supE44 relA1 lac [F^- proAB $lacI^qZ\Delta M15$ Tn10(Tet^R)]

2.4 Plasmids and Primer

2.4.1 Plasmids

Name	
pLPCX	*Clontech*
pVSVG	*Clontech*
pLPCX PS1-WT	Kind gift of E. Koo
pLPCX PS1-ΔExon9	Kind gift of D. Kang
pLPCX PS1-Δ291-319	
pLPCX PS1-M292D	
pLPCX PS1-S290C	
pLPCX PS1-S290C/M292D	
pLPCX PS1-M292D/M146L	
pLPCX PS1-P117L	
pLPCX PS1-L166P	

pLPCX PS1-G384A	

2.4.2 Primer

Name	Sequence
PS1 seq for	GCT GAC ATT GAA ATA TGG CG
PS1 seq rev	TGA TGG AAT GCT AAT TGG TCC
pLNCX seq for	AGC TCG TTT AGT GAA CCG TCA GAT C
pLNCX seq rev	ACC TAC AGG TGG GGT CTT TCA TTC CC
PS1 NotI for	TTT TGC GGC CGC CTA GAT ATA AAA TTG ATG GAA TGC
PS1 XhoI rev	TTT TCT CGA GAT GAC AGA GTT ACC TGC ACC
PS1 S290C in M292D for	CTC ATT TAC TCC TGT ACA GAC GTG TGG
PS1 S290C in M292D rev	CCA CAC GTC TGT ACA GGA GTA AAT GAG
PS1 S290C for	CTC ATT TAC TCC TGT ACA ATG GTG TGG
PS1 S290C rev	CCA CAC CAT TGT ACA GGA GTA AAT GAG
PS1 C290S in ΔExon9 for	GCT CTC ATT TAC TCC AGC ACA GAA AGG GAG TCA CAA G
PS1 C290S in ΔExon9 rev	CTT GTG ACT CCC TTT CTG TGC TGG AGT AAA TGA GAG C
PS1 G384A for	GAG TAA AAC TTG GAT TGG CAG ATT TCA TTT TCT ACA GTG TTC TGG
PS1 G384A rev	CCA GAA CAC TGT AGA AAA TGA AAT CTG CCA ATC CAA ATC CAA GTT TTA CTC
PS1 P117L for	GGC AGC TAA TCT ATA CCC TAT TCA CAG AAG ATA CCC A
PS1 P117L rev	TCG GTA TCT TCT GTG AAT AGG GTA TAG ATT AGC TGC C
PS1 G384A for	GGG AGT AAA ACT TGG ATT GGC AGA TTT CAT TTT CTA CAG TGT T
PS1 G384A rev	AAC ACT GTA GAA AAT GAA ATC TGC CAA TCC AAG TTT TAC TCC C
PS1 M146L for	CAG TGT CAT TGT TGT CTT GAC TAT CCT CCT GGT GG
PS1 M146L rev	CCA CCA GGA GGA TAG TCA AGA CAA CAA TGA CAC TG

PS1 L166P for	GTC ATC CAT GCC TGG CCT ATT ATA TCA TCT CTA TTG TTG C
PS1 L166P rev	GCA ACA ATA GAG ATG ATA TAA TAG GCC AGG CAT GGA TGA C
PS1 M292D for	CCT CAA CAG ACG TGT GGT TG
PS1 M292D rev	CAA CCA CAC GTC TGT TGA GG

2.5 Antibodies

2.5.1 Primary antibodies

Name	**Antigen**	**Species**	**Type**	
26D6	Human Aβ	mouse	monoclonal	(Lu, Rabizadeh et al. 2000)
CT152Z	C-terminal 15 aa of human APP	rabbit	polyclonal	(Sisodia, Koo et al. 1993)
PSN2	N-terminus of human PS1	mouse	monoclonal	(Okochi, Ishii et al. 1997)
BAP-24	Human Aβ40	mouse	monoclonal	(Brockhaus, Grunberg et al. 1998)
BAP-15	Human Aβ42	mouse	monoclonal	
BAP-29	Human Aβ38	mouse	monoclonal	
6E10	Human Aβ	mouse	monoclonal	*Signet laboratories*
IC16	Human Aβ	mouse	monoclonal	unpublished
Ab9	Human Aβ	Mouse	monoclonal	(Das, Howard et al. 2003)

2.5.2 Secondary antibodies

Antigen	**Conjugate**	**Species**	
Biotin	HRP		*New England Biolabs*
Mouse IgG	HRP	Goat	*Sigma*
Mouse IgG	Biotin	Goat	*Linaris*
Rabbit IgG	HRP	Donkey	*Jackson ImmunoResearch lab. Inc.*

2.6 Reagents

2.6.1 Chemicals

1-Step Ultra TMB ELISA	Pierce, Bonn
30 % Acrylamide 37.5 :1, Bis-Acrylamide	National Diagnostics, USA
Acetonitrile	Sigma, Deisenhofen
Acrylamide, 99.9 %	Biorad, Munich
Agar	Roth, Karlsruhe
Ammoniumpersulfate (APS)	Sigma, Deisenhofen
BIS	Biorad, Munich
BisTris	Calbiochem, Darmstadt
Boric acid	Sigma, Deisenhofen
Bromphenolblue	Roth, Karlsruhe
BSA	Sigma, Deisenhofen
Coomassie brilliant blue	Sigma, Deisenhofen
Desoxynucleotide-tri-phosphate (dNTP)	New England Biolabs
Dimethylsulfoxide (DMSO)	Sigma-Aldrich, Steinheim
Dithiothreiotol (DTT)	Sigma, Deisenhofen
DMEM	Invitrogen, Karlsruhe
Dry-milk (fat-free)	VONS, USA
Ethanol	Roth, Karlsruhe
Ethidiumbromide	Sigma, Deisenhofen
Ethylendiaminetetraacetic acid (EDTA)	Roth, Karlsruhe
Fetal Calf Serum (FCS)	Invitrogen, Karlsruhe
GeneJuice Transfection Reagent	Merck, Darmstadt
Glacial Acetic Acid	Merck, Darmstadt
Glycerine	Roth, Karlsruhe
Hydrochloric acid (HCl)	Sigma, Deisenhofen
Igepal (NP40)	Sigma, Deisenhofen
Immobilion™ Western HRP Substrate Luminol Reagent	Millipore, USA
Immobilion™ Western HRP Substrate Peroxidase	Millipore, USA
Isopropanol	Roth, Karlsruhe
Magnesium-chloride ($MgCl_2$)	Roth, Karlsruhe
Methanol	Roth, Karlsruhe
methanol:acetonitrile:water (36%:56%:8%)	Agilent, Santa Clara, USA
Nitrocellulose transfer membrane	Hartenstein, Würzburg

Non-essential amino acids	Invitrogen, Karlsruhe
Opti-MEM	Invitrogen, Karlsruhe
Ponceau S	Sigma, Deisenhofen
Potassium chloride (KCl)	Sigma, Deisenhofen
Potassium di-hydrogen phosphate (KH_2PO_4)	Roth, Karlsruhe
Protease inhibitor cocktail tablets, EDTA-free	Roche, Mannheim
Seakem LE Agarose	Cambrex, USA
Sodium azide (NaN_3)	Merck, Darmstadt
Sodium chloride (NaCl)	Roth, Karlsruhe
Sodium di-hydrogen phosphate (NaH_2PO_4)	Merck, Darmstadt
Sodium dodecyl sulfate (SDS)	BioRad, Munich
Sodium hydroxide (NaOH)	Merck, Darmstadt
Sodium pyruvate	Invitrogen, Karlsruhe
Streptavidin-HRP conjugate	Amersham, Munich
Sulfuric acid	Merck, Darmstadt
TEMED (N,N,N+,N+-Tetramethylendiamine)	BioRad, Munich
Trifluoracetic acid	Sigma, Deisenhofen
Tris hydrochloride (HCL)	Roth, Karlsruhe
Tris-Base	Roth, Karlsruhe
Trypsin/EDTA	Invitrogen, Karlsruhe
Tryptone	Roth, Karlsruhe
Tween-20	Roth, Karlsruhe
Urea	Merck, Darmstadt
Yeast Extract	Roth, Karlsruhe
α-cyano-4-hydroxycinnamic acid	Sigma, Deisenhofen

2.6.2 Antibiotics

Ampicillin	Sigma, Deisenhofen
G418	Sigma, Deisenhofen
Penicillin/Streptomycin	Invitrogen, Karlsruhe
Puromycin	Merck, Darmstadt

2.6.3 γ-secretase modulators and inhibitors

DAPT	Merck, Darmstadt
GSM-1	Roche, Basel
Ibuprofen	Biomol GmbH, Hamburg
Indomethancine	Biomol GmbH, Hamburg
L-685,458	Sigma, Deisenhofen
LY-411575	Eli Lilly, USA
Sulindac sulfide	Alexis Biochemicals, Lausen

2.6.4 Size standards

Biotinylated protein ladder	New England Biolabs, Ipswich
2-log DNA ladder	New England Biolabs, Ipswich

2.6.5 Enzymes

2.6.5.1 General enzymes

Name	**Buffer**	
Antarctic Phosphatase	10 x Antarctic phosphatase buffer	New England Biolabs
PfuUltra High-fidelity DNA polymerase	10 x Reaction buffer	Stratagene
Phusion high-fidelity DNA polymerase	5 x Phusion HF buffer	Finnzymes
T4 DNA ligase	10 x Ligase buffer	New England Biolabs
Taq DNA polymerase	10 x Taq polymerase buffer	New England Biolabs

2.6.5.2 Restriction endonucleases

Name	**Buffer**	
DpnI	10 x Reaction buffer	Stratagene
NotI	NEB3 + BSA	New England Biolabs
XhoI	NEB2 + BSA	New England Biolabs

2.6.6 Kits

BCA Protein Assay Kit	Pierce, Bonn
EZ-link Plus Activated Peroxidase and Kit	Pierce, Bonn
JetStar Plasmid Maxi-Prep Kit	Genomed, Bad
NucleoSpin Plasmid Kit	Macherey-Nagel Oeyenhausen
QIAquick Gel Extraction Kit	Qiagen, Hilden
QuikChange II Site-Directed Mutagenesis Kit	Stratagene
Slide-A-Lyzer Dialysis Kit	Pierce, Bonn

2.7 Laboratory hardware and appliances

Centrifuges	Eppendorf, Hamburg Hettich, Tuttingen
Cryo Freezing Container	Nunc, Wiesbaden
Flat bed shaker	Infors, Bolmingen, Schweiz
Fluorescence microscope	Olympus, Japan
Freezers and fridges	-80°C Heraeus -20°C Liebherr
Gene Ray UV-Photometer	Biometra, Göttingen
Glassware	Schott, Mainz
Heating block	Grant, Berlin
Incubator	Binder, Tuttlingen
Laminar flow	Nunc, Wiesbaden
Light-optical microscope	Wilovert, Wetzlar
Magnetic stirrer	Heidolph, Kehlheim
Microwave	Media Markt
4800 MALDI-TOF-TOF	Applied Biosystems, USA
M-series M8 Analyzer	Bioveris, USA
Multiscan RC Thermo	Labsystems, Finnland
Pasteur pipettes	Roth, Karlsruhe
pH meter	inoLab, Weinheim
Pipettes 0.2 µl – 1 ml	Gilson, USA
Pipettor AccuJet	VWR, Darmstadt
RunOne Electrophoresis Cell System	EmbiTec, San Diego

Scales	Sartorius, Göttingen
Semi-dry blotter	Hoefer, USA
Spectrophotometer	Beckmann, Krefeld
T3 Thermocycler	Biometra, Göttingen
Tank Blotter	CBS Scientific, USA
Waterbath	Julabo, Seelbach
X-ray film developer	FUJI Photo, Japan

2.8 Consumables

0.2 ml reaction tubes	Eppendorf, Hamburg
1.5 ml reaction tubes	Eppendorf, Hamburg
10 cm Petri dishes (bacteria)	Sarstedt, Nümbrecht
10 cm Petri dishes (cell culture)	Nunc, Wiesbaden
12-well plates	Nunc, Wiesbaden
15 ml tubes	Sarstedt, Nümbrecht
2 ml reaction tubes	Eppendorf, Hamburg
48-well plates	Nunc, Wiesbaden
50 ml tubes	Sarstedt, Nümbrecht
6-well plates	Nunc, Wiesbaden
Aluminium-foil	Aro, Metro
Cell Scraper	TPP, Schweiz
Cryotubes	Nunc, Wiesbaden
Disposable gloves	Semperit, Wien
High performance chemiluminescence film	Amersham Biosciences,UK
Immobilion-P Transfer Membrane	Millipore, USA
Microtiter plates, 96-well	Nunc, Wiesbaden
Microtiterplates, high binding, Corning	Sigma, Deisenhofen
PE-foil	BioRad, Munich
Pipet tips	Starlab, Ahrensburg
Pipettes (5 ml – 25 ml)	Sarstedt, Nümbrecht
Whatman paper	Whatman, Dassel

2.9 Software

Adobe Design Standard CS3

ApE

Fuji Imaging Software

Microsoft Office 2003

Prism GraphPad 5.0

SE Central

3 Methods

3.1 Treatment of mice with γ-secretase inhibitors

Treatment of transgenic mice with γ-secretase inhibitor and quantification of Aβ levels in brain was done in collaboration with Dr. Dorner-Ciossek and Sandra Fleißner at Boehringer Ingelheim.

Five month old Tg2576 mice or 2 months old APPPS mice were orally dosed with 15 mg/kg of the γ-secretase inhibitor LY-411575 dissolved in 0.5 % tylose or vehicle alone. The mice were sacrificed 3 h post-administration and brains were homogenized in Tris buffer containing 0.2% Triton X-100. After centrifugation for 1 h at 200000 x g, soluble Aβ42 levels in the supernatant were quantified by sandwich ELISA using commercial kits from Biosource according to the manufacturer's protocol. For ELISA determination of the soluble Aβ40 levels, monoclonal antibody 6E10 was employed as capture antibody and combined with alkaline phosphatase-coupled Aβ40 specific detection antibody. All animal studies were performed according to the German animal welfare law.

3.2 Tissue Culture

Routine cell culture was performed under sterile working conditions in S1 or S2 qualified laboratories. Cell culture glassware was kept separately which included separate washing and autoclaving. Pipettes, dishes, plates, filter tips, 15 ml, 50 ml, and 1.5 ml tubes, syringes and sterile filters were single-use plastic items and cell culture qualified. All solutions and media were stored at 4°C unless otherwise indicated by the manufacturer. Media were pre-warmed before use in a 37°C waterbath. Cell growth and morphology was checked on a daily basis and mycoplasm tests performed semi-annually.

Cell culture media

DMEM complete:	DMEM (+ 4.5 g/l glucose, + L-glutamine, - Pyruvate) 10 % FCS 1 % Penicillin/Streptomycin (10000 U/ml Penicillin/10000 µg/ml Streptomycin) 1 mM Na-Pyruvate
α-MEM complete:	α-MEM

	10 % FCS 1 % Penicillin/Streptomycin (10000 U/ml Penicillin/10000 µg/ml Streptomycin) 1 mM Na-Pyruvate 2 mM L-Glutamine
CHO APP cells:	α-MEM complete 200 µg/ml G418
CHO APP cells + PS1:	α-MEM complete 200 µg/ml G418 2 µg/ml Puromycin
GP2 293 cells:	DMEM complete

3.1.1 Passaging of adherent cell lines

In general, adherent cell lines such as CHO or HEK293 cells were cultured in 10 cm cell culture dishes. If cells were cultured in smaller or larger vessels the volumes were adjusted accordingly.

- Remove cell culture medium from dish.
- Add 5 ml 1 x PBS (Gibco, Invitrogen), sway dish, and remove buffer.
- Add 1 ml 1 x trypsin/EDTA (Gibco/Invitrogen) and sway dish, incubate for 1 min to 5 min at RT.
- Add 10 ml of the appropriate culture medium containing FCS and pipet up and down to achieve a single cell suspension.
- Transfer cell suspension into a 15 ml tube and centrifuge for 4 min at 1000 x g.
- Remove supernatant and resuspend cell pellet in 10 ml medium.
- Add 10 ml cell culture medium into a new 10 cm culture dish and add 1 ml of the cell suspension.

3.1.2 Cryopreservation of cells

For long-term storage and preservation cell lines were frozen and stored in liquid nitrogen.

- Trypsinize cells and resuspend in 10 ml fresh media.
- Spin down at 1000 x g for 4 min.
- Resuspend pellet in freezing media (90% FCS/10% DMSO), 1 ml per 10 cm dish.
- Transfer cell suspension in 1 ml screw cap cryo-vials and place on ice. Incubate for 10 min.
- Transfer vial to freezing container and place at -80°C over night.
- Place vial in liquid nitrogen tank for long-term storage.

3.1.3 Thawing of frozen cell stocks

- Prepare 15 ml tube with pre-warmed culture medium.
- Place cryo-vial in 37 °C water bath and thaw cells.
- Transfer cells into the 15 ml tube and spin down at 1000 x g for 4 min.
- Remove supernatant and resuspend cells in culture medium.
- Transfer cells onto a 10 cm dish and place in incubator.

3.1.4 Compound treatment

To evaluate the effects of compounds on a cellular basis, cells were treated for 24 h with the respective drugs and vehicle control and supernatants and lysates were collected. Treatment was performed in media lacking selection antibiotics and in half of the regular culture volume to achieve a higher concentration of secreted proteins.

Day 1:

- Remove cell culture medium from cells.
- Add 5 ml 1 x PBS (Gibco, Invitrogen), sway dish, and remove buffer.
- Add 1 ml 1 x trypsin/EDTA (Gibco/Invitrogen) and sway dish, incubate for 1 min to 5 min at RT.
- Add 10 ml of the appropriate culture medium containing FCS and pipet up and down to achieve a single cell suspension.
- Transfer cell suspension into a 50 ml tube and centrifuge for 4 min at 1000 x g.
- Remove supernatant and resuspend cell pellet in 30 ml medium without selection antibiotics (e.g. G418, Puromycin, etc.).
- Count cells in Neubauer chamber.

- Seed 300000 cells/well on a 12-well plate.
- Carefully sway plate to achieve even distribution of cells.
- Place plate in incubator over night.

Day 2:

- Dilute compounds and vehicle control in pre-warmed culture medium without selection antibiotics.
- Remove medium from cells, but not from more than 2 wells at a time.
- Add 500 µl medium with vehicle or compound per well.

Day 3:

- Collect supernatants and lysates if necessary.

3.1.5 Generation of retroviral particles

When working with retroviral particles, adhere to biosafety level 2 (S2) rules, these include (but are not limited to):

- Work only in S2 qualified rooms and at S2 qualified cell culture benches.
- Wear lab-coat at all times.
- Double-glove with nitril gloves.
- Wear arm protection.
- Keep disinfectant ready at hand.
- Use plastic pipettes and filtered pipette tips; no glassware!
- Inactivate liquid waste by incubation with 70% ethanol or disinfectant before autoclaving.
- Double-bag solid waste and autoclave on a regular basis.

Day 1:

- Coat 10 cm dishes with poly-L-lysine (5 µg/ml in 1 x PBS; sterile filtered) for 1 h at RT and wash once with 1 x PBS.
- Split a confluent plate of GP2-293 cells 1:4 on the lysine coated dishes, if the original plate is completely overgrown split 1:5.

Day 2:

- Cell density should be 70 – 80%.
- Prepare transfection mixture for each plate:
    - Add 800 µl Optimem (Invitrogen) to a sterile 1.5 ml tube.

- Add 45 µl Gene Juice and incubate for 5 min at RT.
- Add 7.5 µg retroviral shuttle plasmid (e.g. pLPCX, pLHCX, etc.) and 7.5 µg pVSVG plasmid to the transfection mixture. The total volume of the DNA should not exceed 100 µl.
- Incubate for 15 – 20 min at RT.
- Carefully change medium on the GP2-293 cells.
- Add the transfection mix in a dropwise manner onto the cells and carefully sway the plate.
- Place in incubator.

Day 4:

- Take off supernatant and inactivate with disinfectant.
- Carefully add 5 ml fresh medium and place cells in incubator.

Day 5:

- Transfer supernatant containing the retroviral particles into a fresh 50 ml tube.
- Discard cells.
- Sterile filter supernatant (0.2 µm filter) to remove cells and debris and make 1 ml aliquots in screw cap tubes.
- Store virus particles at -80°C.

3.1.6 Infection with retroviral particles

To produce cell lines with stable expression of transgenes, cells were infected with retroviral particles and then subjected to selection with the appropriate antibiotic depending on the resistance gene encoded on the plasmid.

Day 1:

- Seed target cells on 6-well plates. Cell density should be adjusted so that cell lines reach confluency about 48 – 72 h later.
  Seed CHO cells at 300000 cells/well on a 6-well plate.

Day 2:

- Add 1 ml fresh medium and 2 µl polybrene stock solution (5 mg/ml) to a 15 ml tube.
- Thaw retroviral particles quickly in a 37°C waterbath.
- Mix 1 ml retroviral particles with the medium and polybrene in the 15 ml tube.
- Remove medium from cells in the 6-well plate and add the retroviral particle mix. Add 2 ml fresh media to another well as control.
- Incubate for 24 h.

Day 3:

- Remove medium and retroviral particles. Wash each well with 1 x PBS and add fresh medium.
- Incubate for 24 h.

Day 4:

- Trypsinize the infected cells and the non-infected control and resuspend in 10 ml medium containing the appropriate concentration of selection antibiotic.
- Plate cells on a 10 cm dish. For CHO cells split cells 1:10.

- Change media every 2 – 3 days and add selection antibiotic until stable cell clones appear. Make sure the control cells are all dead.
- Check expression of transgene by Western Blot analysis.
- Do not remove selection antibiotic until stable clones are frozen for long-term storage.

3.1.7 Killing curve

To evaluate the concentration of selection antibiotic needed to select for transfected cells, cell lines without expression of the transgene were subjected to treatment with different concentrations of the selection antibiotic. The concentration range was dependent on the antibiotic used:

Hygromycin	100 µg/ml to 800 µg/ml
Puromycin	0.5 µg/ml to 6 µg/ml
G418	100 µg/ml to 800 µg/ml
Blasticidine	1 µg/ml to 8 µg/ml

- Seed cells at low density in 6-well plates. For CHO cells use 100000 cells/well.
- After 24 h change medium to medium containing the selection antibiotic and keep 1 well in regular medium.
- Exchange medium every 2 – 3 days and add fresh selection antibiotic.
- Depending on the cell line selection takes 1 – 2 weeks. Check cells regularly and note at which concentration all cells are dead.

For selection of cell lines with transgenes use the concentration at which all cells were dead and in addition one lower concentration at which approximately 80% of all cells were dead or dying. Sometimes selection at lower concentrations yields higher expression levels.

3.1.8 Subcloning of cell lines

If the expression of the transgene in a stable mass culture was not high enough, the mass culture was subjected to subcloning to identify single clones with higher expression. Single clones could then either be used directly or several single clones were pooled.

- Trypsinize mass culture and count cells in a Neubauer chamber.
- Dilute cells in media containing the selection antibiotic to a density of 0.5 cells/100 µl and 1 cell/100 µl.
- Plate cells on 96-well plates, add 100 µl of the dilution per well.
- Observe growth on plate on a regular basis and mark wells with single clones.
- When the single clones have reached confluency in the 96-well, split the whole well into one well of a 24-well plate.
- Expand the single clones and check for expression.
- Keep selection antibiotic on the cells at all times!

3.2 Protein Biochemistry

3.2.1 Harvesting of secreted proteins

To investigate secreted proteins, cell culture supernatants were harvested. Supernatants were stored at -80°C.

- Prepare and label two sets of 1.5 ml tubes for each sample.
- Add 25 x complete protease inhibitor stock solution to one set of tubes. 20 µl per 500 µl of supernatant.
- Place cell culture dish or plate on ice.
- Pipet supernatant into the set of tubes containing the protease inhibitor.
- Spin samples for 3 min at 16000 x g.
- Transfer supernatant to fresh tubes and store at -80°C.

25 x Complete Protease Inhibitor: dissolve one tablet in 2 ml Milli-Q water
(EDTA-free; Roche)

3.2.2 Harvesting of cellular lysates

To investigate intracellular proteins, cells were lysed in NP40-buffer. Lysates were stored at – 20°C.

- Prepare and label two sets of 1.5 ml tubes for all samples.
- Place 1 x PBS on ice.
- Dilute the Complete protease inhibitor stock in NP40 lysis buffer to a final concentration of 1 x.
- Place cell culture dishes or plates on ice.
- Remove supernatant and wash cells once with cold 1 x PBS.
- Add 1 ml 1 x PBS onto the cells and scrape them off the plate.
- Transfer cells into 1.5 ml tube and centrifuge for 3 min at 16000 x g.
- Discard supernatant and add appropriate amount of NP40 lysis-buffer with protease inhibitor.
- Incubate for 20 min on ice and vortex every 5 min.
- Centrifuge for 20 min at 16000 x g.
- Transfer supernatant into fresh tube.
- Store at -20°C.

NP40 Lysis Buffer:	50 mM Tris-HCl, pH 7.8	
	150 mM	NaCl
	1 %	NP40
	Store at 4°C.	
10 x PBS, pH 7.4:	137 mM	NaCl
	2.7 mM	KCl
	10 mM	Na_2HPO_4
	10 mM	KH_2PO_4
	Store at RT.	
25 x Complete Protease Inhibitor: (EDTA-free; Roche)	Dissolve one tablet in 2 ml Milli-Q water. Store at -20°C.	

3.2.3 Bicinchonic acid protein assay (BCA)

To load equal amount of protein on gels or use equal amounts of protein for experiments, the concentration of the samples was determined by a bicinchonic acid (BCA) protein assay. Protein concentrations were measured using the BCA Protein Assay Kit (Pierce) according to the manufacturer's protocol.

- Prepare two sets of 1.5 ml tubes for the protein standard and one set for the samples.
- Pre-heat heating-block to 60 °C.
- Dilute BSA standard (1 mg/ml) for the standard curve:

Final concentration [µg/ml]	Volume NP40 buffer [µl]	Volume BSA standard [µl]
0	100	0
100	90	10
200	80	20
300	70	30
400	60	40
500	50	50
600	40	60

- Transfer 50 µl of each standard mixture into a fresh tube and discard the rest.
- Add 45 µl NP40 buffer into 1.5 ml tubes and add 5 µl samples.
- Mix BCA Reagent A and B in a 50:1 ratio.
- Add 1 ml of BCA reagent mix to each sample and standard.
- Incubate for 30 min at 60 °C.
- Load samples and standard in duplicates onto a clear 96-well microtiterplate.
- Measure OD at 540 nm and calculate sample concentration.

NP40 Lysis Buffer: 50 mM Tris-HCl, pH 7.8
150 mM NaCl
1 % NP40
Store at 4 °C.

BSA and BCA reagents are supplied with the kit.

3.2.4 SDS-Polyacrylamide gelelectrophoresis (SDS-PAGE)

SDS-Polyacrylamide gelelectrophoresis allows the separation of denatured proteins according to their molecular weight. The loading buffer for the proteins contains SDS which results in an overall negative charge of the proteins, therefore their separation is not influenced by any intrinsic charges.

NuPage Novex Gels

- Prepare resolving gel mixture:

	10 %		12 %	
	1 gel	2 gels	1 gel	2 gels
30% Acrylamide 37.5 :1	2.20 ml	4.40 ml	2.64 ml	5.28 ml
1.6 M Bis-Tris, pH 6.4	1.65 ml	3.30 ml	1.65 ml	3.30 ml
MilliQ-water	2.70 ml	5.40 ml	2.26 ml	4.52 ml
10% APS stock solution	33 µl	66 µl	33 µl	66 µl
Temed	11 µl	22 µl	11 µl	22 µl

- Gently mix the resolving gel mixture and fill 3/4 of the Novex gel cassette.
- Carefully overlay the gel mixture with isopropanol and wait until the polymerization is complete (~ 15 – 20 min).
- Pour off the isopropanol and wash the gel surface with MilliQ water. Carefully drain all the water out of the gel cassette and dry the inside with a small piece of Whatman paper. Do not touch the gel surface!

- Prepare the stacking gel mixture:

	4 %	
	1 gel	2 gels
30% Acrylamide 37.5 :1	260 µl	520 µl
1.6 M Bis-Tris buffer	500 µl	1.00 ml
MilliQ-water	1.23 ml	2.46 ml
10% APS stock solution	20 µl	40 µl
Temed	5 µl	10 µl

- Gently mix the stacking gel mixture and pour it onto the gel cassette up to the top.

- Add the comb and wait until the gel is polymerized.
- Gels can be stored at 4 °C if wrapped in wet paper towels and cling wrap or immediately used.
- Remove comb and wash each slot with MilliQ water to remove un-polymerized acrylamide.
- Place gel in running chamber and fill with 1 x MES running buffer.
- Load samples and run gel at 150 V for approximately 45 min.

Bis-Tris gel-buffer:	1.6 M Bis-Tris, pH 6.4 Store at RT.
10 % APS:	10 % Ammoniumpersulfate in MilliQ water Store at -20°C.
20 x MES:	1 M MES 1 M Tris-Base 69.3 mM SDS 20.5 mM EDTA Store at RT.
1 x MES:	1:20 dilution of 20 x stock in MilliQ water
4 x SDS sample buffer:	1.44 M Bis-Tris 0.64 M Bicine 4 % SDS 100 mM DTT 0.05 % Bromphenoleblue Store at -20°C.

3.2.5 Western-Blot

- Soak two pieces of 3 mm Whatman paper and two blotting sponges in 1 x transfer buffer.
- Soak nitrocellulose membrane in 1 x transfer buffer or PVDF membrane in Methanol.
- Build blotting stack:

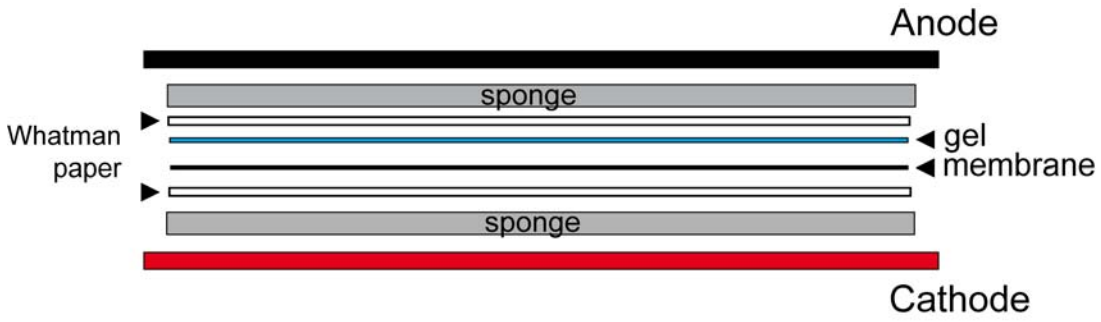

- Fill blotting tank with 1x transfer buffer and place stack in the tank.
- Blot for 2 h at 200 mA or over night at 30 V.

10 x Transfer buffer:	250 mM Tris-Base
	1920 mM Glycin
	Store at RT.

1 x Transfer buffer:	25 mM Tris-Base
	192 mM Glycin
	20 % Methanol

3.2.6 High-resolution urea gelelectrophoresis

All high resolution urea gels were done in collaboration with Dr. Wiltfang and Dr. Esselmann at the Univerity of Erlangen.
This gel system allowed the separation of different Aβ peptide species to a very high resolution. The peptides are not separated according to their size, but depending on their hydrophobicity, therefore the longer peptides run faster than the shorter peptides.

- The gel contains three different gel layers and the height of the different gels has to be marked on the glass plates before the gel solutions are prepared.

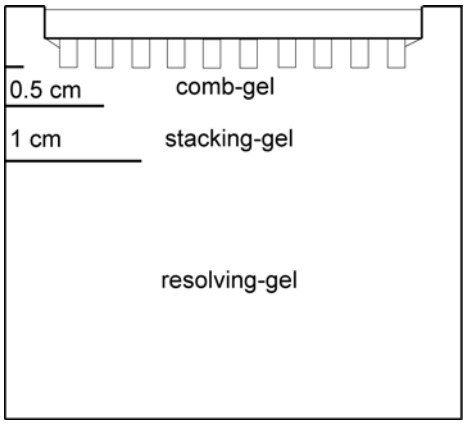

- Prepare resolving gel mixture:

	2 gels
Urea	4.8 g
Resolving gel buffer	2.5 ml
60%/5% acrylamide mix	1.67 ml
10 % SDS	0.25 ml
MilliQ water	1.84 ml
10 % APS	40 µl
Temed	5 µl

- Fill glass plates with resolving gel mixture up to the mark and overlay with isopropanol.
- After polymerization, wash the gel surface with MilliQ water and drain excess water.
- Prepare stacking gel solution:

	4 gels
Stacking gel buffer	2.0 ml
60%/3% acrylamide mix	0.4 ml
10 % SDS	1.0 ml
MilliQ water	0.6 ml
10 % APS	21 µl
Temed	7 µl

- Fill glass plates with stacking gel mixture up to the second mark and overlay with isopropanol.
- After polymerization, wash the gel surface with MilliQ water and drain excess water.
- Prepare comb gel solution:

	4 gels
Comb gel buffer	2.5 ml
60%/3% acrylamide mix	0.4 ml
10 % SDS	1.0 ml
MilliQ water	0.6 ml
10 % APS	24 µl
Temed	8 µl

- Fill the glass plates with comb gel mixture up to the top and add comb.
- Let gel polymerize.
- Place gel in electrophoresis chamber and add Anode and Cathode buffer.
- Mix samples 1:1 with 2 x Sample buffer and boil 5 min at 95 °C.
- Load samples on gel and run at 100 V.
- Prepare blotting paper and PVDF membrane for semi-dry blotting.
    - Cut 4 pieces of 3 mm Whatman paper per gel according to the gel size.
    - Cut 1 PVDF membrane per gel.
    - Fill blotting buffers in dish and let equilibrate to RT.
    - Soak PVDF membrane in Methanol, wash briefly in MilliQ water and place in Blotbuffer B.
    - Place two pieces of paper in Blotting buffer C, one piece in Blotting buffer A, and one piece in Blotting buffer B. Let paper soak for 15 min.
    - Briefly soak gel in Blotting buffer C and build the blotting stack.

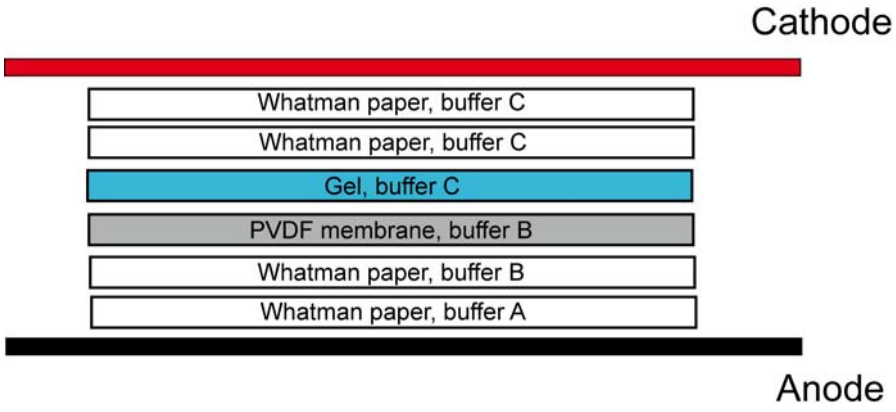

- Apply current. 1 mA per cm2 membrane for 45 min or 30 min with 0.75 mm and 0.5 mm gels, respectively.
- After blotting rinse membrane in MilliQ water and boil in MilliQ water for 5 min.
- Block membrane for 1 h in 5% dry milk in TBS-T at RT.

- Incubate membrane with 6E10 antibody diluted 1:100 in 5 % dry milk in TBS-T over night at 4°C.
- Wash membrane 6 x 10 min with TBS-T.
- Incubate membrane with biotinylated anti-mouse antibody diluted 1:3000 in TBS-T for 1 h at RT.
- Wash membrane 3 x 10 min with TBS-T.
- Incubate membrane with Streptavidin-HRP diluted 1:3000 in TBS-T for 1 h at RT.
- Wash membrane 3 x 10 min with TBS-T.
- Wash membrane 1 x with TBS.
- Develop using enhanced chemiluminescence.

2 x Sample buffer:	0.72 M Bis-Tris 0.32 M Bicine 30 % (w/v) Sucrose 2 % SDS 0.1 % Bromphenolblue
60%/3% Acrylamide mix:	58.2 g Acrylamide 99.9 % 1.8 g BIS 40 ml MilliQ water Stir at RT for 2 h under the fume hood, then add MilliQ water to a final volume of 100 ml. Store in dark at RT.
60%/5% Acrylamide mix:	57 g Acrylamide 99.9 % 3.0 g BIS 40 ml MilliQ water Stir at RT for 2 h under the fume hood, then add MilliQ water to a final volume of 100 ml. Store in dark at RT.
Resolving gel buffer:	1.6 M Tris-base 0.4 M H_2SO_4 pH is self adjusting!
Stacking gel buffer:	0.8 M Bistris 0.2 M H_2SO_4 pH is self adjusting!

Comb gel buffer:	0.72 M Bistris 0.32 M Bicine
Anode buffer:	200 mM Tris-HCl 50 mM H_2SO_4 pH is self adjusting!
Cathode buffer, pH 8.2:	200 mM Bicine 100 mM NaOH 0.25 % SDS
Blotting buffer A:	210 mM Tris-Base, pH 10.4 30 % Methanol
Blotting buffer B:	25 mM Tris-Base, pH 10.4 30 % Methanol
Blotting buffer C:	25 mM Tris-Base 0.025 % SDS pH to 9.0 with 5 M boric acid
10 x TBS, pH 7.4:	1.37 M NaCl 27 mM KCl 0.25 M Tris-Base
1 x TBS:	1:10 dilution of 10 x TBS
1 x TBS-T:	1:10 dilution of 10 x TBS 0.01 % Tween-20

3.2.7 Immunostaining of membranes

- Block membrane in 5% dry-milk/1 x TBS-T, 3% BSA/1 x TBS-T, or 1 x TBS-T alone, for 1 h at RT while shaking. Blocking conditions depend on the antibody used.
- Wash blocking solution of the membrane to avoid contamination of the primary antibody. 3 x 5 min with 1 x TBS-T.

- Dilute primary antibody in 1x TBS-T and add 0.01% NaN_3. Incubate for 2 h at RT or 4°C over night with gentle shaking. Dilution depends on the antibody.
- Wash the membrane at least 3 x 10 min or longer with 1 x TBS-T while shaking.
- Incubate membrane with HRP-coupled secondary antibody for 1 h at RT with gentle shaking. Antibody is diluted in 1 x TBS-T or blocking solution.
- Wash the membrane at least 3 x 10 min or longer with 1 x TBS-T while shaking.
- Wash the membrane once with 1 x TBS.
- Visualize proteins with enhanced chemiluminescence and expose to film or CCD camera.

10 x TBS, pH 7.4:	1.37 M NaCl 27 mM KCl 0.25 M Tris-Base
1 x TBS:	1:10 dilution of 10 x TBS
1 x TBS-T:	1:10 dilution of 10 x TBS 0.01 % Tween-20

3.2.8 PonceauS staining of membranes

- Rinse the membrane in MilliQ water.
- Place membrane in PonceauS solution and incubate for ~ 1 min.
- Transfer membrane into MilliQ water and gently swirl until bands are clearly visible.
- To destain place membrane in 1 x TBS-T.

Ponceau S solution:	0.2 % PonceauS 3 % Glacial acetic acid
10 x TBS pH 7.4:	1.37 M NaCl 27 mM KCl 0.25 M Tris-Base
1 x TBS-T:	137 mM NaCl 2.7 mM KCl 25 mM Tris-Base

0.1 % Tween-20

3.2.9 Coomassie staining

Coomassie brilliant blue is a non-reversible protein stain that was used to detect proteins in acrylamide gels.

- Place gel in Coomassie staining solution and incubate for 2 h or longer with gentle shaking.
- Remove Coomassie solution (do not discard, can be reused multiple times) and rinse gel once with water.
- Add destain solution and incubate at RT while shaking until the background staining is removed and the proteins bands are clearly visible. If necessary renew destain solution multiple times.

Coomassie staining solution:	10 % glacial acetic acid
	25 % isopropanol
	2.5 % coomassie brilliant blue
Destain solution:	10 % glacial acetic acid
	12.5 % isopropanol

3.2.10 HRP-coupling of antibodies

To facilitate the use of the Aβ peptide species specific antibodies in the ELISA assay they were coupled to HRP. For the coupling procedure we used the Pierce EZ-Link™ Plus Activated Peroxidase and Kit. For the dialysis before and after coupling we used the Pierce Slide-A-Lyzer® Dialysis Kit 10000 MWCO.

- Remove dialysis cassette from pouch and immerse in Carbonate buffer for 30 sec.
- Remove access liquid by tapping the cassette on a paper towel.
- Fill the syringe with 1 mg antibody in a volume of 500 µl to 1 ml. If the volume of the antibody is lower adjust by adding Carbonate buffer.
- Insert the syringe in one of the syringe ports and inject the sample.
- Remove excess air from the cassette and place it in the buoy.

- Dialyse the antibody against 1 l of Carbonate buffer over night at 4°C with gentle stirring.
- To remove the sample, fill the syringe with a volume of air equal to the sample size. Insert the needle into a different syringe port than before and introduce the air into the cassette.
- Turn the unit so the needle is at the bottom ad allow sample to collect near the port. Withdraw sample into syringe.
- Inject the sample (volume ~ 500 µl to 1 ml) directly into the HRP vial.
- Incubate 1 h at RT.
- Add 10 µl reductant solution and incubate another 15 min at RT under the fume hood.
- Ass 20 µ Quench buffer and react at RT for an additional 15 min.
- Dialyse against 1 x PBS over night at 4°C.
- For long term storage dilute 1:1 in Pierce SuperFreeze™ peroxidase conjugate stabilizer. Aliquot and store at -20°C. Protein concentration can be measured by BCA. Do not add NaN_3!

Carbonate buffer, pH 9.4:	0.06 M	$NaHCO_3$
	0.14 M	Na_2CO_3
	Autoclave before use. Store at RT.	

1 x PBS, pH 7.2:	13.7 mM	NaCl
	0.27 mM	KCl
	1 mM	Na_2HPO_4
	1 mM	KH_2PO_4

3.2.11 Enzyme-linked immunosorbent assay (ELISA)

Day 1:

- Coat 96-well high binding plates with capture antibody IC16. Dilute antibody 1:250 in 1 x PBS, pH 7.2 and add 100 µl per well.
- Cover plate.
- Incubate over night at 4°C with gentle shaking.

Day 2:

- Dilute synthetic Aβ peptide standard in assay buffer.

Final concentration in 96-well	Volume assay buffer	Synthetic Aβ peptide [10 ng/µl]
3 ng/ml	5 ml	6 µl
1.5 ng/ml	1:1 dilution: 2.5 ml assay buffer + 2.5 ml of previous conc.	
0.75 ng/ml	1:1 dilution: 2.5 ml assay buffer + 2.5 ml of previous conc.	
2 ng/ml	5 ml	4 µl
1 ng/ml	1:1 dilution: 2.5 ml assay buffer + 2.5 ml of previous conc.	
0.5 ng/ml	1:1 dilution: 2.5 ml assay buffer + 2.5 ml of previous conc.	
0.25 ng/ml	1:1 dilution: 2.5 ml assay buffer + 2.5 ml of previous conc.	

- Pour capture antibody off the plate and add 50 µl assay buffer per well.
- Load Aβ standard, 50 µl per well in duplicates.
- Load samples. Amount of sample depends on the respective peptide, cell lines, and experimental setup. In general, load 10 µl cell culture supernatant for Aβ40, 50 µl cell culture supernatant for Aβ42, and 100 µl cell culture supernatant for Aβ38.
- Dilute HRP-coupled detection antibodies in assay buffer:
  Aβ40-HRP 1:1000
  Aβ42-HRP 1:500
  Aβ38-HRP 1:125
- Add 50 µl HRP-coupled detection antibody to each well.
- Adjust the amount of serum in each well and fill up to a total volume of 200 µl.
  Example:

Standard:		Samples:	
50 µl	assay buffer	50 µl	assay buffer
50 µl	Aβ peptide standard	10 µl	sample/cell culture supernatant
50 µl	detection antibody	50 µl	detection antibody
10 µl	fresh cell culture medium	/	
40 µl	assay buffer	90 µl	assay buffer

  The final volume in each well should be 200 µl and all samples should contain the same amount of serum.
- Cover plate and incubate at 4°C over night with gentle shaking.

Day 3:

- Let substrate solution warm to RT.
- Pour samples off plate and wash each well 5 x with 200 µl PBS-T.

- Wash once with 1 x PBS and tap plate on paper towels to remove buffer.
- Add 100 µl TMB ultra substrate solution to each well.
- Incubate for 3 min to 15 min (do not exceed 30 min) in dark.
- Stop reaction by adding 100 µl 2 M H2SO4 per well.
- Read OD at 450 nm.

10 x PBS pH 7.2:	137 mM NaCl 2.7 mM KCl 10 mM Na_2HPO_4 10 mM KH_2PO_4 Store at RT.
1 x PBS pH 7.2:	1:10 dilution of 10 x PBS
1 x PBS-T pH 7.2:	1 x PBS 0.05 % Tween-20 Store at RT.
2 M H_2SO_4	
Assay buffer:	1 x PBS 0.05 % Tween-20 0.5 % BSA Make fresh every time! Sterile filter before use!

3.2.12 Liquid-phase electrochemiluminescence assay (LPECL)

LPECL assays were done in collaboration with Dr. Baumann at Hoffmann-La Roche, Basel, and performed by myself or with the help of Robert Schubenel.
The LPECL is an antibody enzyme-based assay for the quantification of Aβ peptides. Similar to the peptide species specific ELISA, the Aβ peptides are initially detected by a capture antibody that recognizes the first 16 amino acids of the Aβ sequence, therefore binding to all Aβ peptide species. This biotinylated capture antibody is coupled to streptavidin coated magnetic beads and incubated together with the sample and the detection antibodies. The detection antibodies are specific for the different Aβ species and are coupled to an

electrofluorescence tag. In the detection chamber an electric current is applied and the fluorescence of the tag bound to the Aβ peptides is quantified.

- Dilute biotinylated 6E10 capture antibody to 1 µg/ml (1:1000) in assay buffer and add 1:80 diluted streptavidin coated Dynabeads M-280.

Assay buffer	50 ml
Beads	625 µl
6E10-bio	50 µl

- Incubate beads and antibody for 1 h at RT while shaking.
- Dilute Aβ peptide standards:
  Stock concentration is 1 µg/ml, dilute 1:100 to achieve starting concentration of 10 ng/ml. Make 1 ml of 10 ng/ml and perform more dilutions in Assay buffer. Make a serial dilution by sequentially mixing 500 µl of standard with 500 µl of Assay buffer.

ng/ml	10	5	2.5	1.25	0.63	0.31	0.16	0.08	working conc.
ng/ml	2	1.0	0.5	0.25	0.125	0.063	0.031	0.016	endconc. in assay

- Dilute detection antibodies in Assay buffer.

BAP29-TAG	(Aβ38)	0.375 µg/ml
BAP24-TAG	(Aβ40)	0.063 µg/ml
BAP15-TAG	(Aβ42)	0.063 µg/ml

- Pipet 50 µl buffer or 50 µl standard per well. (Costar 96-well plates).
- Pipet 50 µl medium or cell culture supernatant per well.
- Add 100 µl detection antibody per well.
- Add 50 µl pre-incubated capture antibody/dynabeads per well.
- Incubate for 3 h at RT while shaking.
- Measure electrochemiluminsecence on an M-Series M8 analyzer.

Assay buffer, pH 7.4: 50 mM Tris-HCl
60 mM NaCl
0.5 % BSA
1 % Tween-20
Sterile filter and store at 4°C.

3.2.13 Matrix-assisted desorption/ionization time of flight (MALDI-TOF)

All MALDI experiments were done in collaboration with Dr. Koo at the University of California, San Diego and performed by Barbara Cottrell and Justin Torpey.
Matrix-assisted desorption/ionization time of flight (MALDI-TOF) mass spectrometry of Aβ peptides was performed on a 4800 MALDI-TOF-TOF. Aβ peptides were immunoprecipitated from conditioned medium with Ab9 antibody covalently coupled to Seize Beads. Peptides were eluted from the beads with 25% 0.1% trifluoracetic acid : 75% acetonitrile. Samples were mixed 1 : 1 with α-cyano-4-hdroxycinnamic acid matrix in methanol : acetonitrile : water (36% : 56% : 8%) and spotted on the MALDI target. Mass spectra were aquired from m/z 3500 – 5000 Da in reflector positive mode at 10000 shots per spectrum using single shot protection and a delayed extraction time of 420 ns. The area of the isotopic pattern (isotopic cluster area) was used as a measure of apparent relative abundance and expressed as a % of total.

3.3 Molecular Biology

3.3.1 DNA preparation

Plasmid DNA from bacteria was isolated using a combination of alkaline lysis and ion-exchange columns which are the basis for almost all commercially available DNA extraction kits. For large scale DNA extraction from 250 ml bacterial cultures we used the JETstar plasmid purification system form Genomed, for small scale DNA extraction from 4 ml of bacterial culture we used the NucleoSpin Plasmid kit from Macherey-Nagel. Both kits contained all the necessary buffers and solutions and the DNA extraction was performed according to the manufacturer's protocol.

3.3.2 Agarose gelelectrophoresis

To analyse DNA fragments they are separated depending on their size in an electric field on an agarose-gel matrix.

- Boil agarose in 1 x TAE buffer. The percentage of agarose depends on the size of the DNA fragments that are analyzed. 1 % agarose in 1 x TAE is most commonly used.
- Swirl the dissolved agarose and let it cool down to approximately 65°C.

- Pour agarose in gel cassette and place comb in the gel.
- Wait until the gel is solid.
- Remove comb and place in running chamber filled with 1 x TAE.
- Load samples and size standard and run at 100 V.
- Place gel in ethidiumbromide bath to stain DNA and incubate for 15 min.
- Wash gel once in 1 x TAE and place on UV table to take picture or excise fragments.

10 x TAE:	0.80 M Tris-Base 20 mM EDTA 1 % glacial acetic acid
1 x TAE:	1:10 dilution of 10 x TAE in MilliQ water.
Ethidiumbromide bath:	1 x TAE 10 µl of 10 mg/ml Ethidiumbromide solution.

3.3.3 Restriction-enzyme digest

Digestion of DNA with restriction enzymes leads to formation of either sticky or blunt ended DNA. Sticky ends have single stranded base overlaps that can anneal to sticky ends of a different DNA fragment which was digested with the same enzyme. The recognition sequences of restriction enzymes are palindromic stretches of DNA of four, six, or eight base pairs length.
For an analytic digest 1 µg DNA was digested in a final volume of 20 µl with either one or two enzymes at the same time. The analytic digests were incubated at 37°C or the respective optimal temperature for the enzyme, for 1 h. For preparative digests the volume was increased due to the larger amounts of enzyme and DNA used. Preparative digests were incubated for 3 – 4 h at 37°C or, in the case of PCR-product double-digests, over night at 37°C.

Analytic digest:

DNA	1 µg	
Enzyme	0.5 µl	(at least 1 U)
100 x BSA stock	0.2 µl	
10 x Enzyme buffer	2 µl	
Water	x µl	(adjust total volume to 20 µl)

Preparative digest:

DNA	5 – 8 µg	
Enzyme	2 µl	
100 x BSA stock	0.5 µl	
10 x Enzyme buffer	5 µl	
Water	x µl	(adjust total volume to 50 µl)

3.3.4 Gelelution

To purify PCR products from the plasmid template DNA or to remove the vector backbone after restriction digests, the DNA was loaded onto an agarose gel and the respective band excised with a razor blade. The DNA was eluted from the gel slice using the Qiagen Gel Extraction Kit according to the manufacturer's protocol. DNA was eluted in 30 µl sterile filtered MilliQ water pH 8.0.

3.3.5 Dephosphorylation of DNA

To avoid re-ligation of a vector after digestion with restriction enzymes it was treated with a phosphatase which removed the 5' phosphoryl groups from DNA. The Antarctic phosphatase was only active in its own buffer, but instead of purifying the digest prior to phosphatase treatment the buffer could be added directly into the digest mixture together with the Antarctic phosphatase enzyme.

Example reaction:

Digest	50 µl
10 x Antarctic phosphatase buffer	6 µl
Antarctic phosphatase	1 µl
Water	3 µl

- Incubate reaction for 1 h at 37°C.
- Heat inactivate enzyme for 20 min at 65°C.
- Purify reaction.

3.3.6 Ligation of DNA

The ligation of cohesive or blunt ended DNA was performed in a total volume of 20 µl. Plasmid and insert were mixed in a 1:1 molar ratio. With the notably smaller size of the insert fragment this translated into an approximately 1:3 mixture of plasmid to insert. The concentration of the fragments was estimated from their signal on an agarose gel. The enzyme used for the ligation was the T4 DNA ligase which catalyzes the formation of a phosphodiester-bond between two juxtaposed 5' phosphate and 3' hydroxyl termini in duplex DNA.

- Thaw 10 x ligase buffer on ice. Contains ATP! Avoid storage at RT or 4°C.
- Prepare ligation mixture in a small volume, preferably 20 µl or less.

Plasmid DNA	x µl
Insert DNA	x µl
10 x buffer	2 µl
Ligase	1 µl
Water	x µl to a final volume of 20 µl

- Also prepare a ligation control containing water instead of the insert DNA to assess possible re-ligation of the vector.
- Incubate for approximately 30 min at RT and then transform into bacteria.

3.3.7 Transformation

To propagate plasmids the DNA was transformed into bacteria, positive clones confirmed, and DNA preparations performed.

- Thaw competent bacteria on ice.
- Add DNA (plasmid or ligation) and incubate for 30 min on ice.
- Heat shock for 90 sec in a 42 °C waterbath.
- Place on ice for 2 min.
- Add 1 ml pre-warmed (37°C) SOC.
- Incubate at 37°C for 1 h.
- Pellet bacteria by centrifugation at 1000 x g for 3 min.

- Resuspend pellet in 100 µl SOC and spread on agar plate with appropriate selection antibiotic.
- Incubate over night at 37 °C.

SOB medium:
8 g tryptone
2 g yeast extract
0.2 g NaCl
400 ml de-ionized water
Autoclave and store at 4°C.

SOC medium:
10 ml SOB medium
200 µl 2 M Glucose (sterile filtered)
Store at 4°C.

LB medium:
1 % Trypton
0.5 % Yeast extract
1 % NaCl
Store at 4°C.

LB-agar:
1 % Trypton
0.5 % Yeast extract
1 % NaCl
1.5 % Agar
Store at 4°C.

Ampicillin Stock:
50 mg/ml Ampicillin
Sterile filter and store at -20°C.

3.3.8 Polymerase chain reaction (PCR)

PCR facilitates in vitro amplification of specific DNA sequences using a thermostable DNA polymerase. During the PCR the DNA becomes thermally denatured and hybridizes with short oligonucleotides that are subsequently elongated by a DNA polymerase. These steps, denaturation, hybridization/annealing and elongation are repeated several times and result in amplification of the DNA stretch that was flanked by the primer sequences.

PCR protocols vary, depending on the template DNA, the oligonucleotide sequence, the polymerase and the length of the amplified DNA fragment.

3.3.9 Colony-PCR

To test bacterial colonies for positive clones we performed colony PCRs. The colony PCR allowed fast testing of many colonies at the same time by performing a PCR on the bacteria themselves without prior DNA isolation.

- Prepare PCR mix. Prepare one for each colony to test, one for a positive and one for a negative control, plus one for pipetting errors. Keep on ice!

	for 1 PCR	for 10 PCRs (master mix)
PCR grade water	16.3µl	163 µl
10 x buffer	2 µl	20 µl
dNTPs (100 mM each)	0.5 µl	5 µl
Primer for (100 pM)	0.5 µl	5 µl
Primer rev (100 pM)	0.5 µl	5 µl
Taq Polymerase (10 u/µl)	0.2 µl	2 µl

- Aliquot PCR master mix into PCR tubes, 20 µl per tube.
- As positive control add 50 ng vector. The negative control contains no DNA.
- Use a sterile pipet tip to scrape a bacterial colony off the plate.
- First, re-streak the bacteria on a new agar plate with appropriate selection antibiotic. Do not forget to number the colonies!
- Then dip the same pipet tip into the master mix in the PCR tube and stir.
- Run the PCR.

  PCR program:

95 °C	2 min	
95 °C	1 min	} 25 cycles
Xx °C	30 sec	
72 °C	1 min	
72 °C	3 min	
4 °C	hold	

  The annealing temperature (Xx) depends on the primer pair.

3.3.10 Site directed mutagenesis

Site directed mutagenesis was used to introduce point mutations into cDNAs. Two different approaches were utilized, QuikChange in vitro site-directed site-directed mutagenesis and a two-step PCR-based approach.

3.3.10.1 QuikChange site-directed mutagenesis

The QuikChange site-directed mutagenesis is PCR-based. The primer pair is complementary to each other and contains the mutated bases in the middle. During the PCR the whole plasmid is amplified and the newly synthesized DNA contains the mutant sequence. The PCR is then treated with DpnI which digests the methylated and hemi-methylated DNA that was used as a template. The treated DNA is then transformed into competent bacteria and propagated. Mutagenesis was performed according to the manufacturer's protocol, except for small changes in the PCR program.

95 °C	60 sec	
95 °C	50 sec	} 18 cycles
55 °C	50 sec	
68 °C	10 min	
68 °C	10 min	
4 °C	hold	

3.3.10.2 Two-step PCR mutagenesis

This method was used to introduce base pair exchanges into DNA fragments. Two sets of DNA oligonucleotides/primers were used. One pair was set at the outer end of the DNA fragment (outer primer) and one pair was complementary to the mutagenesis-site (inner primer). For the design of the two inner primers it was essential that the base exchange and the resultant mismatch was located in the middle of the primer, and that there were at least 15 matching bases on both sides of the mutant site. The first PCRs were performed with an oligonucleotide pair consisting of one outer and one inner primer. These PCRs resulted in two products, which overlapped in the middle and which both contained the mutagenized site. In a second PCR these two PCR products were mixed and the outer primer pair alone was used for amplification, which resulted in a PCR product that comprised the whole DNA

fragment with the introduced mutation. It was absolutely crucial that these PCRs were performed using a proof-reading DNA polymerase to avoid additional mutations in the final PCR product.

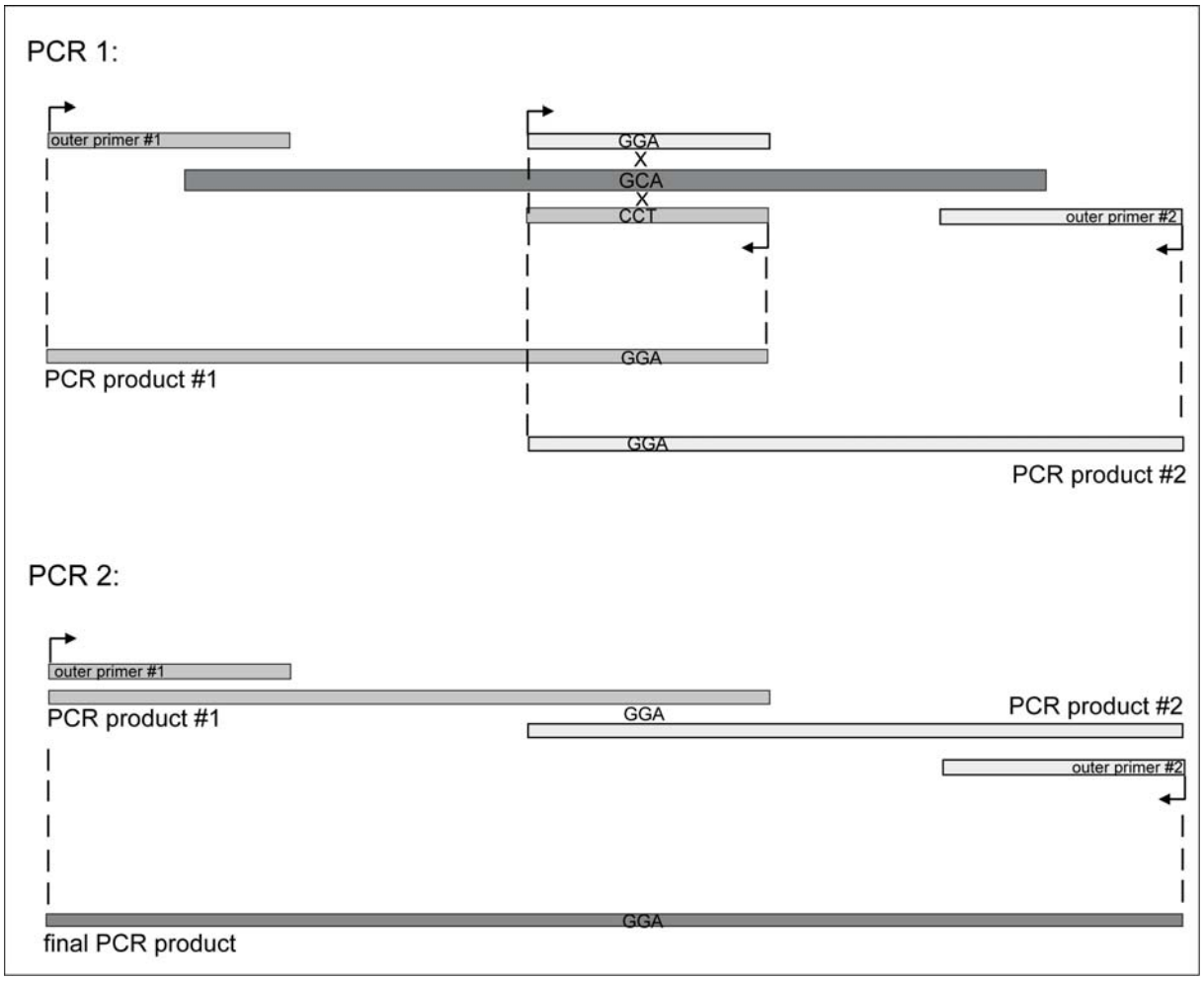

3.3.11 DNA-Sequencing

All DNA constructs were sequenced at the Institute for Immunology and Genetics in Kaiserlsautern.

4 Results

4.1 Presenilin-1 mutations strongly affect the cellular response to γ-secretase modulators and inhibitors *in vitro* and *in vivo*

4.1.1 Genetic dissection of the PS1-ΔExon9 mutation

The PS1-ΔExon9 mutation is unusual as a splice site mutation results in the deletion of a whole exon and, in addition, generates a point mutation (S290C) at the newly formed border of exon8 to exon10 (Perez-Tur, Froelich et al. 1995) (Fig. 4.1.1.1). In contrast, virtually all other FAD associated PS1 mutations are missense mutations.

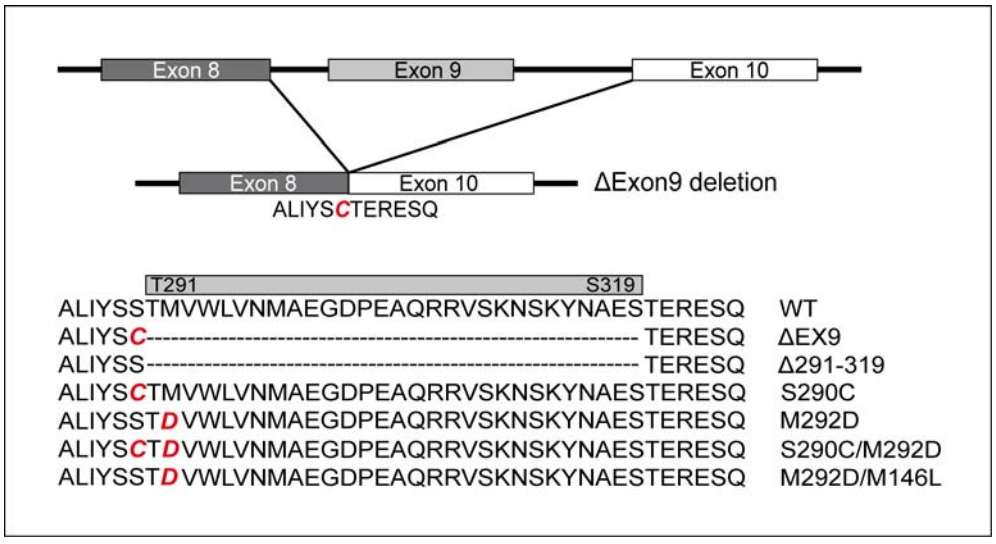

Fig. 4.1.1.1 cDNA constructs for the dissection of the PS1-ΔExon9 mutation. The PS1-ΔExon9 mutation consists of a deletion of amino acids 291-319 and an additional point mutation (S290C) at the newly formed border of exon8 to exon10. The deleted region also contains the endoproteolytic cleavage site of PS1. The cDNA constructs incorporate either one or two of the characteristics of the complex PS1-ΔExon9 mutation: the deletion alone (Δ291-319), the point mutation alone (S290C), lack of endoproteolytic cleavage (M292D), or a combination of the lack of endoproteolytic cleavage with the point mutation (S290C/M292D). The PS1-M292D/M146L construct combines the lack of endoproteolytic cleavage with the FAD associated PS1-M146L mutation, which was previously shown to enhance the effect of Aβ42-lowering NSAIDs. All cDNAs were cloned into the retroviral vector pLPCX.

The deleted region also contains the endoproteolytic cleavage site of PS1 and the mutant protein accumulates in cells in its full-length form (Perez-Tur, Froelich et al. 1995). A previous study had investigated the reasons for the pathological increase in the Aβ42/40

ratio caused by the PS1-ΔExon9 mutation (Steiner, Romig et al. 1999). It was shown that reversion of the S290C point mutation back to the wild-type sequence, resulting in a mutant protein harbouring only the deletion of amino acids 291-319 (PS1-Δ291-319) was sufficient to restore the wild-type PS1 (PS1-WT) phenotype. The PS1-Δ291-319 mutant displayed a similar Aβ42/40 ratio as PS1-WT cells, but the mutant protein still lacked endoproteolytic cleavage. To exclude the possibility that the lack of endoproteolysis of PS1-ΔExon9 and PS1-Δ291-319 mutant or conformational changes associated with the deleted region had any impact on the Aβ42/40 ratio the authors generated an artificial PS1 point-mutation, PS1-M292D. This M292D mutation was shown to completely suppress endoproteolysis, but without any effect on the Aβ42/40 ratio. From these results the authors concluded that the pathogenic increase in the Aβ42/40 ratio of the PS1-ΔExon9 mutation must be caused by the S290C point mutation (Steiner, Romig et al. 1999).

Cells expressing PS1-ΔExon9 were previously shown to have a dramatically attenuated response to treatment with γ-secretase odulators (GSMs) as compared to PS1-WT cells (Weggen, Eriksen et al. 2003), but the mechanistic basis for this effect is unknown. We now wanted to investigate three different possibilities that could explain the diminished response to Aβ42-lowering GSMs. First, the attenuated response could be caused by its lack of endoproteolytic cleavage. We therefore introduced the M292D mutation into the human PS1-WT cDNA. As described above, this mutation was previously shown to suppress processing of PS1 into the N-terminal and C-terminal fragment, but the mutant protein is still fully functional in γ-secretase dependent cleavage and does not change the Aβ42/40 ratio (Steiner, Romig et al. 1999). Second, the reduced response could be due to the S290C point mutation, and to investigate this possibility we generated a cDNA encoding PS1-S290C. Third, the attenuated Aβ42-response could reside in the Δ291-319 deletion or in conformational changes in the regions flanking exon9 caused by the deletion. To test this idea, we mutagenized the cysteine at position 290 in the PS1-ΔExon9 cDNA to a serine, thereby correcting the S290C mutation. All the resulting cDNAs were subcloned into the retroviral shuttle vector pLPCX. Subsequently, Chinese hamster ovary (CHO) cells with stable overexpression of APP751 (APP CHO cells) were infected with retroviral particles for each mutant, and stable pools were selected and used for all further investigations. Previously generated cell lines with stable overexpression of APP751 and PS1-WT or PS1-ΔExon9 were employed as controls (Weggen, Eriksen et al. 2003).

4.1.2 The pathogenic increase in the Aβ42/40 ratio induced by the PS1-ΔExon9 mutation is caused by a synergistic effect of the S290C point mutation and the lack of endoproteolytic cleavage

Stable expression of all PS1 constructs in the APP CHO cells was verified by Western Blotting using the human-specific PS1 monoclonal antibody PSN2 (Okochi, Ishii et al. 1997). In accordance with earlier results, we detected only full-length PS1 (flPS1) at the expected size of 43 kDa in lysates of the cell lines expressing the deletion mutants, PS1-ΔExon9 and PS1-Δ291-319, and in lysates of the cell lines containing the M292D mutation (Fig. 4.1.2.1 A) (Steiner, Romig et al. 1999). In contrast, cells expressing PS1-WT and PS1-S290C showed endoproteolytic cleavage and we detected flPS1 and the PS1 N-terminal fragment at 23 kDa (Fig. 4.1.2.1 A). Subsequently, Aβ40 and Aβ42 levels in conditioned media of all cell lines were quantified by Aβ liquid phase electrochemiluminescence assay (LPECL) to determine the cause for the pathogenic increase in the Ab42/40 ratio associated with the PS1-ΔExon9 mutation. The LPECL assay utilizes Aβ-species specific antibodies coupled to a voltage sensitive luminescent tag and allows the quantification of the electrochemiluminescence depending on the amounts of the specific Aβ peptides (Czirr, Leuchtenberger et al. 2007). We performed five independent experiments and analyzed the data by one-way ANOVA (analysis of variance). Confirming previous results, we found that expression of the PS1-ΔExon9 mutation increased the Aβ42/40 ratio 3-fold compared to PS1-WT expressing cells, while both the PS1-Δ291-319 and the PS1-M292D mutant cell lines displayed a normal Aβ42/40 ratio (Fig. 4.1.2.1 B). Surprisingly, expression of the PS1-S290C point mutation did also not influence the levels of Aβ40 or Aβ42 either and the ratio between the peptides in the mutant cell line was indistinguishable from the PS1-WT expressing cell line (Fig. 4.1.2.1 B). These results were confirmed in three independently generated mass cultures of cells expressing the PS1-S290C mutation. Because these mutants did not clarify the reason for the elevated Aβ42/40 ratio caused by the PS1-ΔExon9 mutation, we generated another cDNA with the S290C point mutation and the M292D mutation (Fig. 4.1.1.1), thus combining two of the three characteristics of the PS1-ΔExon9 mutation. As expected the PS1-S290C/M292D mutant failed to be cleaved, and only flPS1 was detected (Fig. 4.1.2.1 A). Intriguingly, PS1-S290C/M292D induced a significant 2-fold increase in the Aβ42/40 ratio as compared to PS1-WT (Fig. 4.1.2.1 B). From these results we concluded that a synergistic effect of the S290C point mutation and the lack of endoproteolytic cleavage was sufficient to cause a pathogenic increase in the Aβ42/40 ratio. However, the Aβ42/40 ratio in the PS1-S290C/M292D mutant cell line was only 2-fold increased compared to PS1-WT cell lines while the PS1-ΔExon9 mutation increased the Aβ42/40 ratio more than 3-fold. This intermediate effect showed that the PS1-S290C/M292D mutant did not fully recapitulate the

pathogenic change in the Aβ42/40 ratio caused by PS1-ΔExon9, indicating that the deletion of amino acids 291-319 may further contribute to the strongly elevated Aβ42/40 ratio of the PS1-ΔExon9 mutation.

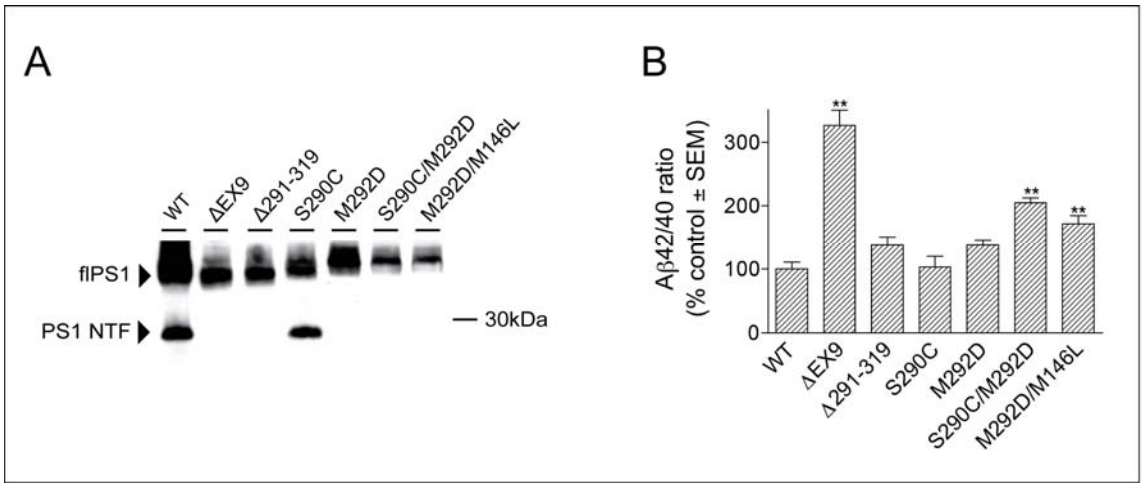

Fig. 4.1.2.1 The increased Aβ42/40 ratio of the PS1-ΔExon9 mutation is caused by a synergistic effect of the lack of endoproteolytic cleavage and the S290C point mutation. (A) The cDNA constructs shown in Fig. 4.1.1.1 were used to generate retroviral particles and employed to infect CHO cells with stable overexpression of human WT-APP (APP CHO), and stable mass cultures were generated. PS1 expression was analyzed by Western Blotting using the human specific N-terminal PS1 antibody PSN2. PS1-WT and PS1-S290C showed endoproteolytic cleavage with detection of flPS1 and the PS1-NTF, at the expected size of 43 kDa and 23 kDa. As expected, mutants PS1-ΔExon9, PS1-Δ291-319, PS1-M292D, PS1-S290C/M292D, and PS1-M292D/M146L did not undergo endoproteolysis due to lack of or mutated endoproteolytic cleavage site, and accumulated as full-length proteins. (B) Aβ40 and Aβ42 levels in conditioned media were determined, Aβ42/40 ratios for each cell line calculated and normalized to PS1-WT. The PS1-ΔExon9 mutation caused a 3-fold increase in the Aβ42/40 ratio compared with PS1-WT. PS1-Δ291-319, PS1-M292D, and PS1-S290C displayed a normal Aβ42/40 ratio similar to PS1-WT. Only PS1-S290C/M292D mimicked the effect of the PS1-ΔExon9 mutation and increased the Aβ42/40 ratio, though not as much as PS1-ΔExon9. This indicated that the pathogenic increase in Aβ42/40 ratio observed with the PS1-ΔExon9 mutation results at least partially from a synergistic effect of the lack of endoproteolytic cleavage and the S290C point mutation. PS1-M292D/M146L displayed a smaller, but significant increase in Aβ42/40 ratio as expected. n = 5; one-way ANOVA, **p<0.01 Dunnett's post tests.

We also generated a cell line with stable expression of the M292D mutation in combination with the FAD associated M146L mutation. The PS1-M146L mutation alone leads to an increase in the Aβ42/40 ratio and it was shown that cell lines with stable expression of this FAD mutation display an enhanced response to Aβ42-lowering NSAIDs (Weggen, Eriksen et al. 2003). Expression of the PS1-M292D/M146L mutant protein led to an approximately 2-fold increase in the Aβ42/40 ratio compared to PS1-WT cells (Fig. 4.1.2.1 B).

4.1.3 The attenuated response of PS1-ΔExon9 to γ-secretase modulators is mainly caused by its lack of endoproteolytic cleavage

To investigate the diminished response of the PS1-ΔExon9 mutation to GSMs, we subjected the cell lines expressing the different PS1 mutations (Fig. 4.1.2.1 A) to treatment with increasing concentrations of the Aβ42-lowering NSAID sulindac sulfide. For these experiments, the cells were repeatedly treated with DMSO vehicle alone, 30 μM sulindac sulfide, or 60 μM sulindac sulfide, and Aβ42 and Aβ40 levels in conditioned media were quantified by LPECL. The Aβ42-response of individual cell lines in five independent dose-response experiments was then compared by one-way ANOVA. It had been previously shown that in this concentration range, sulindac sulfide did not induce toxicity in CHO cells (Weggen, Eriksen et al. 2001; Weggen, Eriksen et al. 2003) In agreement with these findings, we observed that Aβ40 levels were not significantly changed by sulindac sulfide treatment in any of the cell lines as compared to DMSO control condition (Fig. 4.1.3.1 A). We also confirmed earlier findings that the Aβ42-response of the PS1-ΔExon9 cells is strongly diminished as compared to PS1-WT control cells (Fig. 4.1.3.1B and Table 4.1.3.1) (Weggen, Eriksen et al. 2003). In contrast, the Aβ42 response of PS1-S290C expressing cells was not significantly different from PS1-WT control cells, excluding the possibility that the S290C point mutation is responsible for the attenuated response of the PS1-ΔExon9 mutation. However, cells expressing PS1-Δ291-319 behaved similar to PS1-ΔExon9 cells and exhibited a diminished Aβ42 response (Fig. 4.1.3.1 B and Table 4.1.3.1). To further explore whether the loss of endoproteolytic cleavage caused by the deleted region or the deleted region itself was critical, we examined cells expressing the PS1-M292D mutation. These cells also displayed a significantly reduced response to sulindac sulfide treatment when compared to PS1-WT expressing cells. When we combined the M292D mutation with the S290C mutation a trend towards more pronounced attenuation was observed (Fig. 4.1.3.2 and Table 4.1.3.2). However, none of the cell lines with individual or combined characteristics of the PS1-ΔExon9 mutation could fully recapitulate the effect size of this complex FAD PS1 mutant. Interestingly, when the M292D mutation was combined with the M146L mutation, which was previously shown to enhance the response to Aβ42-lowering NSAIDs (Weggen, Eriksen et al. 2003), the resulting M292D/M146L mutant behaved similar to PS1-WT and displayed a normal response to sulindac sulfide treatment (Fig. 4.1.3.1 B and Table 4.1.3.1). Taken together, these results indicate that the attenuated response of the PS1-ΔExon9 mutation to treatment with GSMs is mainly caused by its lack of endoproteolytic cleavage. However, the other characteristics of PS1-ΔExon9, the deletion of amino acids

291-319 and the S290C point mutation, also contribute to the observed phenotype of this complex mutation.

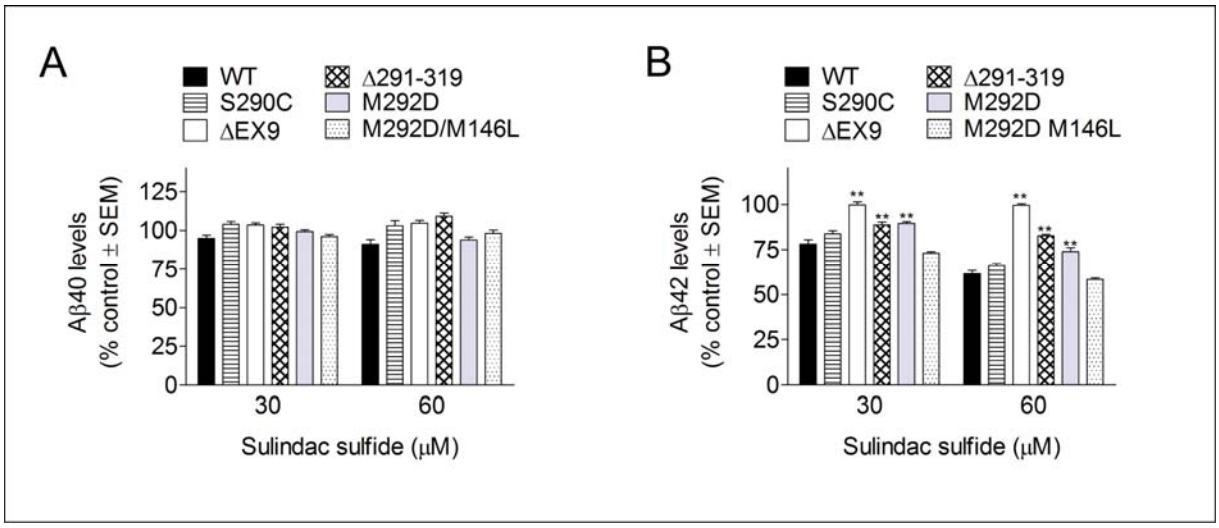

Fig. 4.1.3.1 The diminished response of the PS1-ΔExon9 mutation to sulindac sulfide treatment is mainly caused by its lack of endoproteolytic cleavage. APP CHO cells with stable expression of mutant PS1 or PS1-WT were treated with increasing concentrations of the Aβ42-lowering NSAID sulindac sulfide, and Aβ40 and Aβ42 levels in conditioned media were quantified. The graphs depict the Aβ levels in percentage of DMSO vehicle treated controls. (A) Treatment with 30 µM or 60 µM sulindac sulfide did not cause significant changes in Aβ40 levels as expected. (B) Cells overexpressing PS1-ΔExon9 displayed a strongly attenuated Aβ42 response compared to PS1-WT expressing cells as reported previously. In contrast, the Aβ42 response of PS1-S290C cells was not significantly different from PS1-WT cells. Cell lines expressing PS1-Δ291-319 and PS1-M292D showed a diminished response to sulindac sulfide treatment as compared to PS1-WT cells, indicating that the attenuated response of the PS1-ΔExon9 mutation is mainly caused by its lack of endoproteolytic cleavage. Introduction of the FAD PS1-M146L mutation into the PS1-M292D endoproteolysis-deficient background rescued this effect, and PS1-M292D/M146L cells behaved similar to PS1-WT cells. n = 5; one-way ANOVA, **p < 0.01, Dunnett's post tests.

Table 4.1.3.1 The diminished Aβ42 response of the PS1-ΔExon9 mutation is mainly caused by its lack of endoproteolytic cleavage. Dose-response experiments were analyzed by one-way ANOVA with PS1-WT cells as control group. Aβ levels are shown as percentage of vehicle treated controls. n = 5; **p < 0.01; Dunnett's post tests.

	Aβ42 levels	
	30 µM	60 µM
	% control ± SE	
Cell line		
PS1-WT	78.19 ± 2.37	61.65 ± 1.68
PS1-S290C	83.76 ± 1.75	65.92 ± 1.24
PS1-ΔExon9	99,70 ± 1.63 **	99.49 ± 0.93 **
PS1-Δ291-319	88.71 ± 1.64 **	82.65 ± 0.89 **
PS1-M292D	89.53 ± 1.06 **	73.90 ± 2.19 **
PS1-M292D/M146L	73.19 ± 0.65	58.45 ± 0.82

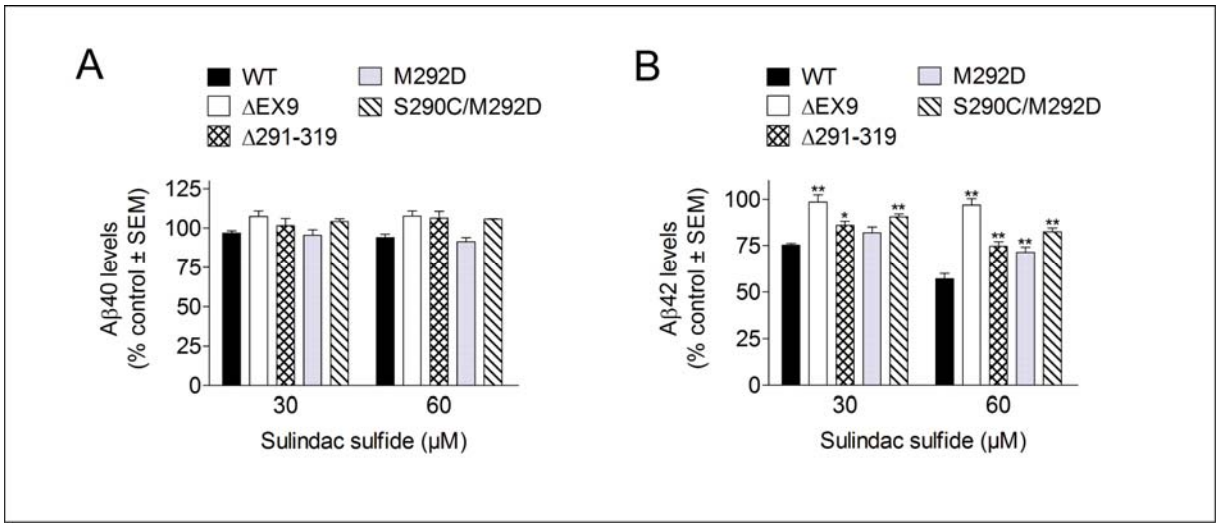

Fig. 4.1.3.2 Single characteristics of the PS1-ΔExon9 mutation do not fully recapitulate the diminished Aβ42 response to sulindac sulfide treatment. APP CHO cells with stable expression of PS1-WT or mutant PS1 were treated with 30 μM or 60 μM of the Aβ42-lowering NSAID sulindac sulfide, and Aβ40 and Aβ42 levels in conditioned media were quantified. The graphs depict the Aβ levels in percentage of DMSO treated controls. (A) Sulindac sulfide treatment did not cause significant changes in Aβ40 levels as expected. (B) Similar to the results shown in figure 4.1.3.1, cells expressing PS1-ΔExon9 displayed an almost completely abolished response to sulindac sulfide treatment, while cell lines expressing the deletion alone (PS1-Δ291-319) or mutant PS1 lacking endoproteolysis (PS1-M292D) also displayed a significant but lesser attenuation than the PS1-ΔExon9 mutant. Combination of the endoproteolysis deficient M292D mutation with the S290C point mutation seemed to further diminish the Aβ42 response as compared to cell lines expressing only single characteristics of the PS1-ΔExon9 mutation. This indicates that all features of the PS1-ΔExon9 mutation, the deletion, lack of endoproteolytic cleavage, and the S290C point mutation contribute to the reduced Aβ42 response after sulindac sulfide treatment. n = 5; one-way ANOVA, **p < 0.01; *p < 0.05 Dunnett's post tests.

Table 4.1.3.2 Single characteristics of the complex PS1-ΔExon9 mutation do not fully recapitulate the diminished Aβ42 response to sulindac sulide treatment. Dose-response experiments were analyzed by one-way ANOVA with PS1-WT cells as control group. Aβ levels are shown as percentage of vehicle treated controls. n = 5; **p < 0.01; *p < 0.05; Dunnett's post tests.

	Aβ42 levels	
	30 μM	60 μM
	% control ± SE	
Cell line		
PS1-WT	75.33 ± 0.89	57.08 ± 2.85
PS1-ΔExon9	98.45 ± 3.94**	96.81 ± 3.49**
PS1-Δ291-319	85.93 ± 2.32*	74.70 ± 2.46**
PS1-M292D	81.90 ± 3.05	71.42 ± 2.67**
PS1-S290C/M292D	90.62 ± 1.36**	82.32 ± 2.06**

4.1.4 Insensitivity to γ-secretase modulators and inhibitors is common among aggressive FAD-associated PS1 mutations

To investigate whether the diminished response of the PS1-ΔExon9 mutation to treatment with GSMs is specific for this mutation or whether other FAD-associated PS1 mutations show a similar effect, we generated cell lines with stable expression of three other aggressive early-onset FAD mutations, PS1-L166P, PS1-P117L, and PS1-G384A. Cell lines were produced as described above by transducing APP CHO cells with retroviral particles for each mutant and pools with stable expression of mutant PS1 protein were selected. Expression of all mutants was confirmed by Western Blotting with PSN2 antibody. All three mutants were endoproteolytically processed and flPS1 as well as PS1-NTF could be detected (Fig. 4.1.4.1 A), and expression of the mutant protein gave rise to an approximately 3-fold increase in the Aβ42/40 ratio as compared to PS1-ΔExon9 (Fig. 4.1.4.1 B).

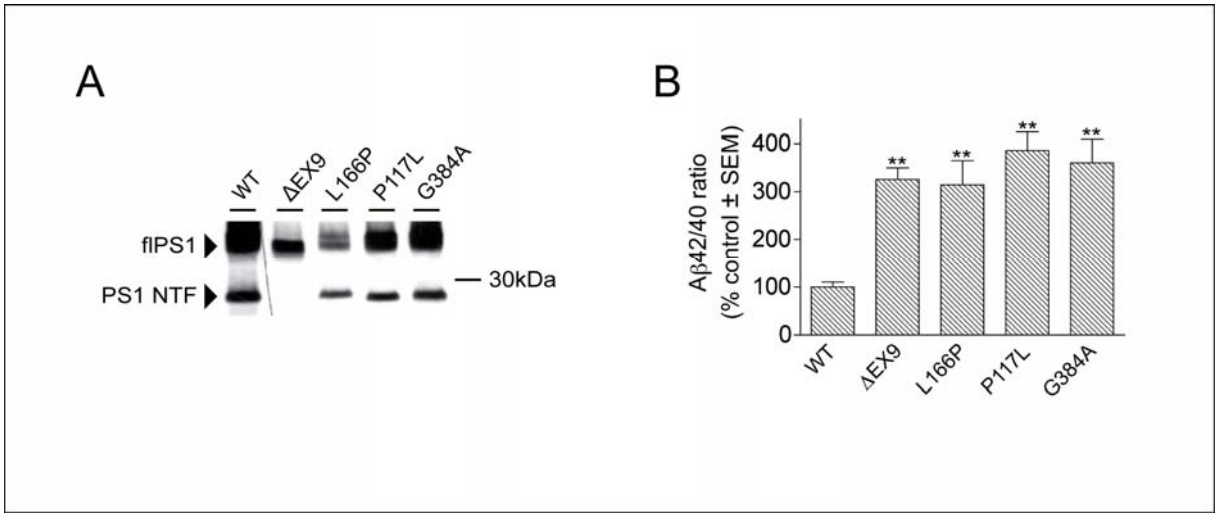

Fig. 4.1.4.1 Aggressive FAD associated PS1 mutations cause a similar increase in the Aβ42/40 ratio. (A) cDNA constructs encoding PS1-WT, PS1-ΔExon9, PS1-L166P, PS1-P117L, and PS1-G384A were cloned, used to generate retroviral particles, employed to infect APP CHO cells, and stable mass cultures were generated. PS1 expression was analyzed by Western Blotting using the human specific N-terminal PS1 antibody PSN2. Cell line PS1-ΔExon9 lacked endoproteolytic cleavage due to deletion of the cleavage site, all other mutant PS1 proteins as well as PS1-WT were endoproteolytically processed and flPS1 as well as the PS1-NTF could be detected. (B) Aβ40 and Aβ42 levels in conditioned media were quantified, the Aβ42/40 ratio calculated, and normalized to PS1-WT. All mutant cell lines increased the Aβ42/40 ratio approximately 3-fold as compared to PS1-WT cells. n = 5; one-way ANOVA, **p = 0.01, Dunnett's post tests.

In terms of the absolute levels of Aβ in ng/ml, expression of all mutant PS1 constructs led to a reduction in Aβ40 and Aβ38 peptide generation and to an increase in the Aβ42/40 ratio. (Table 4.1.4.1). Expression of FAD PS1 mutants PS1-L166P, PS1-P117L, and PS1-G384A

caused an increase in Aβ42 production, whereas Aβ42 levels were decreased in the PS1-ΔExon9 cell line. This is in accordance with previously published results which suggested a partial loss-of-function of some FAD-associated PS1 mutations that leads to a change in the Aβ42/40 ratio both by a reduction in Aβ40 and an increase in Aβ42 production (Bentahir, Nyabi et al. 2006; De Strooper 2007; Shen and Kelleher 2007).

Table 4.1.4.1 Aβ levels in mutant PS1 expressing cell lines are lower than in PS1-WT expressing cells. n = 5

	Aβ levels			Aβ42/40 ratio
	Aβ40	Aβ42	Aβ38	
	ng/ml			
Cell line				
PS1-WT	29.23 ± 1.74	1.89 ± 0.11	2.09 ± 0.11	0.07 ± 0.01
PS1-ΔExon9	2.68 ± 0.07	0.59 ± 0.04	0.18 ± 0.04	0.23 ± 0.03
PS1-L166P	10.84 ± 0.97	2.31 ± 0.23	0.80 ± 0.06	0.22 ± 0.05
PS1-P117L	9.33 ± 0.66	2.43 ± 0.08	0.72 ± 0.03	0.27 ± 0.05
PS1-G384A	11.54 ± 0.80	2.82 ± 0.26	1.16 ± 0.04	0.25 ± 0.07

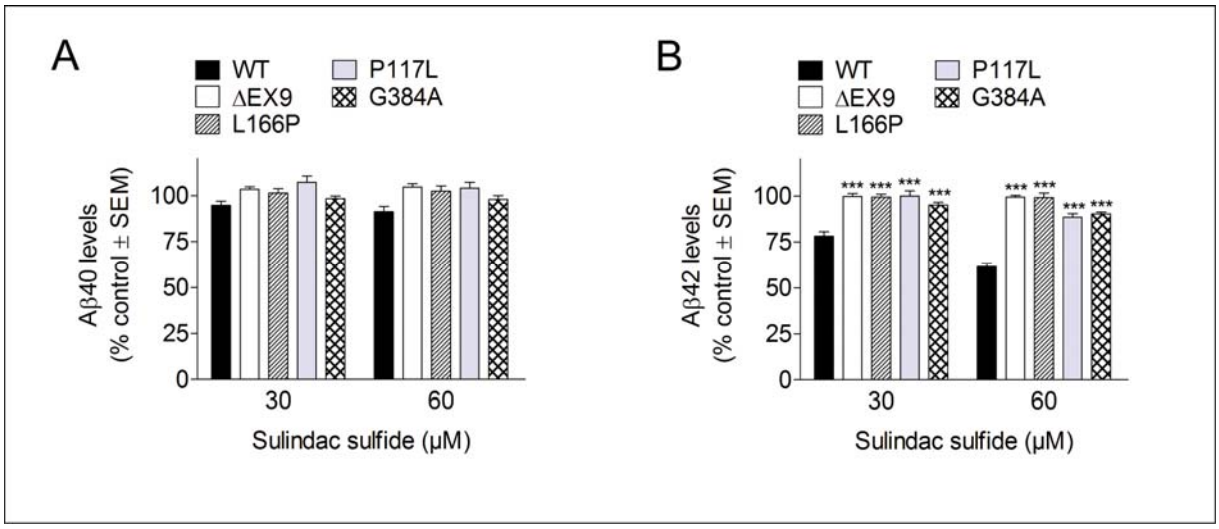

Fig. 4.1.4.2 Insensitivity to Aβ42-lowering NSAIDs is common among aggressive FAD PS1 mutations. APP CHO cells with stable expression of PS1-WT or mutant PS1 were treated with 30 μM or 60 μM of the Aβ42-lowering NSAID sulindac sulfide, and Aβ40 and Aβ42 levels in conditioned media were quantified. The graphs depict the Aβ levels in percentage of DMSO treated controls. (A) Treatment with sulindac sulfide at these concentrations did not cause any significant changes in Aβ40 levels. (B) Cells expressing the FAD PS1 mutations PS1-L166P, PS1-P117L, PS1-G384A, displayed a dramatically reduced response to sulindac sulfide treatment compared to PS1-WT cells. n = 5; one-way ANOVA, ***p = 0.001, Dunnett's post tests.

Table 4.1.4.2 Insensitivity to Aβ42-lowering NSAIDs is common among aggressive FAD associated PS1 mutations. Dose-response experiments were analyzed by one-way ANOVA with PS1-WT cells as control group. Aβ levels are shown as percentage of vehicle treated controls. n = 5; ***p < 0.001; Dunnett's post tests.

	Aβ42 levels	
	30 µM	60 µM
	% control ± SE	
Cell line		
PS1-WT	79.19 ± 2.37	61.65 ± 1.68
PS1-ΔExon9	99.70 ± 1.63***	99.49 ± 0.93***
PS1-L166P	99.45 ± 1.50***	99.16 ± 2.51***
PS1-P117L	99.95 ± 2.76***	88.53 ± 1.98***
PS1-G384A	95.13 ± 1.35***	90.34 ± 0.93***

These cell lines were again subjected to repeated treatment with increasing concentrations of sulindac sulfide and the amounts of Aβ40 and Aβ42 in conditioned media were quantified. All three mutant cell lines displayed a strongly diminished response comparable to the PS1-ΔExon9 cells that were completely refractory to sulindac sulfide treatment (Fig. 4.1.4.2 B and Table 4.1.4.2). As seen in previous experiments levels of Aβ40 were not significantly changed after treatment (Fig. 4.1.4.2 A). These results clearly demonstrate that the reduced response to treatment with GSMs is not a unique characteristic of the PS1-ΔExon9 mutation, but a common feature of aggressive FAD associated PS1 mutations.

We next tested the recently published, highly potent γ-secretase modulator GSM-1 on cell lines expressing PS1-WT or PS1 mutants PS1-ΔExon9, PS1-L166P, PS1-P117L, and PS1- (Page, Baumann et al. 2007). In an initial experiment with PS1-WT cells alone, we observed a dose-dependent reduction in Aβ42 levels with approximately 50 % reduction after treatment with 0.1 µM GSM-1 and almost 80 % reduction at 0.5 µM without any effects on Aβ40 production (data not shown). In a subsequent experiment, we treated PS1-WT and mutant PS1 cell lines with 0.5 µM of GSM-1 or DMSO vehicle. Aβ40 levels were not strongly affected by treatment with GSM-1 although some reduction could be observed in cell lines expressing PS1-ΔExon9, PS1-L166P, and PS1-G384A (Fig. 4.1.4.3 A). Aβ42 levels were reduced by approximately 75 % in PS1-WT cells. In contrast, all mutant cell lines displayed a diminished Aβ42 response to GSM-1 treatment (Fig. 4.1.4.3 B). These results confirm our observations with the Aβ42-lowering NSAID sulindac sulfide.

In a previous study it was shown that the PS1-ΔExon9 mutation is also partially non-responsive to treatment with the transition-state γ-secretase inhibitor L-685,458 (Ikeuchi, Dolios et al. 2003). These results together with our findings that the PS1-ΔExon9 mutation is insensitive to the GSM sulindac sulfide suggested a possible mechanistic link between these two phenotypes.

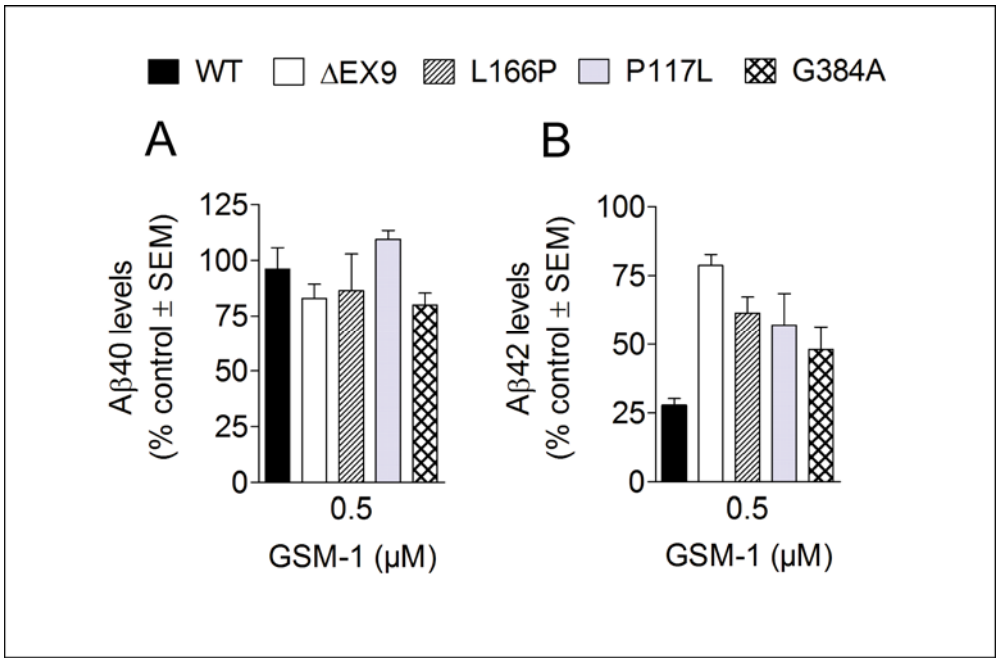

Fig. 4.1.4.3 The Aβ42 response to the highly potent γ-secretase modulator GSM-1 is diminished in FAD PS1 mutant cell lines. (A) APP CHO cells with stable expression of PS1-WT, PS1-ΔExon9, PS1-L166P, PS1-P117L, and PS1-G384A were treated with 0.5 μM GSM-1 or vehicle control, and Aβ40 levels in conditioned media were quantified. Aβ40 levels were slightly reduced in cell lines expressing PS1-ΔExon9, PS1-L166P, and PS1-G384A. (B) Aβ42 levels in the same experiment as above were quantified. Aβ42 levels in PS1-WT cells were reduced by approximately 75 % after treatment with 0.5 μM GSM-1. In contrast, the Aβ42 response in all FAD PS1 cell lines was strongly attenuated with reductions in Aβ42 levels ranging from 25 % in cells expressing PS1-ΔExon9 to 50 % reduction in PS1-G384A cells. The graphs depict the Aβ levels in percentage of DMSO vehicle treated control. n = 1.

To reproduce these earlier results for the PS1-ΔExon9 mutation and to examine whether they are relevant to other FAD PS1 mutations, we treated cell lines expressing PS1-WT, PS1-ΔExon9, and PS1-L166P with the transition-state γ-secretase inhibitor L-685,458.
The cell lines were subjected to repeated treatment with increasing concentrations of the inhibitor, and the cellular response was compared by measuring Aβ40 and Aβ42 levels in conditioned media. Confirming previous results, we observed an attenuated response of the PS1-ΔExon9 cells to treatment with L-685,458 as compared to the PS1-WT expressing cells. At 100 nM L-685,458, levels of Aβ40 and Aβ42 in PS1-WT cells were reduced by around 90% whereas we observed a maximal reduction of only 15% in the PS1-ΔExon9 cells (Fig. 4.1.4.4 A and Table 4.1.4.4). These results could be expanded to another FAD PS1 mutation, PS1-L166P. For PS1-L166P cells, the Aβ40 response was significantly attenuated at the lowest inhibitor concentration of 100 nM with a non-significant trend at higher concentrations.

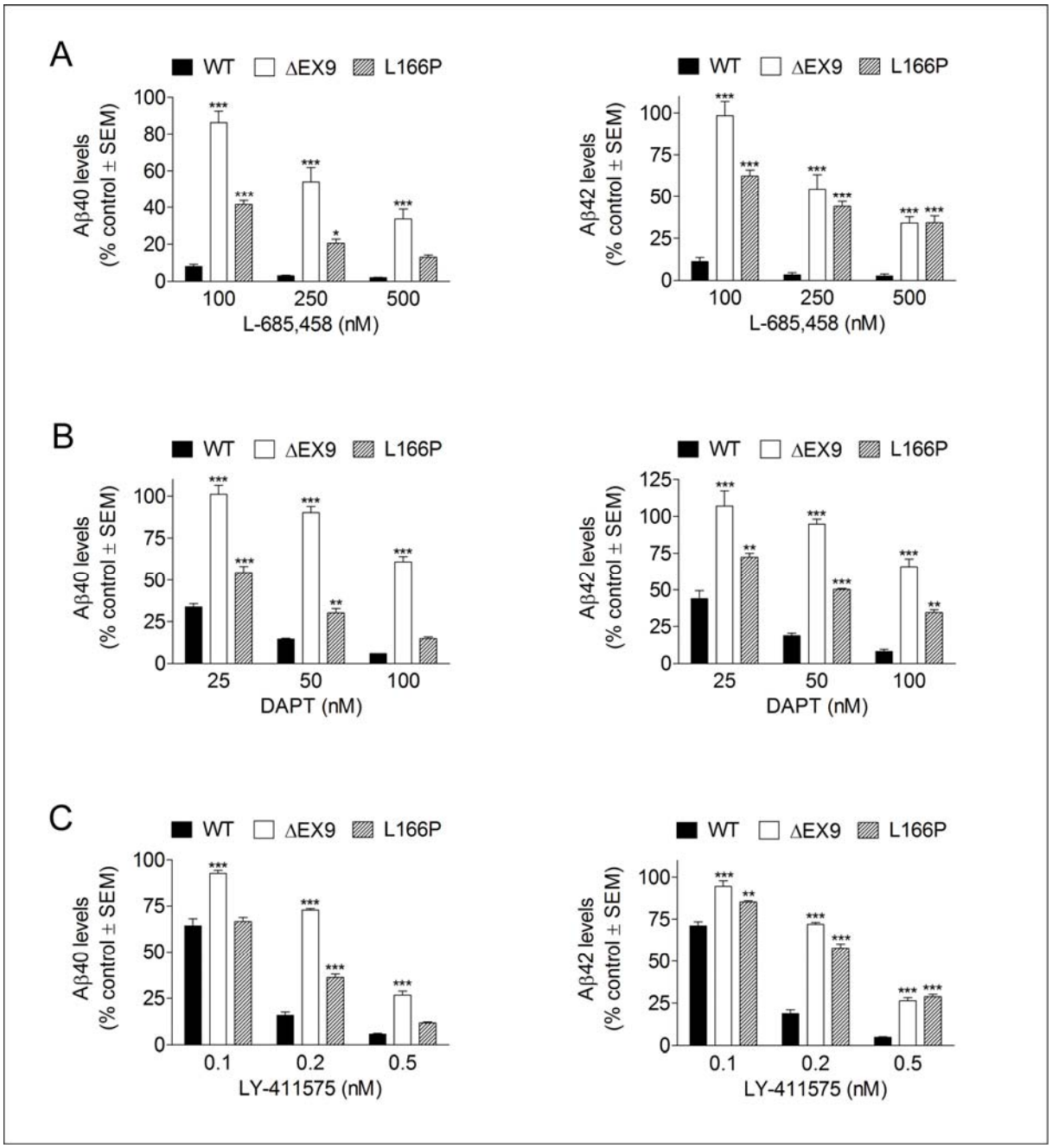

Fig. 4.1.4.4 FAD PS1 mutants are partially insensitive to γ-secretase inhibitors of different structural classes and increasing potencies. APP CHO cells with stable expression of PS1-WT or PS1 mutants PS1-ΔExon9 and PS1-L166P were treated with increasing concentrations of γ-secretase inhibitors. Aβ40 and Aβ42 levels were quantified, and the results were analyzed by one-way ANOVA with PS1-WT cells as control group. The graphs depict the Aβ levels in percentage of vehicle treated controls. (A) PS1-WT and mutant PS1 cells were treated with increasing concentrations of the transition state γ-secretase inhibitor L-685,458. The Aβ40 and Aβ42 response of the PS1-ΔExon9 cells was diminished at all concentrations compared with PS1-WT cells. The Aβ40 (left panel) response of the PS1-L166P cells was attenuated at the lowest concentration of inhibitor with a non-significant trend at higher concentrations. The Aβ42 response (right panel) for the PS1-L166P cells was significantly attenuated at all concentrations tested. (B) Dose-response experiments with the semi-peptidic inhibitor DAPT showed very similar results and an attenuated response to DAPT

treatment of both mutant cell lines was observed. Similar to the results with L-685,458 the attenuation was more pronounced for Aβ42 (right panel) than for Aβ40 (left panel). (C) The cell lines were treated with the highly potent benzodiazepine-like inhibitor LY-411575. Similar to the results with the other γ-secretase inhibitors, a significantly attenuated response of Aβ40 (left panel) and Aβ42 (right panel) was observed with cell lines expressing PS1-ΔExon9 and PS1-L166P as compared with PS1-WT cells. n = 3; one-way ANOVA, ***p < 0.001; **p < 0.01; *p < 0.05 Dunnett's post tests.

Table 4.1.4.3 FAD PS1 mutants are partially insensitive to γ-secretase inhibitors of different structural classes. Aβ levels are depicted in percentage of vehicle trated controls. n = 3; one-way ANOVA, ***p < 0.001; **p < 0.01; *p < 0.05 Dunnett's post tests.

	Aβ40 levels		
	PS1-WT	PS1-ΔExon9	PS1-L166P
		% control ± SE	
L-685,458			
100 nM	8.1 ± 1.14	86.27 ± 6.22***	41.55 ± 2.26***
250 nM	2.95 ± 0.31	54.05 ± 7.86***	20.61 ± 2.20*
500 nM	1.92 ± 0.28	33.37 ± 5.76***	13.07 ± 1.21
	Aβ42 levels		
		% control ± SE	
L-685,458			
100 nM	11.27 ± 2.36	98.33 ± 8.55***	62.31 ± 3.69***
250 nM	3.28 ± 1.22	54.45 ± 8.60***	44.08 ± 3.03***
500 nM	2.59 ± 1.32	34.06 ± 3.79***	34.22 ± 4.05***
	Aβ40 levels		
		% control ± SE	
DAPT			
25 nM	33.76 ± 1.96	101.06 ± 5.38***	54.44 ± 3.65***
50 nM	14.62 ± 0.46	90.18 ± 3.72***	30.26 ± 2.50**
100 nM	5.87 ± 0.13	60.79 ± 3.27***	14.87 ± 0.99
	Aβ42 levels		
		% control ± SE	
DAPT	43.99 ± 5.48	107.06 ± 10.16***	72.35 ± 2.66**
25 nM	18.77 ± 1.65	94.87 ± 3.19***	50.28 ± 0.75***
50 nM	8.13 ± 1.46	65.87 ± 5.07***	34.52 ± 2.01**
100 nM			
	Aβ40 levels		
		% control ± SE	
LY-411575			
0.1 nM	64.23 ± 3.87	92.56 ± 1.62***	66.60 ± 2.20
0.2 nM	15.79 ± 1.81	72.89 ± 0.85***	36.22 ± 1.79***
0.5 nM	5.6 ± 0.62	26.74 ± 2.05***	11.69 ± 0.5
	Aβ42 levels		
		% control ± SE	
LY-411575			
0.1 nM	71.00 ± 2.50	94.43 ± 3.40***	85.20 ± 0.86**
0.2 nM	18.80 ± 2.24	72.01 ± 1.01***	57.68 ± 2.38***
0.5 nM	4.75 ± 0.35	26.47 ± 1.77***	28.74 ± 1.45***

Aβ42 levels in the PS1-L166P cells were significantly higher in response to treatment with L-685,458 at all concentrations tested as compared to PS1-WT cells (Fig. 4.1.4.4 A and Table 4.1.4.3). L-685,458 was designed as a transition state inhibitor for aspartyl proteases, and a photoactivatible derivative was shown to directly bind to the active site of the γ-secretase complex, labelling both the PS1-NTF and the PS1-CTF (Li, Xu et al. 2000). To examine whether the attenuated response of FAD PS1 mutations would be restricted to transition-state inhibitors or could also be observed with inhibitors of other structural classes, we subjected the cell lines to treatment with the structurally different inhibitor DAPT (N-[N-(3,5-Difluorophenacetyl-L-alanyl)]-S-phenylglycine *t*-butyl ester). DAPT is a semi-peptidic inhibitor, and a photoactivatible derivative was shown to bind to the PS1-CTF at a site divergent from the active site of the γ-secretase complex (Morohashi, Kan et al. 2006). Treatment of cells expressing PS1-WT, PS1-ΔExon9, and PS1-L166P with increasing concentrations of DAPT led to similar results as treatment with L-684,458. The response of both mutant cell lines was substantially reduced as compared to PS1-WT expressing cells. For the PS1-L166P cells, the attenuation seemed to be more pronounced for Aβ42 than for Aβ40 (Fig. 4.1.4.4 B and Table 4.1.4.3). DAPT is a γ-secretase inhibitor with medium potency, but high doses were required to significantly reduce brain Aβ levels in an APP transgenic mouse model (Dovey, John et al. 2001). Therefore, to enable *in vivo* experiments, we next evaluated the effect of the highly potent benzodiazepine-like γ-secretase inhibitor LY-411575, which has a reported EC50 value of 119 pM for Aβ40 reduction in HEK293 cells (Lewis, Perez Revuelta et al. 2003). Both mutant cell lines showed a significantly attenuated response to treatment with this highly potent inhibitor, and the attenuation was again more pronounced for Aβ42 inhibition than for Aβ40 inhibition (Fig. 4.1.4.4 C and Table 4.1.4.3).

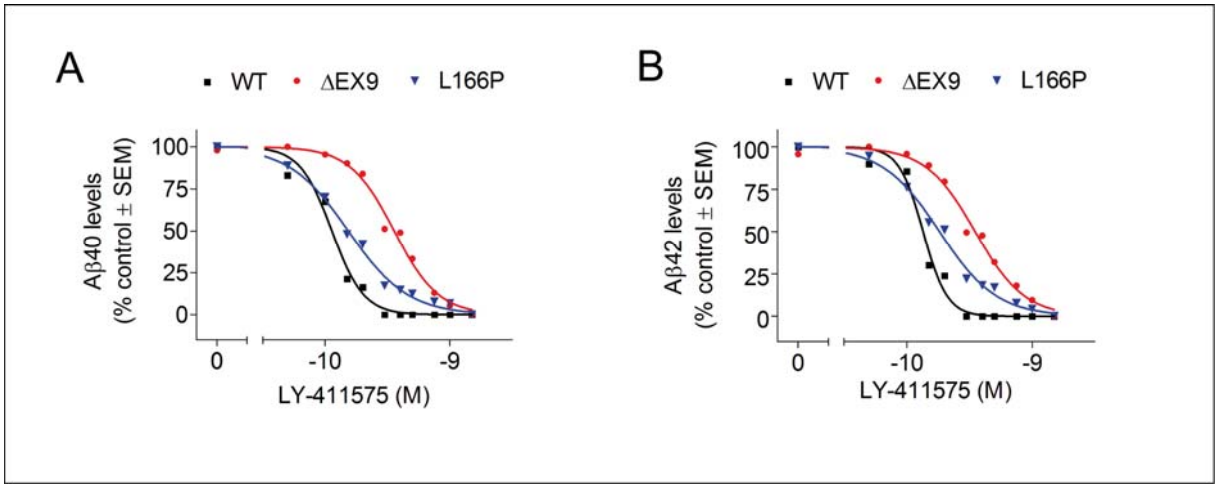

Fig. 4.1.4.5 EC50 values for γ-secretase inhibitor LY-411575 are increased in cell lines expressing FAD PS1 mutants. Cell lines expressing PS1-WT, PS1-ΔExon9, and PS1-L166P were subjected to extended dose-response experiments with 10 different concentrations of the benzodiazepine-like γ-secretase inhibitor LY-411575, Aβ levels in conditioned media were quantified

and dose-response curves generated. (A) The Aβ40 response in both mutant cell lines was attenuated as compared to PS1-WT cells. EC50 values for Aβ40 inhibition were increased from EC50 PS1-WT = 113.5 pM, to EC50 PS1-ΔExon9 = 358.3 pM, and EC50 PS1-L166P = 153.6 pM. (B) The Aβ42 response was similarly affected as the Aβ40 response. EC50 values for Aβ42 inhibition were increased for both mutant cell lines, EC50 PS1-WT =135.2 pM, EC50 PS1-ΔExon9 = 352.1 pM, and EC50 PS1-L166P = 183.1 pM.

A more extended analysis after treatment with 10 different concentrations of LY-411575 revealed a shift in the EC50 values for Aβ40 (Fig. 4.1.4.5 A) and Aβ42 inhibition (Fig. 4.1.4.5 B) in both mutant cell lines. For the PS1-ΔExon9 mutation the EC50 values for Aβ40 (= 358 pM) and Aβ42 (= 352 pM) increased more than 2-fold as compared to PS1-WT cells (Aβ40 = 114 pM and Aβ42 = 135 pM). In summary, cell lines expressing the FAD PS1 mutants PS1-ΔExon9 and PS1-L166P displayed a strongly reduced response to γ-secretase inhibitors of different structural classes and potencies that are known to interact with different sites of PS1.

4.1.5 The higly potent γ-secretase inhibitor LY-411575 failed to reduce Aβ42 levels in brain of an AD mouse model with transgenic expression of the PS1-L166P mutation

We next wanted to test whether the attenuated response of our PS1 mutant cell lines to GSMs and γ-secretase inhibitors might have consequences for the evaluation of such compounds in transgenic animal models of AD. To address this issue, we compared two transgenic animal models of AD in their response to treatment with the LY-411575 inhibitor: single transgenic mice expressing Swedish mutant APP (Tg2576 mice (Hsiao, Chapman et al. 1996)) and double transgenic mice expressing Swedish mutant APP and the PS1-L166P mutation (APPPS mice (Radde, Bolmont et al. 2006)). Both models were orally dosed with 10 mg/kg of LY-411575 or vehicle, and levels of soluble Aβ in brain were determined by ELISA 3 h post-administration. In the Tg2576 mice Aβ40 as well as Aβ42 levels were decreased by more than 80 % after inhibitor treatment as compared to animals treated with vehicle (Fig. 4.1.5.1 A and Table 4.1.5.1). In contrast, while the inhibitor also reduced Aβ40 levels in brains of the double-transgenic APPPS mice by 80%, it failed to significantly reduce Aβ42 levels (Fig. 4.1.5.1 B and Table 4.1.5.1).

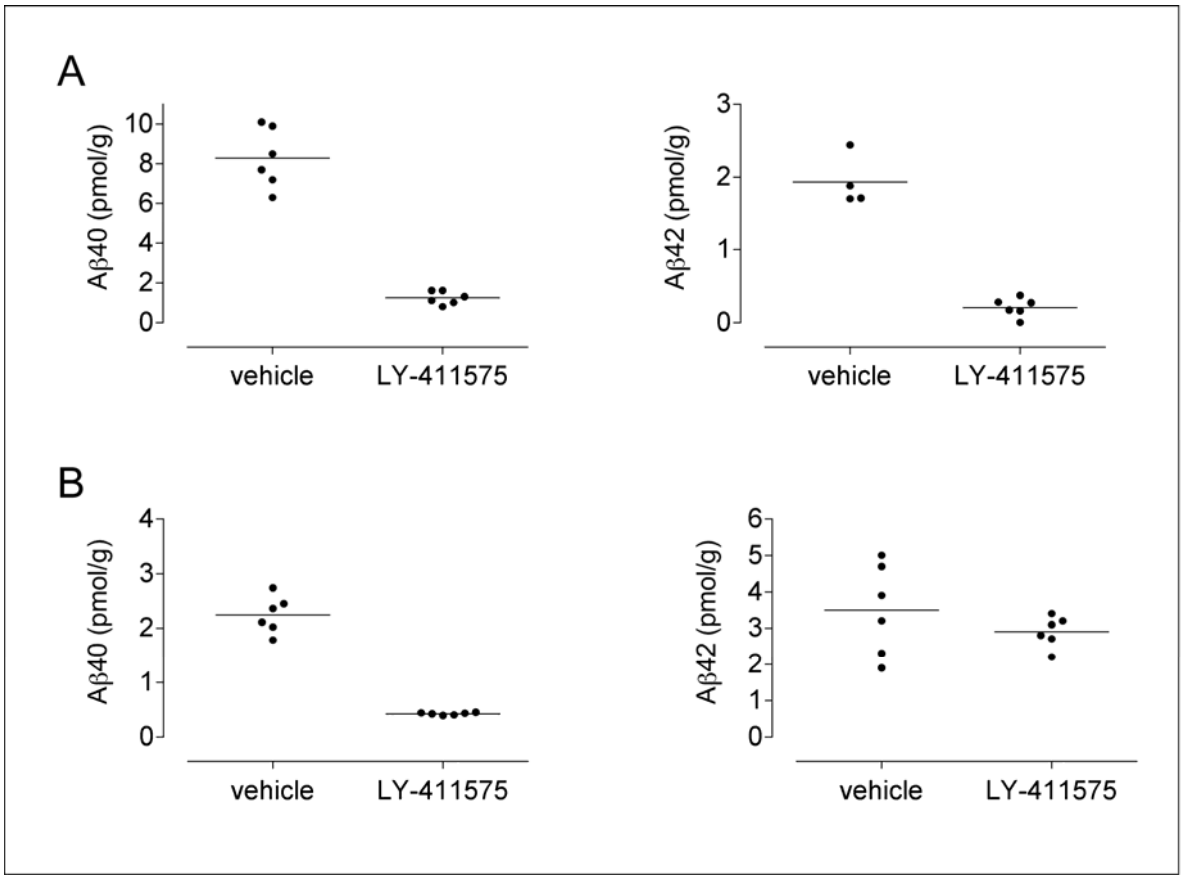

Fig. 4.1.5.1 The highly potent γ-secretase inhibitor LY-411575 failed to reduce Aβ42 levels in brain of PS1-L166P transgenic mice. Single-transgenic mice expressing Swedish mutant APP (Tg2576 mice, n = 4-6) and double-transgenic mice expressing Swedish mutant APP and PS1-L166P (APPPS mice, n = 6) were orally dosed with 10 mg/kg of LY-411575 or vehicle. 3 h post-administration animals were sacrificed and Aβ levels in whole brain homogenates were quantified by ELISA. (A) Tg2576 mice showed more than 85% reduction in Aβ40 (left panel) as well as in Aβ42 (right panel) levels after inhibitor treatment as compared to vehicle treated control animals. (B) In sharp contrast, in APPPS mice, while Aβ40 levels were also reduced by more than 80 % after inhibitor treatment compared to vehicle treated control (left panel), the inhibitor failed to significantly reduce Aβ42 levels (right panel).

Table 4.1.5.1 γ-secretase inhibitor LY-411575 failed to reduce Aβ42 levels in brain of PS1-L166P transgenic mice. n = 4-6; ***p<0.001, paired t-test.

	Tg2576 (APP Swedish)		APPPS (APP Swedish/ PS1-L166P)	
	Aβ40	Aβ42	Aβ40	Aβ42
	pmol/g		pmol/g	
Vehicle	8.23 ± 0.62	1.93 ± 0.17	2.90 ± 0.18	3.5 ± 0.51
LY-411575	1.23 ± 0.13	0.21 ± 0.05	0.42 ± 0.01	2.9 ± 0.18
% reduction	85***	89***	81.2***	17.1

4.2 Independent generation of Aβ42 and Aβ38 peptide species by γ-secretase

4.2.1 γ-secretase modulator treatment of FAD mutant PS1 cell lines increases Aβ38 production despite lack of Aβ42 reduction

Substantial evidence points to a coordinated production of Aβ42 and Aβ38 peptide species. In fact, the generation of these two peptides seems to be inversely regulated. Aβ42 reduction after GSM treatment leads to a concomitant increase in Aβ38 levels. On the contrary, treatment with inverse GSMs such as celecoxib and fenofibrate leads to an increase in Aβ42 levels that is accompanied by a decrease in Aβ38 production (Weggen, Eriksen et al. 2001; Kukar, Murphy et al. 2005). Similarly, treatment of cells with some γ-secretase inhibitors at subinhibitory concentrations increased Aβ42 levels, while decreasing Aβ38 generation. (Zhao, Tan et al. 2007). Furthermore, mutations in the GXXXG motif in the Aβ-region of APP mimic effects of GSMs and lead to a reduction in Aβ42 production while increasing Aβ38 generation (Munter, Voigt et al. 2007). These results clearly point to an interdependence in production of these two peptides. Taken together with findings that Aβ46, Aβ43 and Aβ40 seem to be generated by sequential cleavage of the longer into the shorter peptides, these observations suggested a possible precursor-product relationship between Aβ42 and Aβ38 (Yagishita, Morishima-Kawashima et al. 2006). To further investigate the relation between the production of Aβ38 and Aβ42, we utilized our model system of cell lines that are non-responsive to treatment with GSMs. We measured amounts of secreted Aβ38 in conditioned media of the cell lines expressing PS1-WT, PS1-ΔExon9, PS1-L166P, PS1-P117L, and PS1-G384A after treatment with 30 μM and 60 μM sulindac sulfide. These Aβ38 measurements were performed in the same conditioned media samples as shown in figure 4.1.4.2. While the Aβ42 response to sulindac sulfide treatment in cell lines expressing FAD mutant PS1 was strongly attenuated as compared to PS1-WT cells (Fig. 4.2.1.1 A), there was no significant difference in the Aβ38 increase between cell lines expressing FAD mutant PS1 or PS1-WT (Fig. 4.2.1.1 B and Table 4.2.1.1). Treatment with 30-60 μM sulindac sulfide led to a 1.5-2-fold increase in Aβ38 levels as compared to vehicle treated control. The observed increase was similar in all cell lines. To exclude a compound specific effect, we further treated the cell lines with the structurally divergent Aβ42-lowering NSAID ibuprofen. The cells were subjected to treatment with 250 μM ibuprofen, Aβ levels in conditioned media were quantified, and compared by one-way ANOVA. At this concentration, ibuprofen did not cause toxicity (Weggen, Eriksen et al. 2001), and no significant reductions in Aβ40 production were observed (Fig. 4.2.1.2 A).

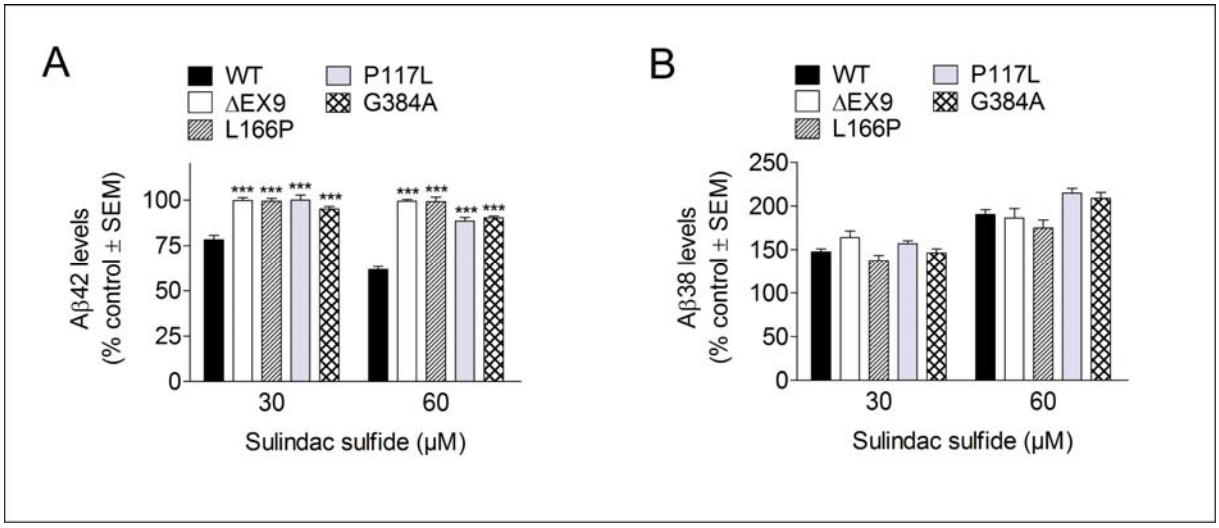

Fig. 4.2.1.1 Independent generation of Aβ42 and Aβ38 peptides by γ-secretase in cell lines expressing aggressive FAD PS1 mutants. APP CHO cells with stable expression of PS1 mutants were subjected to repeated treatment with 30 μM and 60 μM of the Aβ42-lowering NSAID sulindac sulfide or DMSO vehicle. Aβ levels in conditioned media were quantified by sandwich immunoassay and are depicted in percentage of vehicle treated control. (A) The Aβ42 response in the mutant cell lines was strongly attenuated compared to PS1-WT expressing cells. (B) All cell lines showed a similar dose-dependent increase in Aβ38 levels after sulindac sulfide treatment. There was no significant difference in Aβ38 production between cell lines expressing PS-WT or mutant PS1, indicating that Aβ42 and Aβ38 peptides can be generated independently of each other. n = 5; one-way ANOVA, ***p < 0.001; Dunnett's post tests.

Table 4.2.1.1 Aβ38 levels are similarly increased in cell lines expressing PS1-WT or mutant PS1 after treatment with the Aβ42-lowering NSAID sulindac sulfide. Aβ levels are shown in percentage of vehicle treated controls. n = 5.

	Aβ38 levels	
	30 μM	60 μM
	% control ± SE	
Cell line		
PS1-WT	147.88 ± 3.37	190.44 ± 5.65
PS1-ΔExon9	164.01 ± 7.49	186.59 ± 10.81
PS1-L166P	137.77 ± 5.62	175.07 ± 9.19
PS1-P117L	157.00 ± 3.55	215.01 ± 5.55
PS1-G384A	146.37 ± 4.84	209.26 ± 6.56

In PS1-WT control cells, ibuprofen induced a strong reduction in Aβ42 levels whereas all cell lines expressing mutant PS1 displayed a significantly attenuated response (Fig. 4.2.1.2 B and Table 4.2.1.2). In contrast, comparable to our findings with sulindac sulfide, we observed an approximately 1.5-fold increase in Aβ38 levels after ibuprofen treatment in PS1-WT cells and cells expressing FAD PS1 mutants (Fig. 4.2.1.2 C and Table 4.2.1.2). In conclusion, while the Aβ42 response to GSM treatment is strongly attenuated in mutant PS1 expressing cell lines compared to PS1-WT cell lines, the concomitant increase in Aβ38 levels is similar

in all cell lines. This suggests that Aβ42 and Aβ38 peptide species can be generated independently of each other.

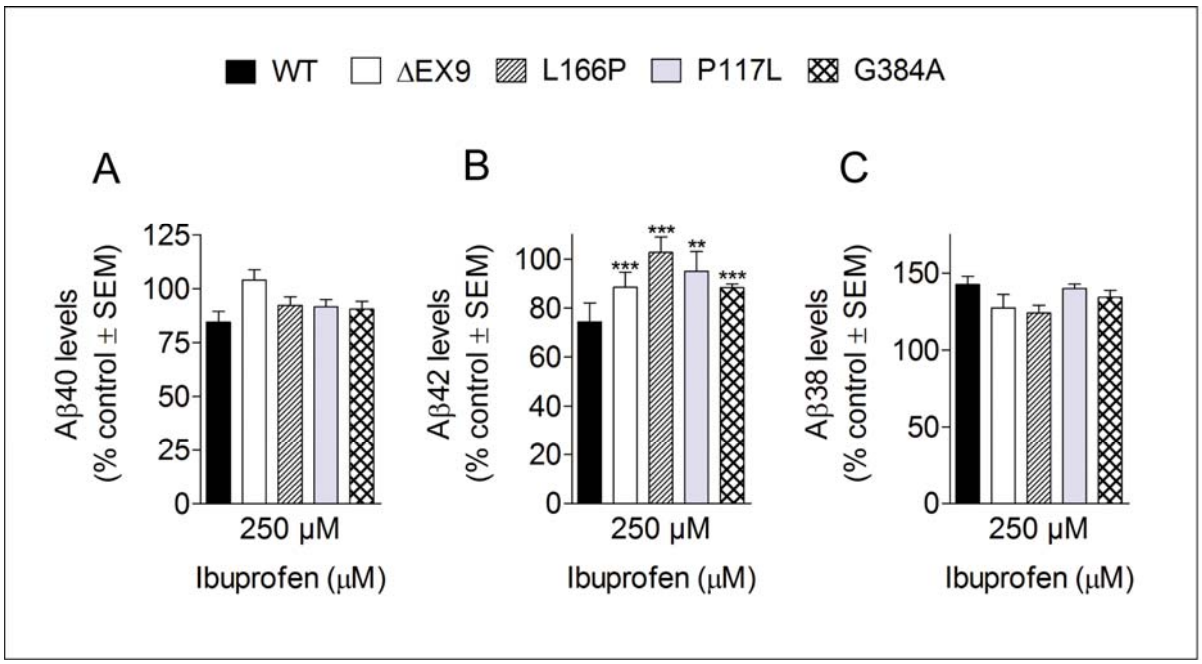

Fig. 4.2.1.2 PS1 mutants are non-responsive to the Aβ42 lowering activity of ibuprofen but display a similar increase of Aβ38 levels as compared to PS1-WT expressing cells. APP CHO cells with stable expression of PS1-WT or mutant PS1 were treated with 250 µM ibuprofen or DMSO vehicle and Aβ peptides were quantified by LPECL. The graphs depict the Aβ levels in percentage of vehicle treated control. (A) Aβ40 levels were not significantly changed after treatment with 250 µM ibuprofen as compared to vehicle treated control. (B) Cells expressing FAD mutant PS1 displayed a strongly diminished Aβ42 response after ibuprofen treatment compared to PS1-WT control cells. (C) In contrast, Aβ38 production was increased to the same level in cells expressing PS1 mutants or PS1-WT. n = 5; one-way ANOVA; ***p < 0.001; **p < 0.01; Dunnett's post tests.

Table 4.2.1.2 PS1 mutants are non-responsive to the Aβ42-lowering activity of ibuprofen, but display a similar increase of Aβ38 levels as compared to PS1-WT. Aβ levels are shown in percentage of vehicle treated controls. n = 5; one-way ANOVA; ***p < 0.001; **p < 0.01; Dunnett's post tests.

	Ibuprofen 250 µM	
Cell line	Aβ42 levels (% control ± SEM)	Aβ38 levels (% control ± SEM)
PS1-WT	62.89 ± 3.31	142.50 ± 5.31
PS1-ΔExon9	94.26 ± 4.21***	127.40 ± 8.52
PS1-L166P	111.40 ± 4.90***	124.10 ± 4.82
PS1-P117L	81.37 ± 3.60**	139.90 ± 2.82
PS1-G384A	88.40 ± 1.80***	134.30 ± 4.44

4.2.2 γ-secretase modulator treatment of non-responsive mutant PS1 cell lines does not cause compensatory changes in other Aβ peptide

To examine the possibility that PS1 mutants would cause overall alterations in the pattern of Aβ peptides, or that GSM treatment would induce compensatory changes of other Aβ peptide species that are not detectable with our C-terminal antibodies that recognize only Aβ40, Aβ42, and Aβ38 we analyzed the full spectrum of Aβ peptides secreted by PS1-WT, PS1-ΔExon9, and PS1-L166P cells by mass spectrometry. The cells were subjected to treatment with 60 µM sulindac sulfide and Aβ peptides from cell culture supernatant were immunoprecipitated with an antibody recognizing the first 16 amino acids of the Aβ sequence, thus allowing precipitation of all C-terminal truncated peptide species. The immunoprecipitated material was then analyzed by MALDI-TOF-TOF.

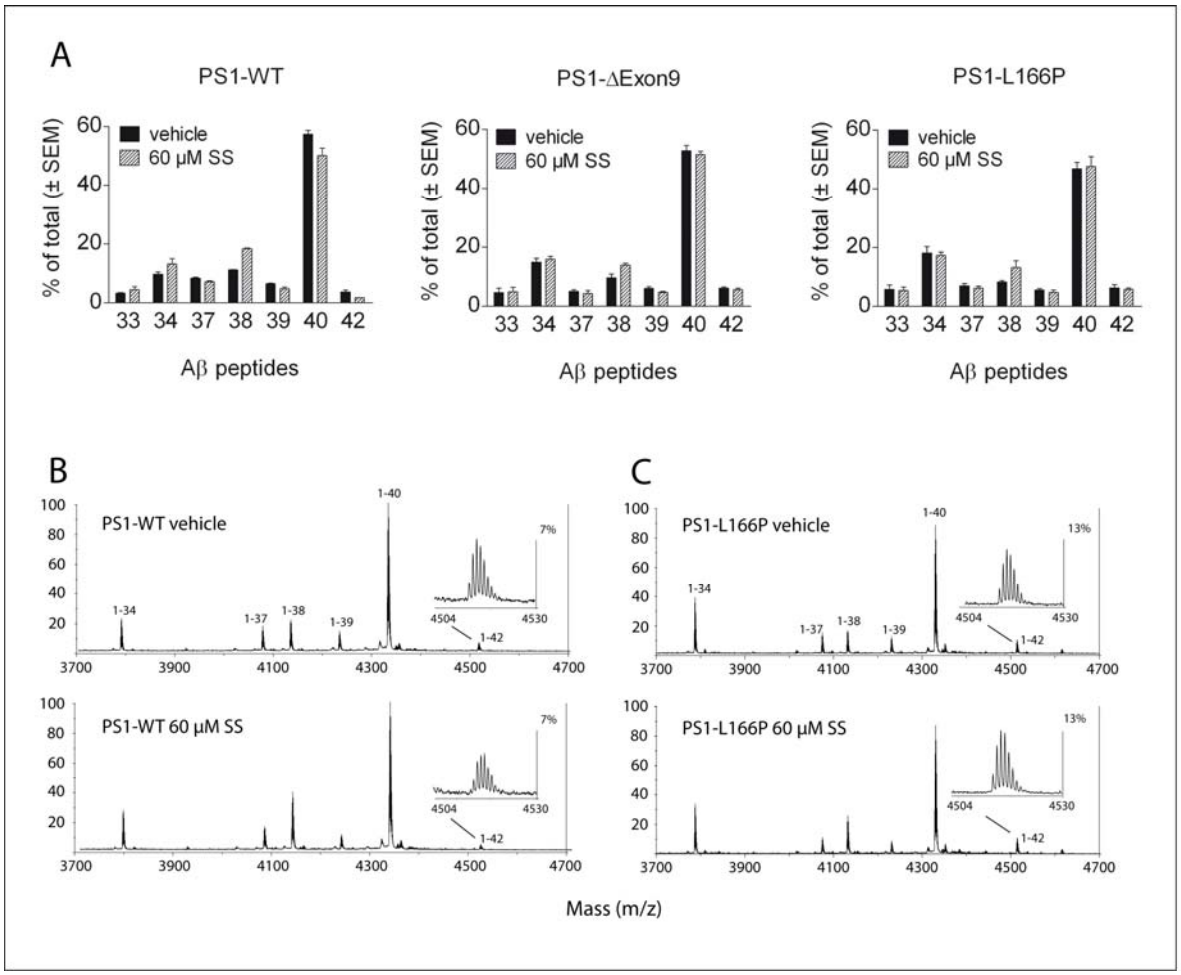

Fig. 4.2.2.1 Mass spectrometry analysis of Aβ peptide species after treatment with the Aβ42-lowering NSAID sulindac sulfide. (A) APP CHO cell with stable expression of PS1-WT, PS1-ΔExon9, and PS1-L166P were treated with 60 µM sulindac sulfide (SS) or DMSO vehicle. Conditioned media were immunoprecipitated with an antibody recognizing the first 16 amino acids of the Aβ sequence, and analyzed by MALDI-TOF-TOF. Peptides ranging from Aβ33 to Aβ40 and Aβ42 were

detected. To determine the relative abundance of individual Aβ peptides, the area of the isotopic cluster from three independent experiments was averaged and then presented as % of total observed signals. Reproducing our sandwich immunoassay results, cell lines expressing PS1 mutants ΔExon9 and L166P displayed an attenuated Aβ42 response to sulindac treatment compared to PS1-WT cells, while Aβ38 levels were induced in all three cell lines. However, no additional changes in the Aβ peptide profile pattern were observed after GSM treatment. (B) Representative mass spectrometry spectra from PS1-WT control cells treated with DMSO vehicle or 60 μM sulindac sulfide. Each spectrum is normalized to the tallest peak (Aβ40) and the percentage of Aβ42 relative to Aβ40 is shown in expanded inserts, Y-axis is relative intensity. (C) Representative mass spectrometry spectra from PS1-WT and PS1-L166P cells treated with DMSO vehicle and 60 μM sulindac sulfide.

To determine the relative abundance of individual Aβ peptides, the area of the isotopic cluster of each peptide was analyzed (Fig. 4.2.2.1 A). The profiles of Aβ peptides produced by cells expressing PS1 mutants have not been examined in detail previously. Interestingly, although the full range of Aβ peptides from Aβ1-33 to Aβ1-40 and Aβ42 was produced, we observed that Aβ34 levels appeared slightly higher in PS1 mutant cells as compared to PS1-WT cells (Fig. 4.2.2.1 A). The mass spectrometry data confirmed our earlier sandwich immunoassay results, showing that the cells expressing mutant PS1 displayed an attenuated Aβ42 response to sulindac sulfide treatment compared to PS1-WT expressing cells, whereas the levels of Aβ38 were increased in all cell lines (Fig. 4.2.2.1). More importantly, the mass spectrometry analysis revealed no further changes in the Aβ peptide profile pattern after sulindac treatment. In addition to the mass spectrometry analysis we analyzed the Aβ peptide profiles on high resolution urea gels. Cell lines expressing PS1-WT, PS1-L166P, and PS1-G384A were treated with 60 μM sulindac sulfide or DMSO vehicle and cell culture supernatants were loaded on high resolution urea gels. The gels were subjected to Western Blotting and Aβ peptides were detected. These experiments again confirmed our sandwich immunoassay and mass spectrometry results: a reduction of Aβ42 in PS1-WT cells after sulindac treatment with a concomitant increase in Aβ38 levels after sulindac sulfide treatment was observed in PS1-WT cells, while no Aβ42 reduction could be observed in cell lines expressing either PS1-L166P or PS1-G384A. Despite this lack of Aβ42 response there was an increase in Aβ38 levels in both mutant cell lines (Fig. 4.2.2.2 A and B). Quantification of three independent experiments also demonstrated no additional changes in the Aβ peptide profile, again confirming the mass spectrometry results (Fig. 4.2.2.2 B).

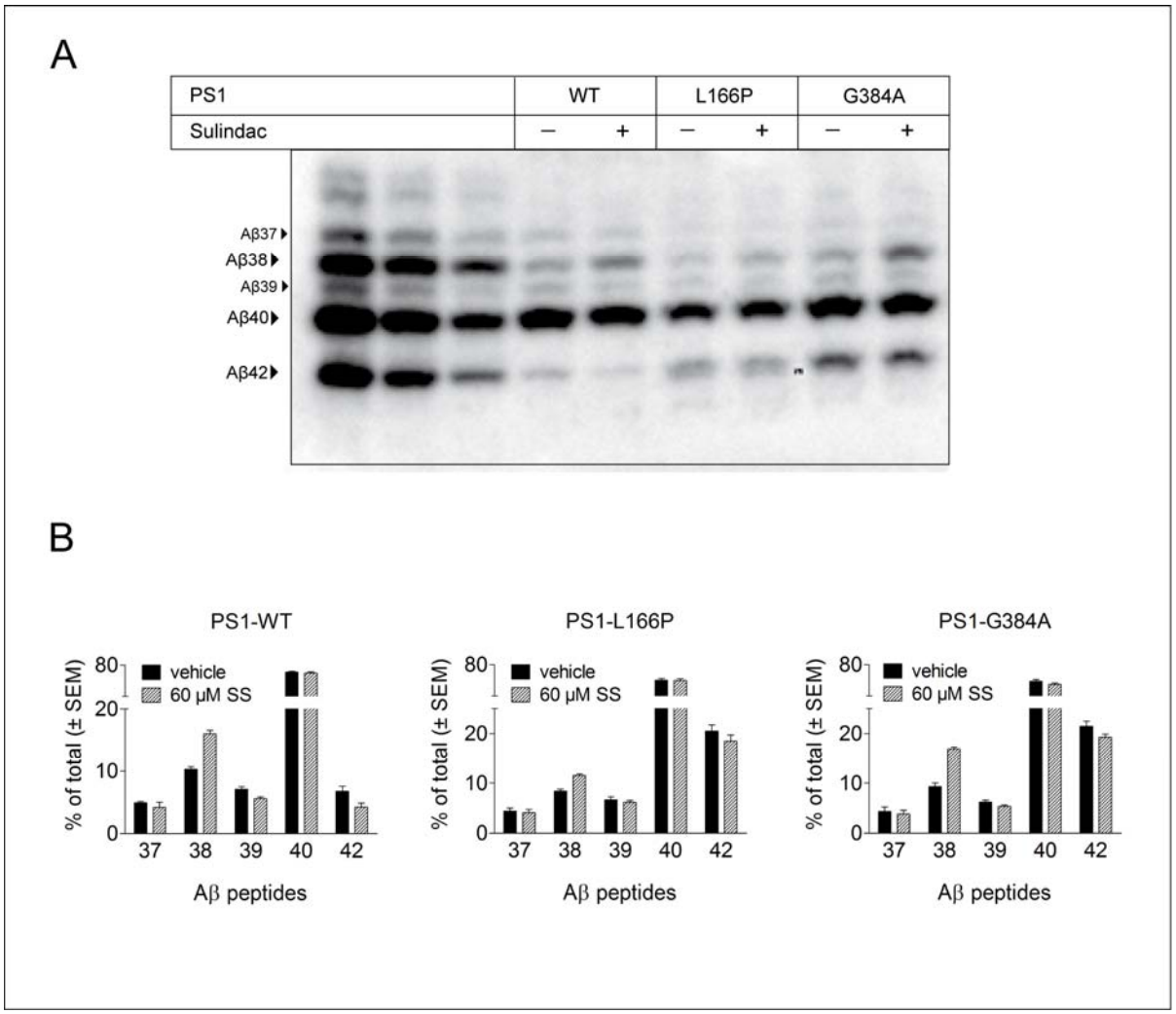

Fig. 4.2.2.2 High resolution urea gel analysis of the Aβ peptide profile of cell lines expressing PS1-WT, PS1-L166P, and PS1-G384A after treatment with the Aβ42-lowering NSAID sulindac sulfide. APP CHO cells were treated with 60 µM sulindac sulfide or DMSO vehicle and conditioned media were loaded on a high resolution urea gel, capable of resolving Aβ37, Aβ38, Aβ39, Aβ40 and Aβ42 peptides. Aβ peptides were detected with an antibody recognizing the first 16 amino acids of the Aβ peptide sequence. (A) Representative Western Blot displaying the attenuated Aβ42 response of cell lines expressing PS1-L166P and PS1-G384A to sulindac treatment as compared to PS1-WT cells. In contrast, Aβ38 levels were increased in all cell lines. Synthetic Aβ peptides in decreasing concentrations were loaded as molecular weight markers in the first three lanes. (B) Three independent experiments were quantified, the relative abundance of each peptide was determined, and displayed as % of all Aβ peptides. While Aβ42 levels in PS1-WT cells were reduced by approximately 40%, both mutant cell lines displayed a maximum reduction of 10%. Aβ38 levels were increased after sulindac treatment in all cell lines, whereas the abundance of all other peptides was unchanged. n = 3.

5 Discussion

γ-secretase is a multiprotein complex consisting of at least four different proteins, presenilin (either PS1 or PS2), APH-1, nicastrin and PEN-2. These four proteins are both necessary and sufficient to form an active γ-secretase complex (Edbauer, Winkler et al. 2003; Kimberly, LaVoie et al. 2003). Presenilin contains the active center of the complex, with two catalytically active aspartates in TMD 6 and 7 (Wolfe, Xia et al. 1999; Nyabi, Bentahir et al. 2003). The whole γ-secretase complex is embedded in the membrane and presenilin adopts a 9 TMD conformation with the N-terminus protruding into the cytoplasm and the C-terminus directed towards the extracellular/lumenal side (Laudon, Hansson et al. 2005; Oh and Turner 2005). During the maturation of the complex presenilin becomes endoproteolytically processed into an NTF and a CTF (Brunkan, Martinez et al. 2005). The γ-secretase complex plays a pivotal role in the generation of the Aβ peptides, the key agents in the development of AD. γ-secretase catalyzes the final step in the proteolytic processing of the β-cleaved APP C-terminal stub, leading to the production of varying Aβ peptides (Haass, Schlossmacher et al. 1992). Moreover, the presenilin genes harbour more than 150 mutations leading to aggressive forms of early-onset AD (Levylahad, Wasco et al. 1995; Rogaev, Sherrington et al. 1995). This makes γ-secretase one of the major targets in AD drug development.

Inhibitors of γ-secretase were first identified in 1998, and since then a number of highly potent inhibitors were synthesized and characterized (Wolfe, Citron et al. 1998; Wolfe, Xia et al. 1999). These compounds belong to different structural classes and were found to target different binding sites in the γ-secretase complex, which seem to be located on the presenilin molecule. Some compounds were modelled after transition-state inhibitors for aspartyl proteases and they directly target the active center of the complex. One example of a transition-state inhibitor is the compound L-685,458. The binding site for these inhibitors is the active center, and in the γ-secretase complex they bind to both the PS1 NTF and CTF, consistent with the location of the active center at the interface of PS1 TMDs 6 and 7 (Esler, Kimberly et al. 2000; Li, Xu et al. 2000). Transition-state inhibitors do not interfere with the binding of the substrate to the γ-secretase complex, indicating that the complex contains an initial substrate binding and recognition site that is different from the active center (Esler, Kimberly et al. 2002). Another class of γ-secretase inhibitors are α-helical peptides modelled after the APP transmembrane domain. These potent inhibitors bind in competition to substrate and block the initial substrate binding site on PS1 (Kornilova, Bihel et al. 2005). A third class of small molecule inhibitors includes arylsulfonamides, dipetidic inhibitors such as DAPT, and benzodiazepine-like compounds such as LY-411575. Photoactivatible derivatives of these compounds were found to target yet another binding site, which is located in the PS1 CTF (Morohashi, Kan et al. 2006).

In addition to these pan-γ-secretase inhibitors a new class of γ-secretase modulators (GSMs) that lower Aβ42 production, but spare Notch processing has been discovered (Weggen, Eriksen et al. 2001). These GSMs such as the NSAIDs sulindac sulfide or ibuprofen also seem to target the γ-secretase complex as indicated by their ability to exert their Aβ42-lowering function in cell-free γ-secretase assays (Eriksen, Sagi et al. 2003; Takahashi, Hayashi et al. 2003; Weggen, Eriksen et al. 2003; Beher 2004; Beher, Clarke et al. 2004). Enzyme kinetics and displacement studies show that GSMs act non-competitively with respect to substrate and to transition-state γ-secretase inhibitors arguing for a novel allosteric binding site (Beher, Clarke et al. 2004). Further support that GSMs target γ-secretase is drawn from the observation that FAD-associated PS1 mutations can modulate the cellular response to treatment with these compounds. The PS1-M146L mutation was shown to enhance the cellular response to treatment with Aβ42-lowering NSAIDs. In contrast, the PS1-ΔExon9 mutation almost completely abolishes the cellular response to GSMs (Weggen, Eriksen et al. 2003). While most of the FAD associated PS1 mutations are point mutations, the PS1-ΔExon9 mutation is a complex mutation with several characteristics (Perez-Tur, Froelich et al. 1995). It is caused by a splice site mutation that leads to the deletion of a whole exon. In addition, the deletion of amino acids 291-319 creates a point mutation (S290C) at the newly formed border of exon 8 to exon 10. The deleted region also contains the endoproteolytic cleavage site of the PS1 molecule. Therefore the mutant protein accumulates in its full-length form (Steiner, Romig et al. 1999). Because the mutation is non-responsive to GSMs and deletes a substantial stretch of amino acids in the PS1 molecule, we speculated that the deleted region might contain either a primary binding site for the GSMs or might cause a dramatic conformational change in PS1 that interferes with GSM binding to the γ-secretase complex. We therefore undertook a genetic dissection of the PS1-ΔExon9 mutation. As a first step, we wanted to determine the cause for the pathogenic increase in Aβ42/40 ratio associated with the PS1-ΔExon9 mutation. This issue had not been fully resolved even though a previous study pointed to the S290C point mutation as expression of mutant PS1 with the Δ291-319 deletion alone did not result in a change in Aβ production (Steiner, Romig et al. 1999). However, these authors did not investigate the effect of the S290C point mutation in a PS1-WT background. Our investigations with different PS1 constructs, which represented the distinct characteristics of the PS1-ΔExon9 mutation clearly showed that the S290C point mutation was not responsible for the pathogenic increase of the Aβ42/40 ratio observed with the PS1-ΔExon9 mutation. In addition, we were able to confirm the previous results that neither the Δ291-319 deletion nor the lack of endoproteolysis caused by the artificial M292D point mutation changed Aβ production (Steiner, Romig et al. 1999). These observations showed that none of the single characteristic of the PS1-Exon9 mutation was sufficient to cause the pathogenic changes in Aβ production associated with

this FAD PS1 mutation. Surprisingly, combining the S290C mutation with the M29D point mutation, and thus placing the S290C point mutation in an endoproteolysis deficient background, resulted in a pathogenic increase in the Aβ42/40 ratio. Our explanation for these findings is that two point mutations which alone did not cause any changes in Aβ production could synergistically force a conformational change in the γ-secretase complex, leading to a pathogenic increase in the Aβ42/40 ratio.

Consistent with these findings, we found that the S290C point mutation was also not responsible for the attenuated Aβ42-response of the PS1-ΔExon9 mutation after treatment with GSMs. In contrast, our results indicate that the diminished response of the PS1-ΔExon9 mutation was mainly caused by its lack of endoproteolytic cleavage as cell lines expressing both the PS1-Δ291-319 deletion and the PS1-M292D mutation displayed a similar attenuation in the Aβ42 response to GSM treatment as the PS1-ΔExon9 mutant cell line. While these results were not able to define a circumscribed binding site for GSMs, they rather argue that conformational changes caused by the lack of endoproteolysis might be responsible for the diminished Aβ42 response and that GSMs might have a lower affinity to the non-cleaved flPS1 molecule. Furthermore, the introduction of the M146L mutation, which was previously shown to enhance the response to GSMs (Weggen, Eriksen et al. 2003), was able to overcome these conformational changes and the PS1-M292D/M146L mutant cell line behaved similar to PS1-WT cells. Further support for the idea that conformational changes are the underlying cause for the increase in the Aβ42/40 ratio as well as for the attenuated response to GSM treatment in the PS1-ΔExon9 mutation comes from FLIM studies of wild-type and mutant PS1. In these studies it was shown that FAD PS1 mutations force a conformational change on PS1, which resulted in a closer proximity of the C-terminus and the N-terminus of the protein. In contrast, treatment of PS1-WT expressing cells with Aβ42-lowering NSAIDs led to an increase in the distance between the ends of the PS1 molecule (Lleo, Berezovska et al. 2004; Berezovska, Lleo et al. 2005).

We next wanted to investigate whether the attenuated response to GSMs is restricted to the PS1-ΔExon9 mutation. In a subsequent screen of FAD PS1 mutants we immediately found three more aggressive early-onset PS1 missense mutations that displayed an equally attenuated Aβ42 response to GSM treatment as the PS1-ΔExon9 mutation. This observation shows that the diminished response to Aβ42-lowering NSAIDs is not a unique characteristic of the PS1-ΔExon9 mutation, but rather common among FAD associated PS1 mutations. In an earlier study it was found that the GSM-insensitive PS1-ΔExon9 mutation was also only partially sensitive to the transition state γ-secretase inhibitor L-685,458 (Ikeuchi, Dolios et al. 2003). We also observed a diminished response of the PS1-ΔExon9 cells to treatment with L-685,458 as compared to PS1-WT cells confirming these earlier results. Given our observations with GSMs, we speculated that this might also be true for other aggressive FAD

PS1 mutations, and were able to show that the PS1-L166P mutation displayed an equally reduced sensitivity to treatment with this γ-secretase inhibitor. Furthermore, we were able to extend these findings to other γ-secretase inhibitors of different structural classes and increasing potencies, the semi-peptidic inhibitor DAPT and the benzodiazepine-like inhibitor LY-411575. Interestingly, the attenuation in Aβ reduction observed in the PS1-L166P mutant cell line after treatment with all of these γ-secretase inhibitors was markedly more pronounced for Aβ42 than for Aβ40.

How these FAD PS1 mutations similarly change the effects of γ-secretase modulators and γ-secretase inhibitors have on Aβ production remains uncertain, as these compounds seem to target different sites in the γ-secretase complex. One possibility is that the binding sites are in close proximity and therefore equally perturbed by conformational changes in the PS1 protein caused by FAD mutations. In fact, it was shown that the initial substrate docking site on PS1 is located close to the active center. α-helical peptides of 10 amino acids were shown to bind to the proposed substrate docking site on PS1, and addition of only 3 more amino acids enhanced the inhibitory properties of the peptide and resulted in blockage not only of the substrate docking site but also of the active center, indicating that these two sites are indeed in close proximity (Bihel, Das et al. 2004; Kornilova, Bihel et al. 2005). Compounds such as DAPT, which were shown to bind to the PS1 CTF, have been proposed to mediate their effect by interfering with the movement of the substrate from the initial docking site on PS1 to the active center (Tian, Ghanekar et al. 2003), which would position their binding site near the active center and the substrate docking site as well. The identity of the allosteric binding site of the GSMs in the γ-secretase complex is unknown. However, the surprising finding that the GSMs also modulate the proteolytic cleavage of signal peptide peptidase (SPP), a protein homologous to PS1 that functions without accessory proteins, favours a location within PS (Sato, Nyborg et al. 2006). Furthermore, in radioligand binding studies GSMs were able to displace transition-state and benzodiazepine γ-secretase inhibitors by non-competitive antagonism, providing further evidence for an allosteric interaction between the binding sites of these compounds (Beher, Clarke et al. 2004; Clarke, Churcher et al. 2006). An alternative explanation could be that the binding sites of γ-secretase inhibitors and γ-secretase modulators are not in close proximity, but that they are nonetheless equally affected by the conformational changes the FAD PS1 mutations force on the γ-secretase complex. In both scenarios, the conformational changes could simply lower the binding affinities of the compounds and thus lead to a reduced cellular response. In accordance with this argument, it was found that photolabelling of PS1-L166P with a transition state inhibitor was less efficient as compared to labelling of PS1-WT (Kornilova, Bihel et al. 2005). In contrast, the PS1-ΔExon9 mutant protein, which in our study was even less responsive to γ-secretase inhibitors than the PS1-L166P mutant, was readily photolabelled by DAPT and the

transition state γ-secretase inhibitor L-685,458 (Li, Xu et al. 2000; Morohashi, Kan et al. 2006). On the other hand, it can not be excluded that the FAD mutations lead to a reduced affinity of the inhibitors beyond the sensitivity of photolabelling studies. A final clarification of the mechanism behind these effects will most likely only be possible when high-resolution structural data of the γ-secretase complex is available.

Apart from these mechanistic aspects, our findings are highly relevant for the use of cellular and animal models of AD for drug discovery efforts aimed at γ-secretase. Cell lines with overexpression of APP are routinely used in small molecule screenings to identify and optimize γ-secretase inhibitors and modulators. In addition, these cell lines often express FAD PS1 mutation to facilitate easy detection of Aβ42. Even more important, while the first AD mouse models that were developed expressed only FAD mutant APP, almost all recent mouse models also express FAD associated PS1 mutations to enhance and accelerate pathology. One of the first mouse models that was developed is the Tg2576 mouse which expresses Swedish mutant APP695 (KM670/671NL) (Hsiao, Chapman et al. 1996). The Swedish mutation in APP enhances total Aβ production by facilitating more efficient BACE cleavage, but it does not affect the ratio between Aβ42 and Aβ40 peptides. The Tg2576 mice develop diffuse and focal Aβ deposits in brain starting at 9 months of age and there is no apparent cell death. One example for a more recent model with enhanced pathology is the APPPS mouse with transgenic expression of Swedish mutant APP and PS1-L166P (Radde, Bolmont et al. 2006). This mouse model is characterized by very fast accumulating amyloid pathology, starting at 6 weeks of age and increasing over time. In contrast to the single transgenic Tg2576 mouse, the additional PS1 mutation leads to a steep increase in the Aβ42/40 ratio in the brains of the APPPS mouse. The massively accelerated amyloid pathology and the higher levels of Aβ42 make double-transgenic mice with expression of FAD mutant APP and PS1 preferred models for treatment strategies targeting the amyloid pathology. Higher levels of Aβ42 facilitate easy detection and earlier onset of pathology allows faster analysis of treatment outcome. Even within the limited number of mutations we have analyzed in our study, three PS1 mutations that are non-responsive to GSMs and γ-secretase inhibitors have been used to generate mouse models of AD: PS1-L166P, PS1-ΔExon9, and PS1-P117L (Table 5.1) (Wen, Shao et al. 2002; Jankowsky, Fadale et al. 2004; Radde, Bolmont et al. 2006). Consistent with our *in vitro* findings, the γ-secretase inhibitor LY-411575 failed to reduce Aβ42 levels in brain of the APPPS mice, while we saw an approximately 80 % reduction in Aβ42 levels in the brain of Tg2576 mice used as control. In accordance with our findings, a recent study by Page et al. showed similar results for the highly potent γ-secretase modulator GSM-1. In their study the authors reported that GSM-1 failed to reduce Aβ42 levels in brains of a double-transgenic mouse model expressing Swedish mutant APP and the FAD associated PS2-N141I mutation, while Aβ42 levels were

strongly decreased in the brain of single transgenic mice expressing only Swedish mutant APP (Page, Baumann et al. 2007). Taken together, these results clearly show that using double-transgenic mouse models with overexpression of both FAD mutant APP and PS might confound *in vivo* studies of the potency and efficacy of GSMs and γ-secretase inhibitors.

Table 5.1 Double-transgenic mouse models of Alzheimer's disease (AD). Mouse models that are non-responsive to treatment with GSMs.

Mouse model	APP	PS	
APPPS	Swedish	PS1-L166P	(Radde, Bolmont et al. 2006)
APP_{sw}/PS1-ΔExon9	Swedish	PS1-ΔExon9	(Jankowsky, Fadale et al. 2004)
APP_{sw}/PS1-P117L	Swedish	PS1-P117L	(Wen, Shao et al. 2002)
APP^{SL} PS1KI	Swedish	PS1-M233T/L235P	(Casas, Sergeant et al. 2004)
APP_{sw}/PS2-N141I	Swedish	PS2-N141I	(Richards, Higgins et al. 2003)

The findings further strongly argue that such cellular and mouse models should be avoided in the preclinical development of novel therapeutic strategies targeting the γ-secretase complex. Finally, our results may also have relevance for future clinical studies of GSMs or γ-secretase inhibitors if these were to include patients with FAD associated PS mutations. Our tissue culture system reflects only insufficiently the situation in a patient with FAD associated PS mutations. The overexpression of PS in cells leads to a replacement of the endogenously expressed PS from the γ-secretase complex because the amount of accessory proteins, APH-1, PEN-2 and nicastrin is limited, and the amount of exogenously expressed mutant PS is much higher than the amount of endogenous PS. Accordingly, the γ-secretase complexes in our cellular model system contain mainly mutant PS1 which is decidedly different from the situation in a heterozygous FAD patient that should express mutant and wild-type PS1 in equal amounts. Therefore, it is possible that the attenuated response of our cell lines and the animal models to GSM and γ-secretase inhibitor treatment would not apply to FAD patients. Nevertheless, the possibility that these patients might respond differently to treatment with γ-secretase targeting drugs than patients with sporadic AD should be taken into consideration. To investigate this possibility better cellular and animal models are needed. Unfortunately, primary fibroblasts from patients with characterized FAD PS mutations are not available in public cell line repositories. To circumvent this problem we have recently obtained fibroblast cell lines from a PS1 knock-in mouse model that expresses a combination of two FAD associated PS1 mutations, PS1-M233T/L235P in the same PS1 molecule (Casas, Sergeant et al. 2004). From these mice we were able to establish cell lines with homozygous

expression of PS1-WT, homozygous expression of mutant PS1-M233T/L235P, or with heterozygous expression of PS1-WT and mutant PS1. This heterozygous cell line more closely reflect the situation of a patient with a FAD associated PS mutation. We were further able to show that the PS1-M233T/L235P mutation, when overexpressed in APP CHO cells, is also completely refractory to treatment with GSMs and γ-secretase inhibitors (E.Czirr, unpublished results). Hence, these cell lines will allow us to further investigate the influence of heterozygous FAD PS1 mutations GSMs and γ-secretase inhibitors, but also on the overall function of γ-secretase.

As mentioned before, γ-secretase dependent processing of the BACE-cleaved APP C-terminal stubs leads to the generation of a number of Aβ peptides that differ in the length of their C-termini, and detectable peptides range from Aβ34 to Aβ48. The exact mechanism through which γ-secretase accomplishes these multiple cleavage events is not known, but the current data points towards a coordinated production of the Aβ peptides, especially for Aβ42 and Aβ38 peptide species. This view is illustrated in the “sequential cleavage” model of Aβ generation, which proposes that longer Aβ peptides are trimmed to generate the shorter species. Such a coordinated production of Aβ peptides is also supported by pharmacological studies with GSMs and γ-secretase inhibitors. Treatment of cell lines with GSMs reduced Aβ42 production and concomitantly increased Aβ38 levels in a dose-dependent manner (Weggen, Eriksen et al. 2001; Eriksen, Sagi et al. 2003). Furthermore, inverse modulators such as fenofibrate were shown to specifically enhance Aβ42 production while decreasing Aβ38 generation (Kukar, Murphy et al. 2005). Similar observations were made with some γ-secretase inhibitors that, when used at sub-inhibitory concentrations, increased Aβ42 and led to an accompanying decrease of Aβ38 (Zhao, Tan et al. 2007). In addition, mutations of a GXXXG motif in the Aβ region of APP led to a decrease in Aβ42 production while increasing Aβ38 generation (Munter, Voigt et al. 2007). All these results point to a tightly connected production of these two peptides and indicate a possible precursor-product relationship. The issue of sequential versus non-sequential cleavage has important implications for the mechanism of action of GSMs but also of γ-secretase in general. In this respect, our model system of cell lines expressing FAD PS1 mutations that are non-responsive to GSMs, allowed us to further evaluate the relationship between Aβ42 and Aβ38 production. Surprisingly, we found that while the FAD PS1 cell lines were almost completely refractory to the Aβ42-lowering activity of the GSMs, their Aβ38 response was similar to the PS1-WT expressing cell lines, and we observed a dose-dependent increase in Aβ38 levels. Moreover, the investigation of the Aβ peptide profile pattern by MALDI-TOF-TOF and high resolution urea gel electrophoresis also excluded compensatory changes in other secreted Aβ peptide species. This observation that Aβ42 and Aβ38 peptides can be generated independently of each other seems to exclude a strict product-precursor relationship between these two

peptides. Similar uncoupling of Aβ42 and Aβ38 production was recently shown not only in mutant PS1 cell lines but also in a mouse model of AD expressing the PS2-N141I mutation (Page, Baumann et al. 2007). While Aβ42 production in the brains of these mice was not significantly affected by treatment with a highly potent GSM the mice displayed a dose dependent increase of Aβ38 levels, confirming our cell based data.

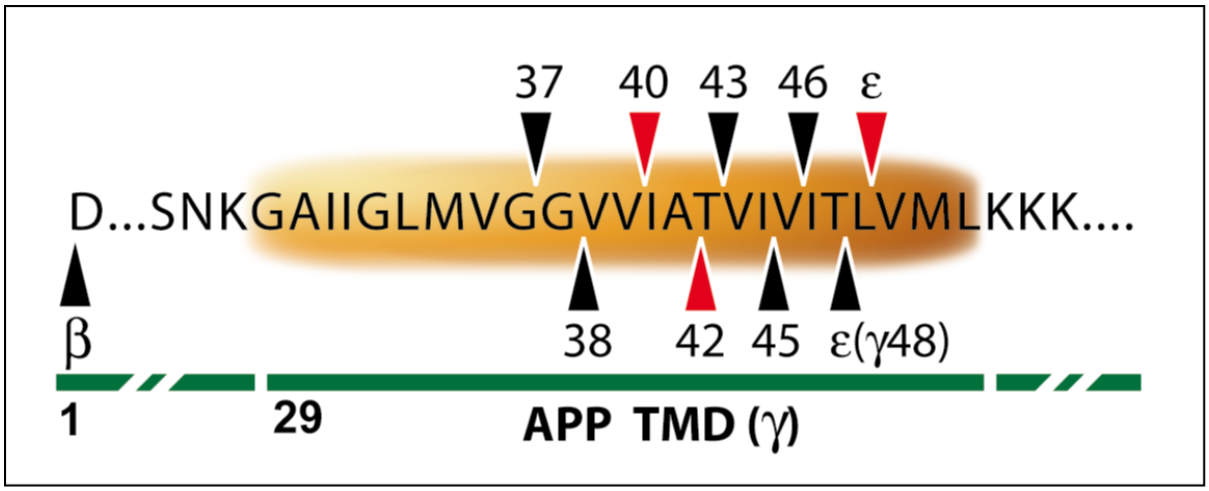

Fig. 5.1 APP transmembrane domain (TMD). Depicted are the different cleavage sites for Aβ peptide generation in the APP TMD. In a proposed α-helical model, the cleavage sites for the AICD (ε), Aβ46, Aβ43, Aβ40 and Aβ37 align on one side of the helix, while cleavage sites for Aβ48, Aβ45, Aβ42 and Aβ38 align on the opposite side of the helix.

Nonetheless, substantial data from other groups supports the sequential cleavage model of Aβ generation. The initial cleavage event seems to be the liberation of the AICD by cleavage at the ε-site, but how exactly the cleavage proceeds from there is unknown. It has been suggested that Aβ40 is to be produced by sequential cleavage of Aβ46 to Aβ43 and then Aβ40 (Yagishita, Morishima-Kawashima et al. 2008), but whether similar precursor-product relationships exist between other peptide species has not been resolved. Evidence indicates that the APP TMD has α-helical conformation with 3.6 residues forming one complete turn (Lichtenthaler, Wang et al. 1999; Wolfe, Xia et al. 1999). This would align cleavage sites for Aβ40, Aβ43, Aβ46, and Aβ49 on one surface of the helix, and cleavage sites for Aβ38, Aβ42, Aβ45, and Aβ48 on the other side (Fig. 5.1). This arrangement would suggests that the different Aβ peptide species could be generated depending on which surface of the helix is exposed to the active site of the γ-secretase complex. GSMs might then exert their Aβ42-lowering function by enhancing the interaction of the substrate Aβ42 with the active site, which would increase the turnover from Aβ42 to Aβ38 and thus lead to a reduction in Aβ42 generation. In contrast, FAD PS1 mutations might reduce the turnover of Aβ42 to Aβ38 and thus lead to an increase in Aβ42 generation. This is compatible with the evidence that some FAD PS1 mutations seem to cause reduced proteolytic activity of the γ-secretase complex.

However, our findings that Aβ42 and Aβ38 production can be uncoupled seem to favour a different model in which Aβ peptides are generated by independent cleavage events. In this model, GSMs might simply change substrate presentation to the active site by vertical movements of the substrate helix, which would more frequently expose the peptide bond after Aβ38 to the active center leading to an increase in Aβ38 and a reduction in Aβ42 generation. In any case, our results do not refute the concept of Aβ generation by sequential cleavage. Our model using PS1 mutations and GSM treatment did only allow to examine secreted Aβ species, but it remains possible that Aβ38 production is increased at the expense of other, longer Aβ peptides such as Aβ45 or Aβ46, which accumulate intracellularly and can not be resolved by mass spectrometry. Furthermore, the FAD PS1 mutations by themselves could lead to the uncoupling of Aβ42 and Aβ38 generation, if production of Aβ peptides by FAD mutant PS1 would be substantially different from generation of Aβ peptides in PS1-WT cells. Taken together, our findings clearly indicate that the sequential cleavage model could be an oversimplification, and that the mechanism of Aβ generation by γ-secretase might be even more complex than previously assumed.

7 Summary

According to the amyloid hypothesis, Alzheimer's disease (AD) is caused by aberrant production or clearance of the amyloid-β (Aβ) peptides, and in particular of the longer more aggregation-prone Aβ42. The Aβ peptides are generated through successive proteolytic cleavage of the amyloid precursor protein (APP) by the *β-site APP cleaving enzyme* (BACE) and γ-secretase. γ-secretase produces Aβ peptides with variable C-termini ranging from Aβ34 to Aβ48, presumably by sequential trimming of longer into shorter peptides. γ-secretase is a multiprotein complex consisting of at least four different proteins and the presenilin proteins (PS1 or PS2) contain the catalytic center of the complex. In 2001 several non-steroidal anti-inflammatory drugs were identified as the founding members of a new class of γ-secretase modulators (GSMs) that can selectively reduce production of Aβ42. Concomitantly, these GSMs increase Aβ38 production indicating closely coordinated generation of Aβ42 and Aβ38 and a potential precursor-product relationship between these peptides. GSMs seem to exert their activity by direct modulation of γ-secretase. Support for this hypothesis is drawn from the finding that some PS mutations associated with early-onset familial AD (FAD) can modulate the cellular response to GSMs and to γ-secretase inhibitors (GSIs), which inhibit production of all Aβ peptides and are known to directly interact with PS.

A particularly interesting FAD PS mutation is PS1-ΔExon9, a complex deletion mutant that blocks endoproteolysis of PS1 and renders cells completely non-responsive to GSMs. Studies presented in this thesis show that the diminished response of PS1-ΔExon9 to GSMs is mainly caused by its lack of endoproteolytic cleavage. Furthermore, we were able to demonstrate that a reduced response to GSMs and GSIs is not limited to PS1-ΔExon9 but is a common effect of aggressive FAD-associated PS1 mutations. Surprisingly, we also found that while the Aβ42 response to GSMs is almost completely abolished by these PS1 mutations, the accompanying Aβ38 increase was indistinguishable to wild-type PS1. Finally, the reduced response to GSIs was confirmed in a mouse model with transgenic expression of an aggressive FAD-associated PS1 mutation as a highly potent GSI failed to reduce Aβ42 levels in brain of these mice.

Taken together, our findings provide clear evidence for independent generation of Aβ42 and Aβ38 peptides, and argue that the sequential cleavage model might be an oversimplification of the molecular mechanism of γ-secretase. Most importantly, our results highlight the significance of genetic background in drug discovery efforts aimed at γ-secretase, and indicate that the use of cellular models with transgenic expression of FAD-associated PS mutations might confound studies of the potency and efficacy of GSMs and GSIs. Therefore, such models should be strictly avoided in the ongoing preclinical development of these promising and potentially disease-modifying therapeutics for AD.

8 References

Andersen, O., J. Reiche, et al. (2005). "Neuronal sorting protein-related receptor sorLA/LR11 regulates processing of the amyloid precursor protein." Proc Natl Acad Sci USA **102**(38): 13461-13466.

Asai, M., C. Hattori, et al. (2003). "Putative function of ADAM9, ADAM10, and ADAM17 as APP alpha-secretase." Biochemical and biophysical research communications **301**: 231-235.

Baek, S., K. Ohgi, et al. (2002). "Exchange of N-CoR corepressor and Tip60 coactivator complexes links gene expression by NF-kB and b-amyloid precursor protein." Cell **110**: 55-67.

Baki, L., J. Shioi, et al. (2004). "PS1 activates PI3K thus inhibiting GSK-3 activity and tau overphosphorylation: effects of FAD mutations." Embo J **23**(13): 2586-96.

Bard, F., C. Cannon, et al. (2000). "Peripherally administered antibodies against amyloid beta-peptide enter the central nervous system and reduce pathology in a mouse model of Alzheimer disease." Nat Med **6**(8): 916-9.

Baron, J. A. and R. S. Sandler (2000). "Nonsteroidal anti-inflammatory drugs and cancer prevention." Annu Rev Med **51**: 511-23.

Baumeister, R., U. Leimer, et al. (1997). "Human presenilin-1, but not familial Alzheimer's disease (FAD) mutants, facilitate Caenorhabditis elegans Notch signalling independently of proteolytic processing." Genes Funct **1**(2): 149-159.

Beher, D. (2004). Assay for gamma-secretase modulators.

Beher, D., E. E. Clarke, et al. (2004). "Selected non-steroidal anti-inflammatory drugs and their derivatives target gamma-secretase at a novel site. Evidence for an allosteric mechanism." J Biol Chem **279**(42): 43419-26.

Beher, D., L. Hesse, et al. (1996). "Regulation of amyloid precursor protein (APP) binding to collagen and mapping of the binding sites on APP and collagen type I." J Biol Chem **271**: 1613-1620.

Bentahir, M., O. Nyabi, et al. (2006). "Presenilin clinical mutations can affect gamma-secretase activity by different mechanisms." J Neurochem **96**(3): 732-42.

Berezovska, O., A. Lleo, et al. (2005). "Familial Alzheimer's disease presenilin 1 mutations cause alterations in the conformation of presenilin and interactions with amyloid precursor protein." J Neurosci **25**(11): 3009-17.

Bihel, F., C. Das, et al. (2004). "Discovery of a Subnanomolar helical D-tridecapeptide inhibitor of gamma-secretase." J Med Chem. **47**(16): 3931-3933.

Borchelt, D. R., G. Thinakaran, et al. (1996). "Familial Alzheimers disease-linked presenilin 1 variants elevate Abeta 1-42/1-40 ratio in vitro and in vivo." Neuron **17**(November): 1005-13.

Brockhaus, M., J. Grunberg, et al. (1998). "Caspase-mediated cleavage is not required for the activity of presenilins in amyloidogenesis and NOTCH signaling." Neuroreport **9**(7): 1481-6.

Brown, M. S., J. Ye, et al. (2000). "Regulated intramembrane proteolysis: a control mechanism conserved from bacteria to humans." Cell **100**(4): 391-8.

Brunkan, A. L., M. Martinez, et al. (2005). "Presenilin endoproteolysis is an intramolecular cleavage." Mol Cell Neurosci.

Bu, G., J. Cam, et al. (2006). "LRP in amylid-beta production and metabolism." Ann N Y Acad Sci. **1086**: 35-53.

Burns, J. C., T. Friedmann, et al. (1993). "Vesicular stomatitis virus G glycoprotein pseudotyped retroviral vectors: Concentration to very high titer and efficient gene transfer into mammalian and nonmammalian cells." Proc Natl Acad Sci USA **90**: 8033-8037.

Cai, H., Y. Wang, et al. (2001). "BACE1 is the major beta-secretase for generation of Abeta peptides by neurons." Nat Neurosci **4**: 233-234.

Cao, X. and T. C. Sudhof (2001). "A transcriptionally [correction of transcriptively] active complex of APP with Fe65 and histone acetyltransferase Tip60." Science **293**(5527): 115-20.

Cao, X. and T. C. Sudhof (2004). "Dissection of amyloid-beta precursor protein-dependent transcriptional transactivation." J Biol Chem **279**(23): 24601-11.

Capell, A., D. Beher, et al. (2005). "Gamma-secretase complex assembly within the early secretory pathway." J Biol Chem.

Casas, C., N. Sergeant, et al. (2004). "Massive CA1/2 Neuronal Loss with Intraneuronal and N-Terminal Truncated A{beta}42 Accumulation in a Novel Alzheimer Transgenic Model." Am J Pathol **165**(4): 1289-1300.

Chen, F., H. Hasegawa, et al. (2006). "TMP21 is a presenilin complex component that modulates gamma-secretase but not epsilon-secretase activity." Nature **440**(7088): 1208-12.

Citron, M., T. Oltersdorf, et al. (1992). "Mutation of the beta-amyloid precursor protein in familial Alzheimer's disease increases beta-protein production." Nature **360**(6405): 672-4.

Citron, M., D. B. Teplow, et al. (1995). "Generation of amyloid beta protein from its precursor is sequence specific." Neuron **14**(3): 661-70.

Citron, M., D. Westaway, et al. (1997). "Mutant presenilins of Alzheimer's disease increase production of 42- residue amyloid beta-protein in both transfected cells and transgenic mice." Nat Med **3**(1): 67-72.

Clarke, E. E., I. Churcher, et al. (2006). "Intra- or inter-complex binding to the gamma -secretase enzyme: A model to differentiate inhibitor classes." J Biol Chem **281**(42): 31279-89.

Czirr, E., S. Leuchtenberger, et al. (2007). "Insensitivity to Abeta 42-lowering non-steroidal anti-inflammatory drugs (NSAIDs) and gamma-secretase inhibitors is common among aggressive presenilin-1 mutations." J Biol Chem **282**(34): 24504-13.

Czirr, E. and S. Weggen (2006). "Gamma-secretase modulation with Abeta42-lowering nonsteroidal anti-inflammatory drugs and derived compounds." Neurodegener Dis **3**(4-5): 298-304.

Das, P. and T. E. Golde (2002). "Open peer commentary regarding Abeta immunization and CNS inflammation by Pasinetti et al." Neurobiol Aging **23**(5): 671-674.

Das, P., V. Howard, et al. (2003). "Amyloid-beta immunization effectively reduces amyloid deposition in FcRgamma-/- knock-out mice." J Neurosci **23**(24): 8532-8.

De Strooper, B. (2007). "Loss-of-function presenilin mutations in Alzheimer disease. Talking Point on the role of presenilin mutations in Alzheimer disease." EMBO Rep **8**(2): 141-6.

De Strooper, B., P. Saftig, et al. (1998). "Deficiency of presenilin-1 inhibits the normal cleavage of amyloid precursor protein." Nature **391**(6665): 387-90.

Donoviel, D. B., A. K. Hadjantonakis, et al. (1999). "Mice lacking both presenilin genes exhibit early embryonic patterning defects." Genes Dev **13**(21): 2801-10.

Dovey, H. F., V. John, et al. (2001). "Functional gamma-secretase inhibitors reduce beta-amyloid peptide levels in brain." J Neurochem **76**(1): 173-81.

Edbauer, D., E. Winkler, et al. (2003). "Reconstitution of gamma-secretase activity." Nat Cell Biol.

Emi, N., T. Friedmann, et al. (1991). "Pseudotype foramtion of murine leukemia virus with the G protein of vesicular stomatitis virus." J. Virol. **65**: 1202-1218.

Eriksen, J. L., S. A. Sagi, et al. (2003). "NSAIDs and enantiomers of flurbiprofen target gamma-secretase and lower Abeta 42 in vivo." J Clin Invest **112**(3): 440-9.

Esch, F. S., P. S. Keim, et al. (1990). "Cleavage of amyloid beta peptide during constitutive processing of its precursor." Science **248**(4959): 1122-4.

Esler, W. P., W. T. Kimberly, et al. (2000). "Transition-state analogue inhibitors of gamma-secretase bind directly to presenilin-1." Nat Cell Biol **2**(7): 428-34.

Esler, W. P., W. T. Kimberly, et al. (2002). "Activity-dependent isolation of the presenilin- gamma -secretase complex reveals nicastrin and a gamma substrate." Proc Natl Acad Sci U S A **99**(5): 2720-5.

Fleisher, A., R. Raman, et al. (2007). "Phase 2 Trial with a γ-secretase inhibitor in mild-to-moderate Alzheimer Disease." Alzheimer's Association International Conference on Prevention of Dementia **Abstract HT-005.**

Fraering, P. C., W. Ye, et al. (2005). "gamma -Secretase substrate selectivity can be modulated directly via interaction with a nucleotide binding site." J Biol Chem.

Games, D., D. Adams, et al. (1995). "Alzheimer-type neuropathology in transgenic mice overexpressing V717F beta-amyloid precursor protein [see comments]." Nature **373**(6514): 523-7.

Gandy, S. and P. Greengard (1994). "Regulated cleavage of the Alzheimer amyloid precursor protein: molecular and cellular basis." Biochimie **76**(3-4): 300-303.

Gasparini, L., L. Rusconi, et al. (2004). "Modulation of beta-amyloid metabolism by non-steroidal anti-inflammatory drugs in neuronal cell cultures." J Neurochem **88**(2): 337-48.

Geling, A., H. Steiner, et al. (2002). "A gamma-secretase inhibitor blocks Notch signaling in vivo and causes a severe neurogenic phenotype in zebrafish." EMBO Rep **3**(7): 688-94.

Gilman, S., M. Koller, et al. (2005). "Clinical effects of Abeta immunization (AN1792) in patients with AD in an interrupted trial." Neurology **64**(9): 1553-1562.

Glenner, G. G. and C. W. Wong (1984). "Alzheimer's disease and Down's syndrome: sharing of a unique cerebrovascular amyloid fibril protein." Biochemical and biophysical research communications **122**(3): 1131-1135.

Golde, T. E., C. B. Eckman, et al. (2000). "Biochemical detection of Abeta isoforms: implications for pathogenesis, diagnosis, and treatment of Alzheimer's disease." Biochim Biophys Acta **1502**(1): 172-87.

Goldgaber, D., M. I. Lerman, et al. (1987). "Isolation, characterization, and chromosomal localization of human brain cDNA clones coding for the precursor of the amyloid of brain in Alzheimer's disease, Down's syndrome and aging." J Neural Transm Suppl **24**(23): 23-8.

Goutte, C., M. Tsunozaki, et al. (2002). "APH-1 is a multipass membrane protein essential for the Notch signaling pathway in Caenorhabditis elegans embryos." Proc Natl Acad Sci USA **99**: 775-779.

Haas, I. G., M. Frank, et al. (2005). "Presenilin-dependent processing and nuclear function of gamma-protocadherins." J Biol Chem **280**(10): 9313-9.

Haass, C., A. Y. Hung, et al. (1993). "beta-Amyloid peptide and a 3-kDa fragment are derived by distinct cellular mechanisms." The Journal of Biological Chemistry **268**(5): 3021-3024.

Haass, C., M. G. Schlossmacher, et al. (1992). "Amyloid beta-peptide is produced by cultured cells during normal metabolism [see comments]." Nature **359**(6393): 322-5.

Haass, C. and H. Steiner (2002). "Alzheimer disease gamma-secretase: a complex story of GxGD-type presenilin proteases." Trends Cell Biol **12**(12): 556-62.

Hardy, J. (1997). "Amyloid, the presenilins and Alzheimer's disease." Trends Neurosci **20**(4): 154-9.

Hardy, J. and D. J. Selkoe (2002). "The amyloid hypothesis of Alzheimer's disease: progress and problems on the road to therapeutics." Science **297**(5580): 353-6.

He, T. C., T. A. Chan, et al. (1999). "PPARdelta is an APC-regulated target of nonsteroidal anti-inflammatory drugs." Cell **99**(3): 335-45.

Heber, S., J. Herms, et al. (2000). "Mice with combined gene knock-outs reveal essential and partially redundant functions of amyloid precursor protein family members." J Neurosci **20**: 7951–7963.

Hébert, S. S., L. Serneels, et al. (2004). "Coordinated and widespread expression of gamma-secretase in vivo: evidence for size and molecular heterogeneity." Neurobiol Dis **17**(2): 260-272.

Hebert, S. S., L. Serneels, et al. (2006). "Regulated intramembrane proteolysis of amyloid precursor protein and regulation of expression of putative target genes." EMBO Rep.

Herms , J., B. Anliker, et al. (2004). "Cortical dysplasia resembling human type 2 lissencephaly in mice lacking all three APP family members." EMBO J **23**: 4106-4115.

Herreman, A., D. Hartmann, et al. (1999). "Presenilin 2 deficiency causes a mild pulmonary phenotype and no changes in amyloid precursor protein processing but enhances the embryonic lethal phenotype of presenilin 1 deficiency." Proc Natl Acad Sci U S A **96**(21): 11872-7.

Herreman, A., G. Van Gassen, et al. (2003). "gamma-Secretase activity requires the presenilin-dependent trafficking of nicastrin through the Golgi apparatus but not its complex glycosylation." J Cell Sci **116**: 1127-36.

Hock, C., U. Konietzko, et al. (2003). "Antibodies against beta-amyloid slow cognitive decline in Alzheimer's disease." Neuron **38**(4): 547-554.

Hom, R. K., A. F. Gailunas, et al. (2004). "Design and synthesis of hydroxyethylene-based peptidomimetic inhibitors of human beta-secretase." J Med Chem **47**(1): 158-164.

Hong, L., G. Koelsch, et al. (2000). "Structure of the protease domain of memapsin 2 (beta-secretase) complexed with inhibitor." Science **290**: 150-153.

Hsiao, K. (1998). "Transgenic mice expressing Alzheimer amyloid precursor proteins." Exp Gerontol **33**(7-8): 883-9.

Hsiao, K., P. Chapman, et al. (1996). "Correlative memory deficits, A beta elevation, and amyloid plaques in transgenic mice." Science **274**(5284): 99-102.

Hu, X., C. W. Hicks, et al. (2006). "Bace1 modulates myelination in the central and peripheral nervous system." Nat Neurosci **9**: 1520-1525.

Hussain, I., D. Powell, et al. (1999). "Identification of a novel aspartic protease (Asp 2) as beta-secretase." Molecular and cellular neurosciences **14**(6): 419-427.

Ikeuchi, T., G. Dolios, et al. (2003). "Familial Alzheimer disease-linked presenilin 1 variants enhance production of both Abeta 1-40 and Abeta 1-42 peptides that are only partially sensitive to a

potent aspartyl protease transition state inhibitor of "gamma-secretase"." J Biol Chem **278**(9): 7010-8.

in t' Veld, B. A., A. Ruitenberg, et al. (2001). "Nonsteroidal antiinflammatory drugs and the risk of Alzheimer's disease." N Engl J Med **345**(21): 1515-21.

Iwata, N., S. Tsubuki, et al. (2001). "Metabolic regulation of brain Abeta by neprilysin." Science **292**(5521): 1550-1552.

Iwatsubo, T., A. Odaka, et al. (1994). "Visualization of A beta 42(43) and A beta 40 in senile plaques with end-specific A beta monoclonals: evidence that an initially deposited species is A beta 42(43)." Neuron **13**(1): 45-53.

Jankowsky, J. L., D. J. Fadale, et al. (2004). "Mutant presenilins specifically elevate the levels of the 42 residue beta-amyloid peptide in vivo: evidence for augmentation of a 42-specific gamma secretase." Hum Mol Genet **13**(2): 159-70.

Jiang, C., A. T. Ting, et al. (1998). "PPAR-gamma agonists inhibit production of monocyte inflammatory cytokines." Nature **391**(6662): 82-6.

Kaether, C., J. Scheuermann, et al. (2007). "Endoplasmic reticulum retention of the gamma-secretase complex component Pen2 by Rer1." EMBO Rep **8**(8): 743-748.

Kang, J., H. G. Lemaire, et al. (1987). "The precursor of Alzheimer's disease amyloid A4 protein resembles a cell-surface receptor." Nature **325**(6106): 733-6.

Kim, H., E. Kim, et al. (2003). "C-terminal fragments of amyloid precursor protein exert neurotoxicity by inducing glycogen synthase kinase-3b expression." FASEB J **17**: 1951-1953.

Kimberly, W. T., M. J. LaVoie, et al. (2003). "Gamma-secretase is a membrane protein complex comprised of presenilin, nicastrin, Aph-1, and Pen-2." Proc Natl Acad Sci U S A **100**(11): 6382-7.

Koo, E. H. (1997). "Phorbol esters affect multiple steps in beta-amyloid precursor protein trafficking and amyloid beta-protein production." Mol Med **3**(3): 204-211.

Kopan, R., J. S. Nye, et al. (1994). "The intracellular domain of mouse Notch: a constitutively activated repressor of myogenesis directed at the basic helix-loop-helix region of MyoD." Development **120**(9): 2385-2396.

Kornilova, A. Y., F. Bihel, et al. (2005). "The initial substrate-binding site of {gamma}-secretase is located on presenilin near the active site." Proc Natl Acad Sci U S A **102**: 3230-5.

Kukar, T., M. P. Murphy, et al. (2005). "Diverse compounds mimic Alzheimer disease-causing mutations by augmenting Abeta42 production." Nat Med **11**(6): 545-50.

Laudon, H., E. M. Hansson, et al. (2005). "A nine-transmembrane domain topology for presenilin 1." J Biol Chem **280**(42): 35352-60.

Launer, L. (2003). "Nonsteroidal anti-inflammatory drug use and the risk for Alzheimer's disease: dissecting the epidemiological evidence." Drugs **63**(8): 731-9.

LaVoie, M. J., P. C. Fraering, et al. (2003). "Assembly of the gamma -secretase complex involves early formation of an intermediate sub-complex of Aph-1 and Nicastrin." J Biol Chem.

Lazarov, V. K., P. C. Fraering, et al. (2006). "Electron microscopic structure of purified, active gamma-secretase reveals an aqueous intramembrane chamber and two pores." Proc Natl Acad Sci USA **103**: 6889-6894.

Lehmann, J. M., J. M. Lenhard, et al. (1997). "Peroxisome proliferator-activated receptors alpha and gamma are activated by indomethacin and other non-steroidal anti-inflammatory drugs." J Biol Chem **272**(6): 3406-10.

Lehrke, M. and M. A. Lazar (2005). "The many faces of PPARgamma." Cell **123**(6): 993-9.

Leissring, M. A., W. Farris, et al. (2003). "Enhanced proteolysis of beta-amyloid in APP transgenic mice prevents plaque formation, secondary pathology, and premature death." Neuron **40**(6): 1087-1093.

Leuchtenberger, S., D. Beher, et al. (2006). "Selective modulation of Abeta42 production in Alzheimer's disease: non-steroidal anti-inflammatory drugs (NSAIDs) and beyond." Curr Pharm Des **12**(33): 4337-4355.

Leuchtenberger, S., M. P. Kummer, et al. (2006). "Inhibitors of Rho-kinase modulate amyloid-beta (Abeta) secretion but lack selectivity for Abeta42." J Neurochem **96**(2): 355-65.

Levitan, D., T. G. Doyle, et al. (1996). "Assessment of normal and mutant human presenilin function in Caenorhabditis elegans." Proc Natl Acad Sci U S A **93**(25): 14940-4.

Levites, Y., T. Amit, et al. (2003). "Neuroprotection and neurorescue against Abeta toxicity and PKC-dependent release of nonamyloidogenic soluble precursor protein by green tea polyphenol (-)-epigallocatechin-3-gallate." FASEB J **17**(8): 952-954.

Levylahad, E., W. Wasco, et al. (1995). "Candidate gene for the chromosome 1 familial Alzheimer's disease locus." Science **269**(5226): 973-977.

Lewis, H. D., B. I. Perez Revuelta, et al. (2003). "Catalytic site-directed gamma-secretase complex inhibitors do not discriminate pharmacologically between Notch S3 and beta-APP cleavages." Biochemistry **42**(24): 7580-6.

Li, Y. M., M. Xu, et al. (2000). "Photoactivated gamma-secretase inhibitors directed to the active site covalently label presenilin 1." Nature **405**(6787): 689-94.

Li, Z. W., G. Stark, et al. (1996). "Generation of mice with a 200-kb amyloid precursor protein gene deletion by Cre recombinase-mediated sitespecific recombination in embryonic stem cells." Proc Natl Acad Sci USA **93**: 6158-6162.

Lichtenthaler, S. F., R. Wang, et al. (1999). "Mechanism of the cleavage specificity of Alzheimer's disease gamma-secretase identified by phenylalanine-scanning mutagenesis of the transmembrane domain of the amyloid precursor protein." Proc Natl Acad Sci U S A **96**(6): 3053-8.

Lleo, A., O. Berezovska, et al. (2004). "Nonsteroidal anti-inflammatory drugs lower Abeta42 and change presenilin 1 conformation." Nat Med **10**(10): 1065-6.

Lu, D. C., S. Rabizadeh, et al. (2000). "A second cytotoxic proteolytic peptide derived from amyloid beta-protein precursor." Nat Med **6**(4): 397-404.

Luo, Y., B. Bolon, et al. (2001). "Mice deficient in BACE1, the Alzheimer's beta-secretase, have normal phenotype and abolished beta-amyloid generation." Nat Neurosci **4**(3): 231-232.

Ma, Q. H., T. Futagawa, et al. (2008). "A TAG1-APP signalling pathway through Fe65 negatively modulates neurogenesis." Nat Cell Biol **Feb 17 [Epub ahead of print]**.

Marambaud, P., J. Shioi, et al. (2002). "A presenilin-1/gamma-secretase cleavage releases the E-cadherin intracellular domain and regulates disassembly of adherens junctions." Embo J **21**(8): 1948-56.

Masliah, E., L. Hansen, et al. (2005). "Abeta vaccination effects on plaque pathology in the absence of encephalitis in Alzheimer disease." Neurology **64**(1): 129-131.

Mattson, M. P., B. Cheng, et al. (1993). "Evidence for excitoprotective and intraneuronal calcium-regulating roles for secreted forms of the beta-amyloid precursor protein." Neuron **10**(2): 243-54.

McGeer, P. L., E. McGeer, et al. (1990). "Anti-inflammatory drugs and Alzheimer disease." Lancet **335**(8696): 1037.

McGowan, E., F. Pickford, et al. (2005). "Abeta42 is essential for parenchymal and vascular amyloid deposition in mice." Neuron **47**(2): 191-9.

Moehlmann, T., E. Winkler, et al. (2002). "Presenilin-1 mutations of leucine 166 equally affect the generation of the Notch and APP intracellular domains independent of their effect on Abeta 42 production." Proc Natl Acad Sci U S A **99**(12): 8025-30.

Morihara, T., T. Chu, et al. (2002). "Selective inhibition of Abeta42 production by NSAID R-enantiomers." J Neurochem **83**(4): 1009-12.

Morohashi, Y., T. Kan, et al. (2006). "Carboxyl-terminal fragment of presenilin is the molecular target of a dipeptidic gamma -secretase-specific inhibitor DAPT." J Biol Chem **281**(21): 14670-6.

Mueller, U., N. Cristina, et al. (1994). "Behavioral and anatomical deficits in mice homozygous for a modified beta-amyloid precursor protein gene." Cell **79**: 755-765.

Multhaup, G. (1994). "Identification and regulation of he high affinity binding site of the Alzheimer's disease amyloid precursor protein (APP) to glycosaminoglycans." Biochimie **76**: 304-311.

Mumm, J. S., E. H. Schroeter, et al. (2000). "A ligand-induced extracellular cleavage regulates gamma-secretase-like proteolytic activation of Notch1." Mol Cell **5**: 197-206.

Munter, L. M., P. Voigt, et al. (2007). "GxxxG motifs within the amyloid precursor protein transmembrane sequence are critical for the etiology of Abeta42." Embo J **26**(6): 1702-12.

Murrell, J. R., A. M. Hake, et al. (2000). "Early-onset Alzheimer disease caused by a new mutation (V717L) in the amyloid precursor protein gene." Arch Neurol. **57**(6): 885-887.

Netzer, W. J., F. Dou, et al. (2003). "Gleevec inhibits beta-amyloid production but not Notch cleavage." Proc Natl Acad Sci U S A **100**(21): 12444-9.

Nicoll, J. A., D. Wilkinson, et al. (2003). "Neuropathology of human Alzheimer disease after immunization with amyloid-beta peptide: a case report." Nat Med **9**(4): 448-452.

Niimura, M., N. Isoo, et al. (2005). "Aph-1 contributes to the stabilization and trafficking of the gamma-secretase complex through mechanisms involving intermolecular and intramolecular interactions." J Biol Chem **280**(13): 12967-12975.

Nilsberth, C., A. Westlind-Danielsson, et al. (2001). "The 'Arctic' APP mutation (E693G) causes Alzheimer's disease by enhanced Abeta protofibril formation." Nat Neurosci **4**(9): 887-93.

Nyabi, O., M. Bentahir, et al. (2003). "Presenilins mutated at Asp-257 or Asp-385 restore Pen-2 expression and Nicastrin glycosylation but remain catalytically inactive in the absence of wild type Presenilin." J Biol Chem **278**(44): 43430-6.

Oakley, H., S. L. Cole, et al. (2006). "Intraneuronal beta-amyloid aggregates, neurodegeneration, and neuron loss in transgenic mice with five familial Alzheimer's disease mutations: potential factors in amyloid plaque formation." J Neurosci **26**(40): 10129-40.

Obregon, D. F., K. Rezai-Zadeh, et al. (2006). "ADAM10 activation is required for green tea (-)-epigallocatechin-3-gallate-induced alpha-secretase cleavage of amyloid precursor protein." J Biol Chem **281**: 16419-16427.

Oddo, S., A. Caccamo, et al. (2003). "Triple-transgenic model of Alzheimer's disease with plaques and tangles: intracellular Abeta and synaptic dysfunction." Neuron **39**(3): 409-421.

Oh, Y. S. and R. J. Turner (2005). "Topology of the C-terminal fragment of human presenilin 1." Biochemistry **44**: 11821-11828.

Okochi, M., A. Fukumori, et al. (2006). "Secretion of the Notch-1 Abeta -like peptide during Notch signaling." J Biol Chem.

Okochi, M., K. Ishii, et al. (1997). "Proteolytic processing of presenilin-1 (PS-1) is not associated with Alzheimer's disease with or without PS-1 mutations." FEBS Lett **418**(1-2): 162-6.

Okochi, M., H. Steiner, et al. (2002). "Presenilins mediate a dual intramembranous gamma-secretase cleavage of Notch-1." Embo J **21**(20): 5408-16.

Orgogozo, J. M., S. Gilman, et al. (2003). "Subacute meningoencephalitis in a subset of patients with AD after Abeta42 immunization." Neurology **61**(1): 46-54.

Page, R. M., K. Baumann, et al. (2007). "Generation of Abeta 38 and Abeta 42 is independently and differentially affected by FAD-associated presenilin 1 mutations and gamma -secretase modulation." J Biol Chem.

Pardossi-Piquard, R., A. Petit, et al. (2005). "Presenilin-Dependent Transcriptional Control of the Abeta-Degrading Enzyme Neprilysin by Intracellular Domains of betaAPP and APLP." Neuron **46**(4): 541-54.

Park, J. H., D. A. Gimbel, et al. (2006). "Alzheimer precursor protein interaction with the Nogo-66 receptor reduces amyloid-beta plaque deposition." J Neurosci **26**(5): 1386-95.

Parks, A. L. and D. Curtis (2007). "Presenilin diversifies its portfolio." Trends Genet **23**(3): 140-50.

Parks, A. L., K. M. Klueg, et al. (2000). "Ligand endocytosis drives receptor dissociation and activation in the Notch pathway." Development **127**: 1373-1385.

Peretto, I., S. Radaelli, et al. (2005). "Synthesis and Biological Activity of Flurbiprofen Analogues as Selective Inhibitors of beta-Amyloid(1)(-)(42) Secretion." J Med Chem **48**(18): 5705-5720.

Perez-Tur, J., S. Froelich, et al. (1995). "A mutation in Alzheimer's disease destroying a splice acceptor site in the presenilin-1 gene." Neuroreport **7**(1): 297-301.

Perez, R. G., H. Zheng, et al. (1997). "The beta-amyloid precursor protein of Alzheimer's disease enhances neuron viability and modulates neuronal polarity. ." J Neurosci **17**: 9407-9414.

Postina, R., A. Schroeder, et al. (2004). "A disintegrin-metalloproteinase prevents amyloid plaque formation and hippocampal defects in an Alzheimer disease mouse model." J Clin Invest **113**(10): 1456-64.

.

Qi-Takahara, Y., M. Morishima-Kawashima, et al. (2005). "Longer forms of amyloid beta protein: implications for the mechanism of intramembrane cleavage by gamma-secretase." J Neurosci **25**(2): 436-45.

Radde, R., T. Bolmont, et al. (2006). "Abeta42-driven cerebral amyloidosis in transgenic mice reveals early and robust pathology." EMBO Rep **7**(9): 940-6.

Rezai-Zadeh, K., D. Shytle, et al. (2005). "Green tea epigallocatechin-3-gallate (EGCG) modulates amyloid precursor protein cleavage and reduces cerebral amyloidosis in Alzheimer transgenic mice." J Neurosi **25**: 8807-8814.

Richards, J. G., G. A. Higgins, et al. (2003). "PS2APP transgenic mice, coexpressing hPS2mut and hAPPswe, show age-related cognitive deficits associated with discrete brain amyloid deposition and inflammation." JNeurosci **23**(26): 8989-9003.

Ring, S., S. W. Weyer, et al. (2007). "The secreted beta-amyloid precursor protein ectodomain APPs alpha is sufficient to rescue the anatomical, behavioral, and electrophysiological abnormalities of APP-deficient mice." J Neurosci **27**(29): 7817-7826.

Robakis, N. K., H. M. Wisniewski, et al. (1987). "Chromosome 21q21 sublocalization of gene encoding beta-amyloid peptide in cerebral vessels and neuritic (senile) plaques of people with Alzheimer´s disease and Down syndrome." Lancet **1**(384-385).

Rogaev, E. I., R. Sherrington, et al. (1995). "Familial Alzheimer's disease in kindreds with missense mutations in a gene on chromosome 1 related to the Alzheimer's disease type 3 gene." Nature **376**(6543): 775-778.

Rovelet-Lecrux, A., D. Hannequin, et al. (2006). "APP locus duplication causes autosomal dominant early-onset Alzheimer disease with cerebral amyloid angiopathy." Nat Genet **38**(1): 24-6.

Sagi, S. A., S. Weggen, et al. (2003). "The non-cyclooxygenase targets of non-steroidal anti-inflammatory drugs, lipoxygenases, peroxisome proliferator-activated receptor, inhibitor of kappa B kinase, and NF kappa B, do not reduce amyloid beta 42 production." J Biol Chem **278**(34): 31825-30.

Sankaranarayanan, S., E. A. Price, et al. (2007). "In vivo BACE1 inhibition leads to brain A{beta} lowering and increased {alpha}-secretase processing of APP without effect on Neuregulin-1." J Pharmacol Exp Ther.

Sastre, M., I. Dewachter, et al. (2003). "Nonsteroidal anti-inflammatory drugs and peroxisome proliferator-activated receptor-gamma agonists modulate immunostimulated processing of amyloid precursor protein through regulation of beta-secretase." J Neurosci **23**(30): 9796-804.

Sato, C., Y. Morohashi, et al. (2006). "Structure of the catalytic pore of gamma-secretase probed by the accessibility of substituted cysteines." J Neurosci **26**(46): 12081-8.

Sato, T., T. S. Diehl, et al. (2007). "Active gamma -secretase complexes contain only one of each component." J Biol Chem.

Sato, T., A. C. Nyborg, et al. (2006). "Signal Peptide Peptidase: Biochemical Properties and Modulation by Nonsteroidal Antiinflammatory Drugs." Biochemistry **45**(28): 8649-8656.

Schenk, D. (2002). "Amyloid-beta immunotherapy for Alzheimer's disease: the end of the beginning." Nat Rev Neurosci **3**(10): 824-828.

Schenk, D., R. Barbour, et al. (1999). "Immunization with amyloid-beta attenuates Alzheimer-disease-like pathology in the PDAPP mouse." Nature **400**(6740): 173-7.

Scheuner, D., C. Eckman, et al. (1996). "Secreted amyloid beta-protein similar to that in the senile plaques of Alzheimers disease is increased in vivo by the presenilin 1 and 2 and APP mutations linked to familial Alzheimers disease." Nature Medicine **2**(8): 864-9.

Schroeter, E. H., J. A. Kisslinger, et al. (1998). "Notch-1 signalling requires ligand-induced proteolytic release of intracellular domain." Nature **393**(6683): 382-6.

Shah, S., S. F. Lee, et al. (2005). "Nicastrin functions as a gamma-secretase-substrate receptor." Cell **122**(3): 435-47.

Shen, J., R. T. Bronson, et al. (1997). "Skeletal and CNS defects in Presenilin-1-deficient mice." Cell **89**(4): 629-39.

Shen, J. and R. J. Kelleher, 3rd (2007). "The presenilin hypothesis of Alzheimer's disease: Evidence for a loss-of-function pathogenic mechanism." Proc Natl Acad Sci U S A **104**(2): 403-409.

Sherrington, R., E. I. Rogaev, et al. (1995). "Cloning of a gene bearing missense mutations in early-onset familial Alzheimer's disease." Nature **375**(6534): 754-760.

Shirotani, K., D. Edbauer, et al. (2004a). "Immature nicastrin stabilizes APH-1 independent of PEN-2 and presenilin: identification of nicastrin mutants that selectively interact with APH-1." J Neurochem **89**: 1520-1527.

Shirotani, K., D. Edbauer, et al. (2004b). "Identification of distinct gamma-secretase complexes with different APH-1 variants." J Biol Chem **279**(40): 41340-5.

Shuto, D., S. Kasai, et al. (2003). "KMI-008, a novel beta-secretase inhibitor containing a hydroxymethylcarbonyl isostere as a transition-state mimic: design and synthesis of substrate-based octapeptides." Bioorg Med Chem Lett. **13**(24): 4273-4276.

Siemers, E. R., R. A. Dean, et al. (2007). "Safety, tolerability, and effects on plasma and cerebrospinal fluid amyloid-beta after inhibition of gamma-secretase. ." Clin Neuropharmacol. **30**(6): 317-325.

Simmons, D. L., R. M. Botting, et al. (2004). "Cyclooxygenase isozymes: the biology of prostaglandin synthesis and inhibition." Pharmacol Rev **56**(3): 387-437.

Sinha, S., J. P. Anderson, et al. (1999). "Purification and cloning of amyloid precursor protein beta-secretase from human brain." Nature **402**(6761): 537-540.

Sisodia, S. S., E. H. Koo, et al. (1990). "Evidence that beta-amyloid protein in Alzheimer's disease is not derived by normal processing." Science **248**(4954): 492-5.

Sisodia, S. S., E. H. Koo, et al. (1993). "Identification and transport of full-length amyloid precursor proteins in rat peripheral nervous system." J Neurosci **13**(7): 3136-42.

Smith, I. F., K. N. Green, et al. (2005). "Calcium dysregulation in Alzheimer's disease: recent advances gained from genetically modified animals." Cell Calcium **38**(3-4): 427-37.

Smith, R. P., D. A. Higuchi, et al. (1990). "Platelet coagulation factor XIa-inhibitor, a form of Alzheimer amyloid precursor protein." Science **248**: 1126-1128.

Spasic, D., T. Raemaekers, et al. (2007). "Rer1p competes with APH-1 for binding to nicastrin and regulates gamma-secretase complex assembly in the early secretory pathway." J Cell Biol **176**(5): 629-640.

Spasic, D., A. Tolia, et al. (2006). "Presenilin-1 Maintains a Nine-Transmembrane Topology throughout the Secretory Pathway." J Biol Chem **281**(36): 26569-77.

Steiner, H., H. Romig, et al. (1999). "The biological and pathological function of the presenilin-1 Deltaexon 9 mutation is independent of its defect to undergo proteolytic processing." J Biol Chem **274**(12): 7615-8.

Stutzmann, G. E. (2005). "Calcium dysregulation, IP3 signaling, and Alzheimer's disease." Neuroscientist **11**(2): 110-5.

Sung, S., H. Yang, et al. (2004). "Modulation of nuclear factor-kappa B activity by indomethacin influences A beta levels but not A beta precursor protein metabolism in a model of Alzheimer's disease." Am J Pathol **165**(6): 2197-206.

Suzuki, N., T. T. Cheung, et al. (1994). "An increased percentage of long amyloid beta protein secreted by familial amyloid beta protein precursor (beta APP717) mutants." Science **264**(5163): 1336-40.

Takahashi, Y., I. Hayashi, et al. (2003). "Sulindac sulfide is a noncompetitive gamma-secretase inhibitor that preferentially reduces Abeta 42 generation." J Biol Chem **278**(20): 18664-70.

Tanzi, R. E., J. F. Gusella, et al. (1987). "Amyloid ß protein gene: cDNA, mRNA distribution and genetic linkage near the Alzheimer locus." Science **235**: 880-884.

Thomas, P. Q. and P. D. Rathjen (1992). "HES-1, a novel homeobox gene expressed by murine embryonic stem cells, identifies a new class of homeobox genes." Nucleic Acids Res. **20**(21): 5840.

Tian, G., S. V. Ghanekar, et al. (2003). "The mechanism of gamma -secretase. Multiple inhibitor binding sites for transition state analogs and small molecule inhibitors." J Biol Chem **278**(31): 28968-75.

Tolia, A., L. Chavez-Gutierrez, et al. (2006). "Contribution of Presenilin Transmembrane Domains 6 and 7 to a Water-containing Cavity in the {gamma}-Secretase Complex." J Biol Chem **281**(37): 27633-42.

Tomiyama, T., T. Nagata, et al. (2008). "A new amyloid beta variant favoring oligomerization in Alzheimer's-type dementia." Ann Neurol **Epub Feb. 25**.

Tu, H., O. Nelson, et al. (2006). "Presenilins form ER Ca2+ leak channels, a function disrupted by familial Alzheimer's disease-linked mutations." Cell **126**(5): 981-93.

Vardy, E. R., A. J. Catto, et al. (2005). "Proteolytic mechanisms in amyloid-beta metabolism: therapeutic implications for Alzheimer's disease." Trends Mol Med.

Vassar, R., B. D. Bennett, et al. (1999). "Beta-secretase cleavage of Alzheimer's amyloid precursor protein by the transmembrane aspartic protease BACE." Science **286**(5440): 735-41.

von Koch, C., H. Zheng, et al. (1997). "Generation of APLP2 KO mice and early postnatal lethality in APLP2/APP double KO mice." Neurobiol Aging **18**: 661-669.

von Rotz, R., B. Kohli, et al. (2004). "The APP intracellular domain forms nuclear multiprotein complexes and regulates the transcription of its own precursor." J Cell Sci **117**: 4435-4448.

Waldron, E., S. Jaeger, et al. (2006). "Functional role of the low-density lipoprotein receptor-related protein in Alzheimer's disease." Neurodegener Dis. **3**(4-5): 233-238.

Wancata, J., M. Musalek, et al. (2003). "Number of dementia sufferers in Europe between the years 2000 and 2050." Eur Psychiatry **18**(6): 306-13.

Wang, R., P. Tang, et al. (2006). "Regulation of tyrosinase trafficking and processing by presenilins: partial loss of function by familial Alzheimer's disease mutation." Proc Natl Acad Sci U S A **103**(2): 353-8.

Warner, T. D. and J. A. Mitchell (2004). "Cyclooxygenases: new forms, new inhibitors, and lessons from the clinic." Faseb J **18**(7): 790-804.

Wasco, W., K. Bupp, et al. (1992). "Identification of a mouse brain cDNA that encodes a protein related to the Alzheimer disease-associated amyloid beta protein precursor." Proc Natl Acad Sci U S A **89**(22): 10758-62.

Weggen, S., E. Czirr, et al. (2007). Non-steroidal anti-inflammatory drugs (NSAIDs) and derived Abeta42-lowering molecules for treatment and prevention of Alzheimer's disease (AD), Springer USA.

Weggen, S., J. L. Eriksen, et al. (2001). "A subset of NSAIDs lower amyloidogenic Abeta42 independently of cyclooxygenase activity." Nature **414**(6860): 212-6.

Weggen, S., J. L. Eriksen, et al. (2003). "Abeta42-lowering nonsteroidal anti-inflammatory drugs preserve intramembrane cleavage of the amyloid precursor protein (APP) and ErbB-4 receptor and signaling through the APP intracellular domain." J Biol Chem **278**(33): 30748-54.

Weggen, S., J. L. Eriksen, et al. (2003). "Evidence that nonsteroidal anti-inflammatory drugs decrease amyloid beta 42 production by direct modulation of gamma-secretase activity." J Biol Chem **278**(34): 31831-7.

Weidemann, A., G. König, et al. (1989). "Identification, biogenesis, and localisation of precursors of Alzheimer´s disease A4 amyloid protein." Cell **57**: 115-26.

Wen, P. H., X. Shao, et al. (2002). "Overexpression of wild type but not an FAD mutant presenilin-1 promotes neurogenesis in the hippocampus of adult mice." Neurobiol Dis **10**(1): 8-19.

Willem, M., A. N. Garratt, et al. (2006). "Control of Peripheral Nerve Myelination by the {beta}-Secretase BACE1." Science.

Winklhofer, K. F., J. Tatzelt, et al. (2008). "The two faces of protein misfolding: gain- and loss-of-function in neurodegenerative diseases." EMBO J **27**: 336-349.

Wolfe, M. S. (2007). "When loss is gain: reduced presenilin proteolytic function leads to increased Abeta42/Abeta40. Talking Point on the role of presenilin mutations in Alzheimer disease." EMBO Rep **8**(2): 136-140.

Wolfe, M. S., M. Citron, et al. (1998). "A substrate-based difluoro ketone selectively inhibits Alzheimer's gamma-secretase activity." J Med Chem **41**(1): 6-9.

Wolfe, M. S., W. Xia, et al. (1999). "Peptidomimetic probes and molecular modeling suggest that Alzheimer's gamma-secretase is an intramembrane-cleaving aspartyl protease." Biochemistry **38**(15): 4720-7.

Wolfe, M. S., W. Xia, et al. (1999). "Two transmembrane aspartates in presenilin-1 required for presenilin endoproteolysis and gamma-secretase activity [see comments]." Nature **398**(6727): 513-7.

Wong, G. T., D. Manfra, et al. (2004). "Chronic treatment with the gamma-secretase inhibitor LY-411,575 inhibits beta-amyloid peptide production and alters lymphopoiesis and intestinal cell differentiation." J Biol Chem **279**(13): 12876-82.

Wong, P. C., H. Zheng, et al. (1997). "Presenilin 1 is required for Notch1 and DII1 expression in the paraxial mesoderm." Nature **387**(6630): 288-92.

Yagishita, S., M. Morishima-Kawashima, et al. (2008). "Abeta46 is processed to Abeta40 and Abeta43, but not to Abeta42, in the low density membrane domains." J Biol Chem **283**(2): 733-738.

Yagishita, S., M. Morishima-Kawashima, et al. (2006). "DAPT-Induced Intracellular Accumulations of Longer Amyloid beta-Proteins: Further Implications for the Mechanism of Intramembrane Cleavage by gamma-Secretase." Biochemistry **45**(12): 3952-60.

Yan, Q., J. Zhang, et al. (2003). "Anti-Inflammatory Drug Therapy Alters {beta}-Amyloid Processing and Deposition in an Animal Model of Alzheimer's Disease." J Neurosci **23**(20): 7504-7509.

Yan, R., M. J. Bienkowski, et al. (1999). "Membrane-anchored aspartyl protease with Alzheimer's disease beta-secretase activity." Nature **402**(6761): 533-537.

Yankner, B. A., L. R. Dawes, et al. (1989). "Neurotoxicity of a fragment of the amyloid precursor associated with Alzheimer's disease." Science **245**(4916): 417-20.

Yankner, B. A., L. K. Duffy, et al. (1990). "Neurotrophic and neurotoxic effects of amyloid beta protein: reversal by tachykinin neuropeptides." Science **250**(4978): 279-282.

Yu, G., M. Nishimura, et al. (2000). "Nicastrin modulates presenilin-mediated notch/glp-1 signal transduction and betaAPP processing." Nature **407**: 48-54.

Zhang, M., A. Haapasalo, et al. (2006). "Presenilin/{gamma}-secretase activity regulates protein clearance from the endocytic recycling compartment." Faseb J.

Zhang, Y. W., R. Wang, et al. (2007). "Presenilin/gamma-secretase-dependent processing of beta-amyloid precursor protein regulates EGF receptor expression." Proc Natl Acad Sci USA **104**(25): 10613-10618.

Zhao, G., M. Z. Cui, et al. (2005). "gamma -cleavage is dependent on zeta -cleavage during the proteolytic processing of amyloid precursor protein within its transmembrane domain." J Biol Chem **280**(45): 37689-97.

Zhao, G., J. Tan, et al. (2007). "The same gamma-secretase accounts for the multiple intramembrane cleavages of APP." J Neurochem **100**(5): 1234-46.

Zheng, H., M. Jiang, et al. (1995). "ß-amyloid precursor protein-deficient mice show reactive gliosis and decreased locomotor activity." Cell **81**(May 19): 525-31.

Zhou, S., H. Zhou, et al. (2005). "CD147 is a regulatory subunit of the {gamma}-secretase complex in Alzheimer's disease amyloid {beta}-peptide production." Proc Natl Acad Sci U S A.

Zhou, Y., Y. Su, et al. (2003). "Nonsteroidal Anti-Inflammatory Drugs Can Lower Amyloidogenic A{beta}42 by Inhibiting Rho." Science **302**(5648): 1215-1217.

9 Appendix

9.1 *Curriculum vitae*

9.2 Contributions to international meetings

Neuroscience 2007; November 3-7, 2007; San Diego, California, USA

Oral Presentation; Session No. 444, APP processing and function: *Influence of FAD PS1 mutations on the efficacy of γ-secretase modulators and inhibitors: evidence for independent generation of Aβ42 and Aβ38 peptide species.*

Eva Czirr, Stefanie Leuchtenberger, Cornelia Dorner-Ciossek, Barbara Cottrell, Mathias Jucker, Claus U. Pietrzik, Edward H. Koo, Karlheinz Baumann, and Sascha Weggen

PENS Summer School 2007: Novel Molecular Strategies to treat Neurodegenerative Diseases; July 8-15, 2007; Ofir, Portugal

Poster presentation: *Presenilin-1 mutations strongly affect the cellular response to Aβ42-lowering NSAIDs and γ-secretase inhibitors in vitro and in vivo.*

Eva Czirr, Stefanie Leuchtenberger, Cornelia Dorner-Ciossek, Anna Schneider, Mathias Jucker, Edward H. Koo, Claus U. Pietrzik, Karlheinz Baumann, Sascha Weggen

10th International Conference on Alzheimer´s Disease and Related Disorders (ICAD)

July 15-20, 2006; Madrid, Spain

Oral Presentation S01-02 Disease Mechanisms – Presenilins/γ-Secretase: *Genetic dissection of the PS1 ΔExon9 mutation and its attenuated response to Aβ42-lowering NSAIDs.*

Eva Czirr, Stefanie Leuchtenberger, Anna Schneider, Edward H. Koo, Claus U. Pietrzik, Sascha Weggen

9.3 Publications

"Nonsteroidal anti-inflammatory drugs and ectodomain shedding of the amyloid precursor protein."
Leuchtenberger, S., Maler, J., **Czirr, E.,** Ness, J., Lichtenthaler, S.F., Esselmann, H., Pietrzik, C.U., Wiltfang, J., Weggen, S.;
Neurodegenerative Diseases, 2008, Mar 18; [Epub ahead of print].

"Insensitivity to Aβ42-lowering non-steroidal anti inflammatory drugs (NSAIDs) and γ-secretase inhibitors is common among aggressive presenilin-1 mutations."
Czirr, E., Leuchtenberger S., Dorner-Ciossek, C., Schneider, A., Jucker, M., Koo, E.H., Pietrzik, C.U., Baumann, K., Weggen, S.;
Journal of Biological Chemistry, 2007, 282(34):24504-13.

"Non-steroidal anti-inflammatory drugs (NSAIDs) and derived Aβ42-lowering molecules for treatment and prevention of Alzheimer´s disease."
Weggen, S., **Czirr, E.**, Leuchtenberger, S., Eriksen, J.L.;
Pharmacology and Mechanisms in Alzheimer´s Therapeutics (Springer USA), 2008.

"γ-Secretase modulation with Aβ42-lowering non-steroidal anti-inflammatory drugs (NSAIDs) and derived compounds."
Czirr, E. and Weggen, S.;
Neurodegenerative Diseases, 2006, 3(4-5):298-304.

"Inhibitors of Rho-kinase modulate amyloid-beta (Abeta) secretion but lack selectivity for Abeta42."
Leuchtenberger,S., Kummer, M.P., Kukar, T., **Czirr, E.**, Teusch, N., Sagi, S.A., Berdeaux, R., Pietrzik, C.U., Ladd, T.B., Golde, T.E., Koo, E.H., Weggen, S.;
Journal of Neurochemistry, 2006, 96(2):355-65.

"Genetic variation in oocyte phenotype revealed through parthenogenesis and cloning: Correlation with differences in pronuclear epigenetic modification."
Gao, S., **Czirr, E.,** Chung, Y.G., Han, Z., Latham, K.E.;
Biology of Reproduction, 2004, 70(4):1162-70.

"Outer dense fiber protein 2 (ODF2) is a self-interacting protein with affinity for microtubules." Donkor F.F., Monnich, M., **Czirr, E.**, Hollemann, T., Hoyer-Fender, S.;

Journal of Cell Science, 2004, 117: 4643-51.

"Localization of histone macroH2A1.2 to the XY-body is not a response to the presence of asynapsed chromosome axes."
Hoyer-Fender, S., **Czirr, E.**, Radde, R., Turner, J.M., Mahadevaiah, S.K., Pehrson, J.R., Burgoyne, P.S.;
Journal of Cell Science, 2004, 15;117: 189-98.

9.4 Acknowledgements

9.5 Original publications

“Insensitivity to Aβ42-lowering non-steroidal anti inflammatory drugs (NSAIDs) and γ-secretase inhibitors is common among aggressive presenilin-1 mutations.”
Czirr, E., Leuchtenberger S., Dorner-Ciossek, C., Schneider, A., Jucker, M., Koo, E.H., Pietrzik, C.U., Baumann, K., Weggen, S.;
Journal of Biological Chemistry, 2007, 282(34):24504-13.

“γ-Secretase modulation with Aβ42-lowering non-steroidal anti-inflammatory drugs (NSAIDs) and derived compounds.”
Czirr, E. and Weggen, S.;
Neurodegenerative Diseases, 2006, 3(4-5):298-304.